REPORT DOCUMENTATION PAGE

Form Approved OMB NO. 0704-0188

1. REPORT DATE (DD-MM-YYYY)	2. REPORT TYPE	3. DATES COVERED (From - To)
20-08-2015	Final Report	1-Jul-2012 - 30-Jun-2015

4. TITLE AND SUBTITLE
Final Report: Fundamental Properteries and Capabilities of Plasmonic Antennas for Efficient Interaction with Nanoeletronics

5a. CONTRACT NUMBER
W911NF-12-1-0253

5b. GRANT NUMBER

5c. PROGRAM ELEMENT NUMBER
611102

6. AUTHORS
Mona Jarrahi

5d. PROJECT NUMBER

5e. TASK NUMBER

5f. WORK UNIT NUMBER

7. PERFORMING ORGANIZATION NAMES AND ADDRESSES
University of Michigan - Ann Arbor
3003 S. State St
Ann Arbor, MI 48109 -1274

8. PERFORMING ORGANIZATION REPORT NUMBER

9. SPONSORING/MONITORING AGENCY NAME(S) AND ADDRESS (ES)
U.S. Army Research Office
P.O. Box 12211
Research Triangle Park, NC 27709-2211

10. SPONSOR/MONITOR'S ACRONYM(S)
ARO

11. SPONSOR/MONITOR'S REPORT NUMBER(S)
61863-EL-YIP.94

12. DISTRIBUTION AVAILIBILITY STATEMENT
Approved for Public Release; Distribution Unlimited

13. SUPPLEMENTARY NOTES
The views, opinions and/or findings contained in this report are those of the author(s) and should not contrued as an official Department of the Army position, policy or decision, unless so designated by other documentation.

14. ABSTRACT
During the third year of this research program, we extended the powerful capabilities of the nano-plasmonic antennas that we demonstrated during the first two years to achieve record-high power terahertz radiation pulses. In this regard, we presented a novel design of large area photoconductive emitters which incorporates plasmonic contact electrodes to offer significantly higher optical-to-terahertz conversion efficiencies compared to conventional designs. The presented terahertz emitter can offer high power terahertz radiation because of its capacity to handle relatively high optical powers without suffering from the carrier screening effect and thermal

15. SUBJECT TERMS
Plasmonic nano-antenna, Terahertz source, Heterodyne receiver

16. SECURITY CLASSIFICATION OF:			17. LIMITATION OF ABSTRACT	15. NUMBER OF PAGES	19a. NAME OF RESPONSIBLE PERSON
a. REPORT	b. ABSTRACT	c. THIS PAGE			Mona Jarrahi
UU	UU	UU	UU		19b. TELEPHONE NUMBER 734-747-1799

Report Title

Final Report: Fundamental Properteries and Capabilities of Plasmonic Antennas for Efficient Interaction with Nanoeletronics

ABSTRACT

During the third year of this research program, we extended the powerful capabilities of the nano-plasmonic antennas that we demonstrated during the first two years to achieve record-high power terahertz radiation pulses. In this regard, we presented a novel design of large area photoconductive emitters which incorporates plasmonic contact electrodes to offer significantly higher optical-to-terahertz conversion efficiencies compared to conventional designs. The presented terahertz emitter can offer high power terahertz radiation because of its capacity to handle relatively high optical powers without suffering from the carrier screening effect and thermal breakdown. Additionally, it can offer broadband terahertz radiation due to the fact that terahertz radiation is generated by dipole nano-plasmonic antennas embedded within the device active area with dipole lengths much smaller than terahertz radiation wavelength. Moreover, use of plasmonic contact electrodes enables a more efficient separation and acceleration of photocarriers, enhancing the effective dipole moment induced within the device active area in response to an incident optical pump. We demonstrate broadband, pulsed terahertz radiation with record-high radiation power levels as high as 3.8 mW over 0.1-5 THz frequency range, exhibiting an order of magnitude higher optical-to-terahertz conversion efficiency compared to conventional designs.

Enter List of papers submitted or published that acknowledge ARO support from the start of the project to the date of this printing. List the papers, including journal references, in the following categories:

(a) Papers published in peer-reviewed journals (N/A for none)

Received	Paper
07/15/2014 53.00	Shang-Hua Yang , Mona Jarrahi. Enhanced light–matter interaction at nanoscale byutilizing high-aspect-ratio metallic gratings, Optics Letters, (09 2013): 3677. doi:
07/15/2014 54.00	Christopher W. Berry , Mohammed Reza M. Hashemi , Emmanuelle Merced , Nelson Sepúlveda , Mona Jarrahi. Direct Measurement of Vanadium Dioxide DielectricProperties in W-band, Journal of Infrared, Millimeter and Terahertz Waves, (03 2014): 486. doi:
07/15/2014 55.00	Christopher W. Berry, Mohammad R. Hashemi, Mona Jarrahi. Generation of high power pulsed terahertz radiation using a plasmonicphotoconductive emitter array with logarithmic spiral antennas, Applied Phylics letters, (02 2014): 81122. doi:
07/15/2014 56.00	Christopher W. Berry, Mohammad R. Hashemi, Sascha Preu, Hong Lu, Arthur C. Gossard, Mona Jarrahi. High power terahertz generation using 1550nm plasmonic photomixers, Applied Phylics letters, (07 2014): 11121. doi:
07/15/2014 57.00	M. Unlu, M. R. Hashemi, C. W. Berry, S. Li, S.-H. Yang , M. Jarrahi. Switchable Scattering Meta-Surfaces forBroadband Terahertz Modulation, Scientific Reports, (07 2014): 5708. doi:
07/15/2014 58.00	C. W. Berry, M. R. Hashemi, S. Preu, H. Lu, A. C. Gossard, Mona Jarrahi. Plasmonics enhanced photomixing for generating quasi-continuous-wave frequency-tunable terahertz radiation, Optics Letters, (07 2014): 0. doi:
08/20/2015 77.00	Mehmet Unlu, Mohammad Hashemi, Christopher Berry, Shenglin Li, Shang-Hua Yang, Mona Jarrahi. Fully integrated broadband terahertz modulators, SPIE Newsroom, (11 2014): 0. doi: 10.1117/2.1201410.005657
08/20/2015 80.00	Mona Jarrahi. Advanced Photoconductive Terahertz Optoelectronics Based on Nano-Antennas and Nano-Plasmonic Light Concentrators, IEEE Transactions on Terahertz Science and Technology, (05 2015): 0. doi: 10.1109/TTHZ. 2015.2406117
08/20/2015 79.00	Nezih T. Yardimci, Shang-Hua Yang, Christopher W. Berry, Mona Jarrahi. High-Power Terahertz Generation Using Large-Area Plasmonic Photoconductive Emitters, IEEE Transactions on Terahertz Science and Technology, (03 2015): 0. doi: 10.1109/TTHZ. 2015.2395417
08/20/2015 78.00	Mehmet Unlu, Mona Jarrahi. Miniature multi-contact MEMS switch for broadband terahertz modulation, Optics Express, (12 2014): 0. doi: 10.1364/OE.22.032245
08/25/2013 33.00	Christopher Berry, Mohammad Reza Hashemi, Mehmet Unlu, Mona Jarrahi. Design, Fabrication, and Experimental Characterization of Plasmonic Photoconductive Terahertz Emitters, Journal of Visualized Experiments, (7 2013): 0. doi: 10.3791/50517
08/25/2013 34.00	Ning Wang, Mona Jarrahi. Noise Analysis of Photoconductive Terahertz Detectors, Journal of Infrared, Millimeter, and Terahertz Waves, (7 2013): 0. doi: 10.1007/s10762-013-9995-1

08/25/2013	32.00	N. Wang, M.R. Hashemi, M. Unlu, M. Jarrahi, C.W. Berry. Significant performance enhancement in photoconductive terahertz optoelectronics by incorporating plasmonic contact electrodes, Nature Communications, (3 2013): 0. doi: 10.1038/ncomms2638
08/25/2013	36.00	Ning Wang, Mohammad R. Hashemi, Mona Jarrahi. Plasmonic photoconductive detectors for enhanced terahertz detection sensitivity, Optics Express, (07 2013): 0. doi: 10.1364/OE.21.017221
08/25/2013	37.00	Mona Jarrahi, Christopher W. Berry. Principles of Impedance Matching in Photoconductive Antennas, Journal of Infrared, Millimeter, and Terahertz Waves, (9 2012): 0. doi: 10.1007/s10762-012-9937-3
TOTAL:	**15**	

Number of Papers published in peer-reviewed journals:

(b) Papers published in non-peer-reviewed journals (N/A for none)

Received		Paper
08/20/2015	75.00	Christopher W. Berry, Nezih T. Yardimci, Mona Jarrahi. Responsivity Calibration of Pyroelectric Terahertz Detectors, ArXiv arXiv:1412.6878v1, (12 2014): 1. doi:
08/20/2015	76.00	Mona Jarrahi, Imran Mehdi. Emerging technologies for next generation terahertz systems, Microwave Magazine, (11 2014): 30. doi:
TOTAL:	**2**	

Number of Papers published in non peer-reviewed journals:

(c) Presentations

1. M. Jarrahi, "Plasmonics-Enabled Advancements in Terahertz Imaging and Spectroscopy Systems," International Symposium on Frontiers in THz Technology, Hamamatsu, Japan, August 30 - September 2, 2015
2. M. Jarrahi, "New Frontiers in Terahertz Technology," 8th Global Symposium on Millimeter-Waves, Montreal, Canada, May 25-27, 2015
3. M. Jarrahi, "Plasmonics Enabled High Power Terahertz Sources," Proc. International Workshop on Optical Terahertz Science and Technology, San Diego, CA, March 8-13, 2015
4. N. Wang, M. Jarrahi, "Heterodyne Terahertz Receiver Based on Plasmonic Photomixers," Proc. International Workshop on Optical Terahertz Science and Technology, San Diego, CA, March 8-13, 2015
5. M. R. Hashemi, S.-H. Yang, T. Wang, N. Sepúlveda, M. Jarrahi, "Voltage-Controlled Terahertz Phase Modulator based on Vanadium Dioxide," Proc. International Workshop on Optical Terahertz Science and Technology, San Diego, CA, March 8-13, 2015
6. S.-H. Yang , C. W. Berry, N. T. Yardimci, M. R. Hashemi, M. Jarrahi, "High-Aspect Ratio Plasmonic Photoconductive Terahertz Sources," Proc. International Workshop on Optical Terahertz Science and Technology, San Diego, CA, March 8-13, 2015
7. N. T. Yardimci , S.-H. Yang, C. W. Berry, M. Jarrahi, "Significant Terahertz Radiation Enhancement in Large Area Photoconductive Emitters by Incorporating Plasmonic Contact Electrode Gratings," Proc. International Workshop on Optical Terahertz Science and Technology, San Diego, CA, March 8-13, 2015
8. C. W. Berry, M. R. Hashemi, S. Preu, H. Lu, A. Gossard, M. Jarrahi, "Plasmonic Photomixers for High-Power Continuous-Wave Terahertz Generation," Proc. SPIE Photonic West, San Francisco, CA, February 7-12, 2015
9. N. T. Yardimci, S.-H. Yang, C. W. Berry, M. Jarrahi, "High-power and broadband terahertz generation through large-area plasmonic photoconductive emitters," Proc. SPIE Photonic West, San Francisco, CA, February 7-12, 2015
10. S.-H. Yang, N. T. Yardimci, M. Jarrahi, "Compensating the carrier screening effect in plasmonic photoconductive terahertz sources," Proc. SPIE Photonic West, San Francisco, CA, February 7-12, 2015
11. M. Jarrahi, "Plasmonic Terahertz Optoelectronics," SPIE Photonic West, San Francisco, CA, February 7-12, 2015
12. M. Jarrahi, "Plasmonic Terahertz Sources for High Performance Terahertz Imaging and Spectroscopy," Proc. 5th International Symposium on Terahertz Nanoscience, Martinique, December 1-5, 2014
13. M. Jarrahi, "Game-Changing Terahertz Sensor Technologies for Large-Scale Consumer Market," Trillion Sensors Summit, San Diego, CA, November 12-13, 2014
14. M. Jarrahi, "Advanced Terahertz Imaging and Spectroscopy Systems based on Plasmonic Terahertz Optoelectronics," Proc. SPIE Optics and Photonics Conference, San Diego, CA, August 17-21, 2014

Number of Presentations: 14.00

Non Peer-Reviewed Conference Proceeding publications (other than abstracts):

Received		Paper
08/20/2015	87.00	Mohammed R. Hashemi, Shang-Hua Yang, Tongyu Wang, Nelson Sepulveda, Mona Jarrahi. Millimeter-Wave Phase Modulator Based on Vanadium Dioxide Meta-Surfaces, International Antennas and Propagation Symposium. 19-JUL-15, . : ,
10/02/2012	2.00	C. W. Berry, M. R. Hashemi, M. Unlu, and M. Jarrahi. Enhancing optical-to-terahertz conversion efficiency by using plasmonic photoconductive emitters, International Conference on Fiber-Optics and Photonics, Chennai, India, Dec 9-12, 2012 . 09-DEC-12, . : ,
TOTAL:	**2**	

Number of Non Peer-Reviewed Conference Proceeding publications (other than abstracts):

Peer-Reviewed Conference Proceeding publications (other than abstracts):

Received	Paper
07/15/2014	72.00 C. W. Berry, M. R. Hashemi, S. Preu, H. Lu, A. C. Gossard, M. Jarrahi. High Power Terahertz Generation from ErAs:InGaAs Plasmonic Photomixers, International Conference on Infrared, Millimeter, and Terahertz Waves. 14-SEP-14, . : ,
07/15/2014	73.00 Shang-Hua Yang, Mohammad R. Hashemi, Christopher W. Berry, Mona Jarrahi. Three-Dimensional Plasmonic Contact Electrodes for High-Efficiency Photoconductive Terahertz Sources, International Conference on Infrared, Millimeter, and Terahertz Waves. 14-SEP-14, . : ,
07/15/2014	74.00 Nezih T. Yardimci, Shang-Hua Yang, Christopher W. Berry , Mona Jarrahi. Plasmonics Enhanced Terahertz Radiationfrom Large Area Photoconductive Emitters, IEEE Photonics Conference . 12-OCT-14, . : ,
07/15/2014	61.00 Chirstopher W. Berry, Mohammad R. Hashemi, Mehmet Unlu, Mona larrahi. Plasmonics-Enhanced Photoconductive Terahertz Emitters, International Microwave and Optoelectronic Conference. 04-AUG-13, . : ,
07/15/2014	62.00 Ning Wang, Christopher W. Berry, Mohammad R. Hashemi, Mona Jarrahi. Terahertz Detection Sensitivity Enhancement by IncorporatingPlasmonic Gratings in Photoconductive Detectors, International Conference on Infrared, Millimeter, and Terahertz Waves. 01-SEP-13, . : ,
07/15/2014	63.00 M. Unlu, M. R. Hashemi, C. W. Berry, S. Li, S.-H. Yang, M. Jarrahi. Broadband Terahertz Modulation through Reconfigurable Meta-Surfaceswith Diamagnetic Switching Capability, International Conference on Infrared, Millimeter, and Terahertz Waves. 01-SEP-13, . : ,
07/15/2014	64.00 Christopher W. Berry, Mohammed R. Hashemi, Mona Jarrahi. Plasmonic Photoconductive Terahertz Emitters Based on LogarithmicSpiral Antenna Arrays, International Conference on Infrared, Millimeter, and Terahertz Waves. 01-SEP-13, . : ,
07/15/2014	65.00 Christopher W. Berry, Ning Wang, Mohammad R. Hashemi, Mona Jarrahi. Plasmonic Photoconductive Antennas for High-Power Terahertz Generation and High-Sensitivity Terahertz Detection, European Conference on Antennas and Propagation. 06-APR-14, . : ,
07/15/2014	66.00 Shang-Hua Yang, Christopher W. Berry, Mohammad R. Hashemi, Mona Jarrahi. Plasmonic-enhanced optical-to-terahertz conversation efficiency, 4th European Optical Society Topical Meeting on Terahertz Science & Technology. 11-MAY-14, . : ,
07/15/2014	67.00 Shang-Hua Yang, Mohammed R. Hashemi, Christopher W. Berry, Mona Jarrahi. High-Efficiency Terahertz Emitters based onThree-dimensional Metallic Nanostructures, International Microwave Symposium. 01-JUN-14, . : ,
07/15/2014	68.00 C. W. Berry , M. R. Hashemi, S. Preu, H. Lu, A. C. Gossard, Mona Jarrahi. Plasmonic Photomixers for Increased Terahertz RadiationPowers at 1550 nm Optical Pump Wavelength, Conference of Lasers and Electro-Optics. 08-JUN-14, . : ,
07/15/2014	69.00 Mohammed R. Hashemi, Christopher W. Berry, Mona Jarrahi, Shang-Hua Yang. 7.5% Optical-to-Terahertz Conversion Efficiency throughUse of Three-Dimensional Plasmonic Electrodes, Conference of Lasers and Electro-Optics. 08-JUN-14, . : ,

07/15/2014 70.00 C. W. Berry, M. R. Hashemi, S. Preu, H. Lu, A. C. Gossard, M. Jarrahi. Terahertz Radiation Enhancement through Use of Plasmonic Photomixers,
IEEE International Antennas and Propagation Symposium. 06-JUL-14, . : ,

07/15/2014 71.00 Shang-Hua Yang, Mohammed R. Hashemi, Christopher W. Berry, Mona Jarrahi. High-Efficiency Photoconductive Terahertz Antennas based on High-Aspect Ratio Plasmonic Electrodes,
IEEE International Antennas and Propagation Symposium. 06-JUL-14, . : ,

08/20/2015 83.00 Shang-Hua Yang, Christopher W. Berry, Nezih T. Yardimci, Mona Jarrahi. Large Area Plasmonic Photoconductive Emitters for Generating High Power Broadband Terahertz Radiation,
Frontiers in Optics. 19-OCT-14, Tucson, Arizona. : ,

08/20/2015 93.00 Nezih T. Yardimci, Mona Jarrahi. 3.8 mW Terahertz Radiation Generation over a 5 THz Radiation Bandwidth through Large Area Plasmonic Photoconductive Antennas,
International Microwave Symposium. 17-MAY-15, . : ,

08/20/2015 92.00 Mona Jarrahi. High-Efficiency Terahertz Sources based on Plasmonic Contact Electrodes,
International Microwave Symposium. 17-MAY-15, . : ,

08/20/2015 91.00 Nezih T. Yardimci, Mona Jarrahi. 3.8 mW Terahertz Radiation Generation through Plasmonic Nano-Antenna Arrays,
International Antennas and Propagation Symposium. 19-JUL-15, . : ,

08/20/2015 90.00 Mona Jarrahi. Plasmonics Enabled Advances in Photoconductive Terahertz Radiation Sources,
International Conference on Infrared, Millimeter, and Terahertz Waves. 23-AUG-15, . : ,

08/20/2015 89.00 Mohammed R. Hashemi, Shang-Hua Yang, Tongyu Wang, Nelson Sepúlveda, Mona Jarrahi. Fully-Integrated and Electronically-Controlled Millimeter-Wave Phase Modulator,
International Conference on Infrared, Millimeter, and Terahertz Waves. 23-AUG-15, . : ,

08/20/2015 88.00 Nezih T. Yardimci, Shang-Hua Yang, Mona Jarrahi. High Power Pulsed Terahertz Radiation From Large Area Photoconductive Emitters,
International Conference on Infrared, Millimeter, and Terahertz Waves. 23-AUG-15, . : ,

08/20/2015 85.00 Shang-Hua Yang, Tongyu Wang, Nelson Sepúlveda, Mona Jarrahi, Mohammed Reza Hashemi. Efficient Terahertz Phase Modulation Using Vanadium Dioxide Meta-Surfaces,
CLEO: Science and Innovations. 10-MAY-15, San Jose, California. : ,

08/20/2015 86.00 Nezih Yardimci, Shang-Hua Yang, Christopher Berry, Mona Jarrahi. Terahertz Radiation Enhancement in Large-Area Photoconductive Sources by Using Plasmonic Nanoantennas,
CLEO: Science and Innovations. 10-MAY-15, San Jose, California. : ,

08/25/2013 38.00 Christopher W. Berry, Mona Jarrahi. Plasmonic photoconductive antennas for high power terahertz generation,
2012 IEEE Antennas and Propagation Society International Symposium and USNC/URSI National Radio Science Meeting. 08-JUL-12, Chicago, IL, USA. : ,

08/27/2013 39.00 S. Li, M. Unlu, M. Jarrahi. Reconfigurable mesh filters for terahertz modulation,
2012 37th International Conference on Infrared, Millimeter, and Terahertz Waves (IRMMW-THz 2012). 23-SEP-12, Wollongong, NSW, Australia. : ,

08/27/2013 40.00 C. W. Berry, M. Unlu, M. R. Hashemi, M. Jarrahi. Use of plasmonic gratings for enhancing the quantum efficiency of photoconductive terahertz sources,
2012 37th International Conference on Infrared, Millimeter, and Terahertz Waves (IRMMW-THz 2012). 23-SEP-12, Wollongong, NSW, Australia. : ,

08/27/2013 41.00 Christopher W. Berry, Mohammad R. Hashemi, Mehmet Unlu, Mona Jarrahi. Enhancing optical-to-terahertz conversion efficiency by using plasmonic photoconductive emitters,
International Conference on Fibre Optics and Photonics. , Chennai. : ,

08/27/2013 42.00 C. W. Berry, S. Li, S-H. Yang, M. R. Hashemi, M. Unlu, M. Jarrahi. Broadband terahertz modulation using reconfigurable mesh filters,
2013 IEEE 14th Annual Wireless and Microwave Technology Conference (WAMICON). 07-APR-13, Orlando, FL, USA. : ,

08/27/2013 43.00 Mehmet Unlu, Christopher W. Berry, Shenglin Li, Shang Hua Yang, Mohammed Reza Hashemi, Mona Jarrahi. Electromechanically Switchable Diamagnetism for Efficient Terahertz Modulation,
CLEO: QELS_Fundamental Science. , CLEO: QELS_Fundamental Science (2013). : ,

08/27/2013 44.00 Ning Wang, Christopher W. Berry, Mohammed Reza Hashemi, Mona Jarrahi. Ultrafast Plasmonic Photoconductors for High Sensitivity Terahertz Detection,
CLEO: QELS_Fundamental Science. , CLEO: QELS_Fundamental Science (2013). : ,

08/27/2013 45.00 Christopher W. Berry, Mohammed Reza Hashemi, Mehmet Unlu, Mona Jarrahi. Substantial Radiation Enhancement in Photoconductive Terahertz Emitters by Utilizing Plasmonic Contact Electrodes,
CLEO: Science and Innovations. , San Jose, California. : ,

08/27/2013 46.00 M. Unlu, C. W. Berry, S. Li, S.-H. Yang, M. R. Hashemi, M. Jarrahi1. A High-performance Terahertz Spatial Light Modulator based on Reconfigurable Mesh Filters,
4th International Conference on Metamaterials, Photonic Crystals and Plasmonics. , . : ,

08/27/2013 47.00 N. Wang, C. W. Berry, M. R. Hashemi, M. Jarrahi1. Terahertz Detection Sensitivity Enhancement by Use of Plasmonic Photoconductive Detectors,
4th International Conference on Metamaterials, Photonic Crystals and Plasmonics. , . : ,

08/27/2013 48.00 Chirstopher W. Berry, Mohammad R. Hashemi, Mehmet Unlu, Mona Jarrahi. Nanoscale Contact Electrodes for Significant Radiation Power Enhancement in Photoconductive Terahertz Emitters,
IEEE Microwave Symposium Digest. , . : ,

08/27/2013 49.00 Ning Wang, Chirstopher W. Berry, Mohammad Reza Hashemi, Mona Jarrahi. Terahertz Detection Sensitivity Enhancement by Using Plasmonic Contact Electrode Gratings,
IEEE Microwave Symposium Digest. , . : ,

08/27/2013 50.00 C. W. Berry, M. R. Hashemi, M. Unlu, M. Jarrahi. Plasmonic Photoconductive Antennas for Significant Terahertz Radiation Enhancement,
Proc. IEEE International Antennas and Propagation Symposium. , . : ,

08/27/2013 51.00 M. Unlu, C. W. Berry, S. Li, S.-H. Yang, M. R. Hashemi, M. Jarrahi. A Microelectromechanically Reconfigurable Mesh Filter for High-Performance Terahertz Modulation,
Proc. IEEE International Antennas and Propagation Symposium. , . : ,

08/27/2013 52.00 Mohammad R. Hashemi, Mona Jarrahi, Christopher W. Berry. Plasmonic Photoconductors for High-Efficiency Terahertz Generation,
Proc. Optical Society of Americas Sensors topical meeting. , . : ,

TOTAL: 38

Number of Peer-Reviewed Conference Proceeding publications (other than abstracts):

(d) Manuscripts

Received		Paper
07/15/2014	59.00	Mohammad R. Hashemi, Shang-Hua Yang , Christopher W. Berry, Mona Jarrahi. 7.5% Optical-to-Terahertz Conversion Efficiency Offered by Photoconductive Emitters with Three-Dimensional Plasmonic Contact Electrodes, IEEE Transaction on Terahertz Science and Technology (04 2014)
08/20/2015	81.00	Shang-Hua Yang, Mona Jarrahi. Frequency-Tunable Continuous-Wave Terahertz Sources based on GaAs Plasmonic Photomixers , Applied Physics Letters (accepted) (08 2015)
08/20/2015	82.00	Shang-Hua Yang, Mona Jarrahi. Spectral Characteristics of Terahertz Radiation from Plasmonic Photomixers, Optics Express (08 2015)
08/25/2013	30.00	. Enhanced light-matter interaction at nanoscale by utilizing high aspect-ratio metallic gratings, ( )
08/25/2013	24.00	. Broadband Terahertz Modulators based on MEMS-Reconfigurable Mesh Filters, ( )
10/02/2012	3.00	C. W. Berry, M. R. Hashemi, M. Unlu, and M. Jarrahi. Significant Radiation Enhancement in Photoconductive Terahertz Emitters by Incorporating Plasmonic Contact Electrodes, arXiv:1209.1680v1 (09 2012)
10/02/2012	4.00	Christopher W. Berry & Mona Jarrahi. Principles of Impedance Matching in PhotoconductiveAntennas, Journal of Infrared, Millimeter and Terahertz Waves (08 2012)
TOTAL:		**7**

Number of Manuscripts:

Books

Received		Book
TOTAL:		

Received	Book Chapter

TOTAL:

Patents Submitted

1. M. Jarrahi, "Terahertz Endoscopy through Laser-Driven Terahertz Sources and Detectors," Provisional Patent Application No. 62167201, filed 05/27/15
2. M. Jarrahi, "Low-Duty-Cycle Continuous-Wave Photoconductive Terahertz Imaging and Spectroscopy Systems," Pending International Patent Application No. PCT/US2015/035685, filed 06/12/15
3. M. Jarrahi, M. Unlu, M. R. Hashemi, C. W. Berry, and S. Li, "Reconfigurable Device for Terahertz and Infrared Filtering and Modulation," Pending International Patent Application No. PCT/US14/49866, filed 08/06/14
4. M. Jarrahi, C. W. Berry, N. Wang, S.-H. Yang, and M. R. Hashemi, "Photoconductive Device with Plasmonic Electrodes," Pending International Patent Application No. PCT/US2013/022776, filed 01/23/13 (US Serial No. 14/372,779) (European Application number is 13741491.8) (Japanese Application number is 2014-553536)

Patents Awarded

Awards

PI Awards and Recognitions:

IEEE Antennas and Propagation Society (AP-S) Lot Shafai Mid-Career Distinguished Achievement Award (2015)
IEEE Microwave Theory and Techniques Society Distinguished Lecturer (2015)
Kavli Fellow by the National Academy of Sciences (2014)

Student Awards and Recognitions:

SPIE Scholarship in Optics and Photonics received by Nezih Tolga Yardimci (2015)
Taiwanese Government Studying Abroad Scholarship received by Shang-Hua Yang (2015)
University of Michigan Rackham Summer Award received by Shang-Hua Yang (2015)?
Optical Terahertz Science & Technology Conference Best Poster Prize (2nd place) by Ning Wang (2015)
IEEE Antennas and Propagation Society Doctoral Research Award received by Shang-Hua Yang (2014)

Graduate Students

NAME	PERCENT_SUPPORTED	Discipline
Ning Wang	0.30	
Shang-Hua Yang	0.30	
Nezih Tolga Yardimci	0.40	
FTE Equivalent:	**1.00**	
Total Number:	**3**	

Names of Post Doctorates

NAME	PERCENT_SUPPORTED
Mohammed R. Hashemi	0.10
FTE Equivalent:	**0.10**
Total Number:	**1**

Names of Faculty Supported

NAME	PERCENT_SUPPORTED	National Academy Member
Mona Jarrahi	0.10	
FTE Equivalent:	**0.10**	
Total Number:	**1**	

Names of Under Graduate students supported

NAME	PERCENT_SUPPORTED
FTE Equivalent:	
Total Number:	

Student Metrics

This section only applies to graduating undergraduates supported by this agreement in this reporting period

The number of undergraduates funded by this agreement who graduated during this period: 0.00

The number of undergraduates funded by this agreement who graduated during this period with a degree in science, mathematics, engineering, or technology fields:..... 0.00

The number of undergraduates funded by your agreement who graduated during this period and will continue to pursue a graduate or Ph.D. degree in science, mathematics, engineering, or technology fields:..... 0.00

Number of graduating undergraduates who achieved a 3.5 GPA to 4.0 (4.0 max scale):..... 0.00

Number of graduating undergraduates funded by a DoD funded Center of Excellence grant for Education, Research and Engineering:..... 0.00

The number of undergraduates funded by your agreement who graduated during this period and intend to work for the Department of Defense 0.00

The number of undergraduates funded by your agreement who graduated during this period and will receive scholarships or fellowships for further studies in science, mathematics, engineering or technology fields:..... 0.00

Names of Personnel receiving masters degrees

NAME
Total Number:

Names of personnel receiving PHDs

NAME
Ning Wang
Total Number: 1

Names of other research staff

NAME	PERCENT_SUPPORTED

FTE Equivalent:
Total Number:

Sub Contractors (DD882)

Inventions (DD882)

Scientific Progress

Please see the attachment

Technology Transfer

Army Research Office Progress Report

ARO-YIP: Fundamental Properties and Capabilities of Plasmonic Antennas for Efficient Interaction with Nanoelectronics

Contract # W911NF-12-1-0253

Performance Period: 07/01/2012 – 06/30/2013

Program Manager: Dr. James Harvey

Lead Organization: University of Michigan, Ann Arbor

Technical Point of Contact: Mona Jarrahi (mjarrahi@umich.edu)

Administrative Point of Contact: Michelle Chapman (chapman@eecs.umich.edu)

Executive Summary

Here is a list of research activities conducted during the first year of the ARO-YIP program:

- We presented a novel photoconductive terahertz emitter that uses a plasmonic contact electrode configuration to enhance the optical-to-terahertz conversion efficiency by two orders of magnitude. Our technique addresses the most important limitations of conventional photoconductive terahertz emitters, namely low output power and poor power efficiency, which originate from the inherent tradeoff between high quantum efficiency and ultrafast operation of conventional photoconductors. One of the key novelties in our design that led to this leapfrog performance improvement is to design a contact electrode configuration that accumulates a large number of photo-generated carriers in close proximity to the contact electrodes, such that they can be collected within a sub-picosecond timescale. In other words, the tradeoff between photoconductor ultrafast operation and high quantum efficiency is mitigated by spatial manipulation of the photo-generated carriers. Plasmonic contact electrodes offer this unique capability by (1) allowing light confinement into nanoscale device active areas between the plasmonic electrodes (beyond diffraction limit), (2) extraordinary light enhancement at the metal contact and photo-absorbing semiconductor interface. Another important attribute of our solution is that it accommodates large photoconductor active areas without a considerable increase in the parasitic loading to the terahertz radiating antenna. Utilizing large photoconductor active areas enable mitigating the carrier screening effect and thermal breakdown, which are the ultimate limitations for the maximum radiation power from conventional photoconductive emitters. We experimentally demonstrated 50 times higher terahertz powers from a plasmonic photoconductive emitter in comparison with a similar photoconductive emitter with non-plasmonic contact electrodes.

- We experimentally demonstrated that the use of plasmonic contact electrodes not only enhances the output power and efficiency of photoconductive terahertz emitters by a factor of 50, but also enhances the responsivity and detection sensitivity of photoconductive terahertz detectors by a factor of 30. Consequently, our presented plasmonic photoconductive terahertz optoelectronics concept offers more than three orders of magnitude enhancement in the signal-to-noise ratio of time-domain and frequency-domain terahertz spectroscopy and imaging systems. This report is concentrated on the unique attributes of our presented plasmonic terahertz optoelectronics by describing the governing physics, numerical modeling, and experimental verification.

- This research, in the 07/01/2012 – 06/30/2013 performance period, has resulted in 7 peer-reviewed journal papers, 20 peer-reviewed conference papers, 8 conference abstracts, 24 invited/plenary talks, and 2 patents. Additionally, the PI of this project, Mona Jarrahi, has received the Frontiers of Engineering Award from National Academy of Engineering and Grainger Foundation; and the graduate student working on this project, Christopher W. Berry, has received a best student paper award (2^{nd} place) from IEEE International Symposium on Antennas and Propagation and USNC-URSI National Radio Science Meeting, a best student paper award (3^{rd} place) from International Microwave Symposium, a doctoral research award from IEEE Antennas and Propagation Society, and a graduate fellowship from Michigan Space Grant Consortium. The details are as follows:

Awards and Recognitions

Awards and recognitions received by the PI of this project, Mona Jarrahi:

- National Academy of Engineering, The Grainger Foundation Frontiers of Engineering Award
- SPIE Senior Membership
- National Academy of Engineering (NAE) Frontiers of Engineering

Awards and recognitions received by the graduate student working on this project, Christopher Berry:

- IEEE International Symposium on Antennas and Propagation and USNC-URSI National Radio Science Meeting Best Student Paper Award (2nd place
- International Microwave Symposium Best Student Paper Award (3rd place)
- IEEE Antennas and Propagation Society Doctoral Research Award
- Michigan Space Grant Consortium Graduate Fellowship

Journal Publications

1. C. W. Berry, N. Wang, M. R. Hashemi, M. Unlu, M. Jarrahi "Significant Performance Enhancement in Photoconductive Terahertz Optoelectronics by Incorporating Plasmonic Contact Electrodes," *Nature Communications*, 4, 1622, 2013
2. C. W. Berry, M. R. Hashemi, M. Unlu, M. Jarrahi "Design, Fabrication, and Experimental Characterization of Plasmonic Photoconductive Terahertz Emitters," *J. Visualized Experiments*, 77, e50517, doi:10.3791/50517, 2013
3. N. Wang, M. Jarrahi, "Noise Analysis of photoconductive terahertz detectors," *Journal of Infrared, Millimeter and Terahertz Wave*, 34, 519-528, 2013
4. N. Wang, M. R. Hashemi, M. Jarrahi, "Plasmonic photoconductive detectors for enhanced terahertz detection sensitivity," *Optics Express*, 21, 17221–17227, 2013
5. S.-H. Yang, M. Jarrahi, "Enhanced light-matter interaction at nanoscale by utilizing high aspect-ratio metallic gratings," *Optics Letters*, 38, 2013
6. C. W. Berry, M. Jarrahi, "Principles of impedance matching in photoconductive antennas," *Journal of Infrared, Millimeter and Terahertz Waves*, 33, 1182-1189, 2012
7. M. Unlu, C. W. Berry, S. Li, S-H. Yang, M. R. Hashemi, M. Jarrahi, "Broadband terahertz modulators based on MEMS-reconfigurable mesh filters," arXiv:1212.6562v1, 2012

Conference Publications

1. M. Unlu, M. R. Hashemi, C. W. Berry, S. Li, S.-H. Yang, M. Jarrahi, "High-performance terahertz spatial light modulators based on reconfigurable diamagnetic meta-surfaces," *Proc. International Congress on Advanced Electromagnetic Materials in Microwaves and Optics*, Bordeaux, France, September 16-21, 2013
2. C. W. Berry, M. R. Hashemi, M. Jarrahi, "Plasmonic Photoconductive Terahertz Emitters Based On Logarithmic Spiral Antenna Arrays," *Proc. International Conference on Infrared, Millimeter, and Terahertz Waves*, Mainz, Germany, Sep 1-6, 2013
3. M. Unlu, M. R. Hashemi, C. W. Berry, S. Li, S.-H. Yang, M. Jarrahi, "Broadband Terahertz Modulation Through Reconfigurable Meta-Surfaces With Diamagnetic Switching Capability," *Proc. International Conference on Infrared, Millimeter, and Terahertz Waves,* Mainz, Germany, Sep 1-6, 2013
4. N. Wang, C. W. Berry, M. R. Hashemi, M. Jarrahi, "Terahertz Detection Sensitivity Enhancement By Incorporating Plasmonic Gratings In Photoconductive Detectors," *Proc. International Conference on Infrared, Millimeter, and Terahertz Waves*, Mainz, Germany, Sep 1-6, 2013
5. C. W. Berry, M. R. Hashemi, M. Unlu, M. Jarrahi, "Plasmonics-Enhanced Photoconductive Terahertz Emitters," *Proc. International Microwave and Optoelectronic Conference*, Rio de Janeiro, Brazil, August 4-7, 2013

6. C. W. Berry, M. R. Hashemi, M. Jarrahi, "Plasmonic Photoconductors for High-Efficiency Terahertz Generation*" Proc. Optical Society of Americas Sensors topical meeting*, Rio Grande, Puerto Rico, July 14-19, 2013
7. M. Unlu, C. W. Berry, S. Li, M. R. Hashemi, S.-H. Yang, M. Jarrahi, "A Microelectromechanically Reconfigurable Mesh Filter for High-Performance Terahertz Modulation," *Proc. IEEE International Antennas and Propagation Symposium*, Orlando, FL, July 7-12, 2013
8. C. W. Berry, M. R. Hashemi, M. Unlu, M. Jarrahi, "Plasmonic Photoconductive Antennas for Significant Terahertz Radiation Enhancement," *Proc. IEEE International Antennas and Propagation Symposium*, Orlando, FL, July 7-12, 2013 (Best student paper award, 2nd place)
9. C. W. Berry, M. R. Hashemi, M. Unlu, M. Jarrahi, "Substantial Radiation Enhancement in Photoconductive Terahertz Emitters by Utilizing Plasmonic Contact Electrodes," *Proc. Conference of Lasers and Electro-Optics*, San Jose, CA, 9-14 June 2013
10. N. Wang, C. W. Berry, M. R. Hashemi, M. Jarrahi, "Ultrafast Plasmonic Photoconductors for High Sensitivity Terahertz Detection," *Proc. Conference of Lasers and Electro-Optics*, San Jose, CA, 9-14 June 2013
11. M. Unlu, C. W. Berry, S. Li, S.-H. Yang, M. R. Hashemi, and M. Jarrahi, "Electromechanically Switchable Diamagnetism for Efficient Terahertz Modulation," *Proc. Conference of Lasers and Electro-Optics*, San Jose, CA, 9-14 June 2013
12. C. W. Berry, M. R. Hashemi, M. Unlu, M. Jarrahi, "Nanoscale Contact Electrodes for Significant Radiation Power Enhancement in Photoconductive Terahertz Emitters," *IEEE Microwave Symposium Digest*, Seattle, WA, June 2-7, 2013 (Best student paper award, 3rd place)
13. N. Wang, C. W. Berry, M. R. Hashemi, M. Jarrahi, "Terahertz Detection Sensitivity Enhancement by Using Plasmonic Contact Electrode Gratings," *IEEE Microwave Symposium Digest*, Seattle, WA, June 2-7, 2013
14. M. Unlu, C. W. Berry, S. Li, S.-H. Yang, M. R. Hashemi, M. Jarrahi, "Broadband terahertz modulation using reconfigurable mesh filters," *Proc. IEEE Wireless and Microwave Technology Conference*, Orlando, Florida, April 7-9, 2013
15. N. Wang, C. W. Berry, M. R. Hashemi, M. Jarrahi, "Terahertz Detection Sensitivity Enhancement by Use of Plasmonic Photoconductive Detectors," *Proc. 4th International Conference on Metamaterials, Photonic Crystals and Plasmonics*, Sharjah, UAE, 18-22 March, 2013
16. M. Unlu, C. W. Berry, S. Li, S.-H. Yang, M. R. Hashemi, M. Jarrahi, "A High-performance Terahertz Spatial Light Modulator based on Reconfigurable Mesh Filters," *Proc. 4th International Conference on Metamaterials, Photonic Crystals and Plasmonics*, Sharjah, UAE, 18-22 March, 2013
17. C. W. Berry, M. Jarrahi, "Enhancing optical-to-terahertz conversion efficiency by using plasmonic photoconductive emitters," *Proc. International Conference on Fiber-Optics and Photonics*, Chennai, India, Dec 9-12, 2012
18. C. W. Berry, M. Unlu, M. R. Hashemi, M. Jarrahi, "Use of Plasmonic Gratings for Enhancing the Quantum Efficiency of Photoconductive Terahertz Sources," *Proc. International Conference on Infrared, Millimeter, and Terahertz Waves*, Wollongong, Australia, Sep 23-28, 2012
19. S. Li, M. Unlu, M. Jarrahi, "Reconfigurable Mesh Filters for Terahertz Modulation," *Proc. International Conference on Infrared, Millimeter, and Terahertz Waves*, Wollongong, Australia, Sep 23-28, 2012
20. C. W. Berry, M. Jarrahi, "Plasmonic Photoconductive Antennas for High Power Terahertz Generation," *Proc. IEEE International Antennas and Propagation Symposium*, Chicago, IL, July 8-14, 2012

Conference Abstracts

1. C. W. Berry, N. Wang, M. R. Hashemi, M. Jarrahi, "Plasmonics-Enhanced Photoconductive Terahertz Optoelectronics," *Proc. International Conference and Exhibition on Lasers, Optics & Photonics*, San Antonio, TX, October 7-9, 2013

2. M. Unlu, M. R. Hashemi, C. W. Berry, S. Li, S.-H. Yang, M. Jarrahi, "Reconfigurable diamagnetic meta-molecules for broadband terahertz modulation," *Proc. SPIE Optics and Photonics Conference*, San Diego, CA, August 25-29, 2013
3. M. Unlu, M. R. Hashemi, C. W. Berry, S. Li, S.-H. Yang, M. Jarrahi, "Terahertz wave manipulation through electromechanically reconfigurable diamagnetic surfaces," *Proc. International Symposium on Photoelectronic Detection and Imaging*, Beijing, China, June 25-27, 2013
4. N. Wang, C. W. Berry, M. R. Hashemi, M. Jarrahi, "High Sensitivity Photoconductive Terahertz Detectors Based on Plasmonic Contact Electrodes," *Proc. International Workshop on Optical Terahertz Science and Technology*, Kyoto, Japan, April 1-5, 2013
5. C. W. Berry, M. R. Hashemi, M. Unlu, M. Jarrahi, "High Power Photoconductive Terahertz Emitters Utilizing Nanoscale Plasmonic Gratings*," Proc. International Workshop on Optical Terahertz Science and Technology*, Kyoto, Japan, April 1-5, 2013
6. M. Unlu, C. W. Berry, S. Li, S.-H. Yang, M. R. Hashemi, M. Jarrahi, "A Microelectromechanically Controlled Broadband Terahertz Modulator," *Proc. International Workshop on Optical Terahertz Science and Technology*, Kyoto, Japan, April 1-5, 2013
7. C. W. Berry, M. Jarrahi, "Enhanced terahertz emission from photoconductive emitters using plasmonic contact electrodes," *Proc. SPIE Photonic West*, San Francisco, CA, February 2-7, 2013
8. C. W. Berry, M. Jarrahi, "Photoconductive Terahertz Sources based on Plasmonic Gratings," *Proc. SPIE Optics and Photonics Conference*, San Diego, CA, August 12-16, 2012

Invited Talks

1. C. W. Berry, N. Wang, M. R. Hashemi, M. Jarrahi, "Plasmonics-Enhanced Photoconductive Terahertz Optoelectronics," *International Conference and Exhibition on Lasers, Optics & Photonics*, San Antonio, TX, October 7-9, 2013
2. M. Jarrahi, "Plasmonic photoconductive emitters and detectors," *Workshop on Terahertz Technologies (in association with European Microwave Conference)*, October 6-11, Nuremberg, Germany, 2013
3. M. Unlu, M. R. Hashemi, C. W. Berry, S. Li, S.-H. Yang, M. Jarrahi, "High-performance terahertz spatial light modulators based on reconfigurable diamagnetic meta-surfaces," *International Congress on Advanced Electromagnetic Materials in Microwaves and Optics*, Bordeaux, France, September 16-21, 2013
4. M. Unlu, M. R. Hashemi, C. W. Berry, S. Li, S.-H. Yang, M. Jarrahi, "Broadband Terahertz Modulation Through Reconfigurable Meta-Surfaces With Diamagnetic Switching Capability," *International Conference on Infrared, Millimeter, and Terahertz Waves,* Mainz, Germany, Sep 1-6, 2013
5. M. Unlu, M. R. Hashemi, C. W. Berry, S. Li, S.-H. Yang, M. Jarrahi, "Reconfigurable diamagnetic meta-molecules for broadband terahertz modulation," *SPIE Optics and Photonics Conference*, San Diego, CA, August 25-29, 2013
6. C. W. Berry, M. R. Hashemi, M. Unlu, M. Jarrahi, "Plasmonics-Enhanced Photoconductive Terahertz Emitters," *International Microwave and Optoelectronic Conference*, Rio de Janeiro, Brazil, August 4-7, 2013 (plenary lecture)
7. M. Jarrahi, "Plasmonics-Enhanced Terahertz Imaging and Sensing Systems," *CMOS Emerging Technologies Research Symposium*, Whistler, Canada, July 17-19, 2013
8. C. W. Berry, M. R. Hashemi, M. Jarrahi, "Plasmonic Photoconductors for High-Efficiency Terahertz Generation*" Optical Society of Americas Sensors topical meeting*, Rio Grande, Puerto Rico, July 14-19, 2013
9. M. Unlu, M. R. Hashemi, C. W. Berry, S. Li, S.-H. Yang, M. Jarrahi, "Terahertz wave manipulation through electromechanically reconfigurable diamagnetic surfaces," *International Symposium on Photoelectronic Detection and Imaging*, Beijing, China, June 25-27, 2013
10. M. Unlu, C. W. Berry, S. Li, S-H. Yang, M. R. Hashemi, M. Jarrahi, "Broadband terahertz modulation using reconfigurable mesh filters," *IEEE Wireless and Microwave Technology Conference*, Orlando, Florida, April 7-9, 2013

11. N. Wang, C. W. Berry, M. R. Hashemi, M. Jarrahi, "Terahertz Detection Sensitivity Enhancement by Use of Plasmonic Photoconductive Detectors," *4th International Conference on Metamaterials, Photonic Crystals and Plasmonics*, Sharjah, UAE, 18-22 March, 2013
12. M. Unlu, C. W. Berry, S. Li, S.-H. Yang, M. R. Hashemi, M. Jarrahi, "A High-performance Terahertz Spatial Light Modulator based on Reconfigurable Mesh Filters," *4th International Conference on Metamaterials, Photonic Crystals and Plasmonics*, Sharjah, UAE, 18-22 March, 2013
13. M. Jarrahi, "Pushing the Limits of Terahertz Optoelectronics," *Northwestern University, Electrical Engineering and Computer Science Dept.*, Chicago, IL, March 2013
14. M. Jarrahi, "Pushing the Limits of Terahertz Optoelectronics," *University of Illinois at Urbana-Champaign, Electrical and Computer Engineering Dept.*, Urbana, IL, February 2013
15. M. Jarrahi, "Pushing the Limits of Terahertz Optoelectronics", *University of Texas Austin Electrical and Computer Engineering Department*, Austin, TX, January 2013
16. M. Jarrahi, "Pushing the Limits of Terahertz Optoelectronics", *University of California San Diego Electrical and Computer Engineering Department*, San Diego, CA, January 2013
17. C. W. Berry, M. Jarrahi, "Enhancing optical-to-terahertz conversion efficiency by using plasmonic photoconductive emitters", *International Conference on Fiber-Optics and Photonics*, Chennai, India, Dec 9-12, 2012
18. M. Jarrahi, "Pushing the Limits of Terahertz Optoelectronics", *Colombia University Department of Electrical Engineering*, New York, NY, November 2012
19. M. Jarrahi, "Pushing the Limits of Terahertz Optoelectronics", *Stanford University Department of Electrical Engineering*, Stanford, CA, October 2012
20. M. Jarrahi, "Pushing the Limits of Terahertz Optoelectronics", *University of Michigan Dearborn Department of Natural Sciences*, Dearborn, MI, October 2012
21. C. W. Berry, M. Unlu, M. R. Hashemi, M. Jarrahi, "Use of Plasmonic Gratings for Enhancing the Quantum Efficiency of Photoconductive Terahertz Sources", *International Conference on Infrared, Millimeter, and Terahertz Waves*, Wollongong, Australia, Sep 23-28, 2012
22. S. Li, M. Unlu, M. Jarrahi, "Reconfigurable Mesh Filters for Terahertz Modulation," *International Conference on Infrared, Millimeter, and Terahertz Waves*, Wollongong, Australia, Sep 23-28, 2012
23. C. W. Berry, M. Jarrahi, "Photoconductive Terahertz Sources based on Plasmonic Gratings," *SPIE Optics and Photonics Conference*, San Diego, CA, August 12-16, 2012
24. M. Jarrahi, "Plasmonic photoconductors for high-performance terahertz optoelectronics," *Naval Research Laboratory*, Washington, DC, July 2012

Patents

1. M. Jarrahi, M. Unlu, M. R. Hashemi, C. W. Berry, and S. Li, "Reconfigurable Device for terahertz and Infrared Filtering and Modulation," Provisional Patent, Patent Application No. 61/862,730, filed 08/06/2013
2. M. Jarrahi, C. W. Berry, N. Wang, S.-H. Yang, and M. R. Hashemi, "Photoconductive Device with Plasmonic Electrodes," U.S. Patent Pending, Patent Application No. 61/589,486, filed 01/23/13

Detailed Research Summary

There has been a great deal of effort for extending the high frequency limit of radio frequency (RF) sources and the low frequency limit of optical emitters, as well as combining RF and optical techniques to realize high performance terahertz radiation sources [1]. On the RF side, impact ionization avalanche transit-time (IMPATT) diodes, Gunn diodes, resonance tunneling diodes, and chains of frequency multipliers [2-4] have demonstrated very promising compact terahertz sources. However, this category of sources has limited bandwidth, poor power efficiency and low output power levels. On the other hand, electron beam devices such as backward wave oscillators [5] and travelling wave tube regenerative amplifiers [6] can produce reasonable power levels, but their operation has not been demonstrated above 1.5 THz [7]. Additionally, the bulky nature of backward wave oscillators and their requirement for high magnetic fields and vacuum limits their use in various operational settings. On the optical side, quantum-cascade lasers have been under an extensive investigation during the past decade [8], and significant progress has been made, pushing their operation frequency to 1 THz [9] and their operation temperature to ~200 K for a 3.22 THz lasing frequency [10]. Moreover, optical down-conversion to terahertz frequencies based on nonlinear optical effects has been extensively used for generating high power terahertz waves. Optical down-conversion to terahertz frequencies in bulk nonlinear materials is inherently inefficient due to the optical/terahertz phase mismatch limiting the efficient field interaction length. Guided wave nonlinear media [11], quasi-phase-matching in periodically poled media [12, 13], and the use of tilted wave-front pump waves [14] have been employed to offer a better phase-matching control resulting in longer field interaction lengths. However, because of material absorption, the active length in which terahertz waves are generated is limited to centimeter ranges. Because of the field interaction length limitations, the use of high-power optical pumps has been necessary to provide ultra-high peak powers for generating meaningful terahertz powers using nonlinear optical techniques. An additional inherent limitation of nonlinear optical techniques for generating terahertz waves stems from the conservation of energy in a nonlinear optical process, namely the Manley–Rowe rule [15]. In other words, the maximum power efficiency of terahertz sources based on nonlinear optical phenomena is limited to the ratio between the energies of the generated terahertz photon and the pump optical photon.

On the other hand, optical-to-terahertz conversion through photoconduction has demonstrated very promising performance [16-22] and has been the most commonly used technique for generating terahertz waves since the pioneering demonstration of picosecond photoconducting Hertzian dipoles in 1984 [23]. One of the main advantages of photoconductive terahertz emitters compared to the terahertz emitters based on nonlinear optical phenomena is that their power efficiency is not restricted by the Manley-Rowe limit. This is because one electron-hole pair can be generated for each absorbing photon, which can emit several terahertz photons upon reaching the terahertz antenna in a photoconductive emitter. In other words, the optical-to-terahertz conversion efficiency of photoconductive terahertz emitters can reach 100%, orders of magnitude higher than the Manley-Rowe limit. Although the optical-to-terahertz conversion efficiency of photoconductive emitters can theoretically reach 100%, the low quantum efficiency of conventional ultrafast photoconductors imposes substantially lower conversion efficiencies. The low quantum efficiency of conventional ultrafast photoconductors also limits the responsivity and detection sensitivity of photoconductive terahertz detectors, which are

extensively used in combination with photoconductive terahertz emitters in time-domain and frequency-domain terahertz spectroscopy and imaging systems [24, 25].

To address the low quantum efficiency limitation of conventional ultrafast photoconductors, we propose a novel photoconductor concept which incorporates a plasmonic contact electrode configuration to offer high quantum efficiency and ultrafast operation simultaneously. By using nanoscale plasmonic contact electrodes we significantly reduce the average photocarrier transport path to the photoconductor contact electrodes compared to conventional photoconductors. By incorporating plasmonic contact electrodes, we demonstrate enhancing the optical-to-terahertz power conversion efficiency of a conventional photoconductive terahertz emitter by a factor of 50. By use of the same quantum efficiency enhancement mechanism, we also demonstrate increasing the responsivity and detection sensitivity of a conventional photoconductive terahertz detector by a factor of 30. Consequently, our presented plasmonic photoconductive terahertz optoelectronics concept offers more than three orders of magnitude enhancement in the signal-to-noise ratio of time-domain and frequency-domain terahertz spectroscopy and imaging systems.

Plasmonic photoconductors for terahertz generation:

To demonstrate the potential of plasmonic electrodes for enhancing the quantum efficiency of conventional ultrafast photoconductors, we chose to fabricate a proof-of-concept photoconductive emitter and characterize its performance enhancement due to integrating plasmonic gratings as a part of photoconductor contact electrodes. Figure 1a shows the schematic diagram and operation concept of the implemented photoconductive emitter in the absence of plasmonic gratings (conventional scheme). The photoconductive emitter consists of an ultrafast photoconductor with 20 μm gap between the anode and cathode contacts, connected to a 60 μm long bowtie antenna with maximum and minimum widths of 100 μm and 30 μm, respectively. Low-temperature-grown GaAs (LT-GaAs) is used for the photo-absorbing substrate to achieve an ultrafast photoconductor response. When a sub-picosecond optical pump at ~800 nm wavelength range is incident on the ultrafast photoconductor, electron-hole pairs are generated which induce a photocurrent under an applied bias electric field. The induced photocurrent, which follows the envelope of the optical pump, drives the terahertz antenna connected to the photoconductor contact electrodes, generating terahertz radiation. The bandwidth of the terahertz radiation is determined by the optical pulse, antenna characteristics, and the semiconductor carrier lifetime. Since electrons have significantly higher mobilities compared to holes and due to the nonlinear increase in the bias electric field near the contact electrodes, the optical pump is focused onto the photoconductive gap asymmetrically close to the anode contact to maximize terahertz radiation [19, 26, 27]. Similar to any conventional photoconductive terahertz emitter, the quantum efficiency of the described photoconductive emitter is limited by the relatively long carrier transport path lengths to the photoconductor contact electrodes. This is because of the relatively low drift velocity of the carriers in the semiconductor [28], and even if the pump is focused down to a diffraction-limited spot size next to the anode contact, a very small portion of the photo-generated electrons can reach the anode in a sub-picosecond timescale. The remaining majority of the photo-generated carriers recombine in the substrate before reaching the contact electrodes and without efficient contribution to terahertz generation. Figure 1b shows the schematic diagram of the implemented photoconductive emitter that incorporates 20 μm long plasmonic contact electrode gratings designed for enhancing the quantum efficiency of the conventional photoconductive emitter (Fig. 1a).

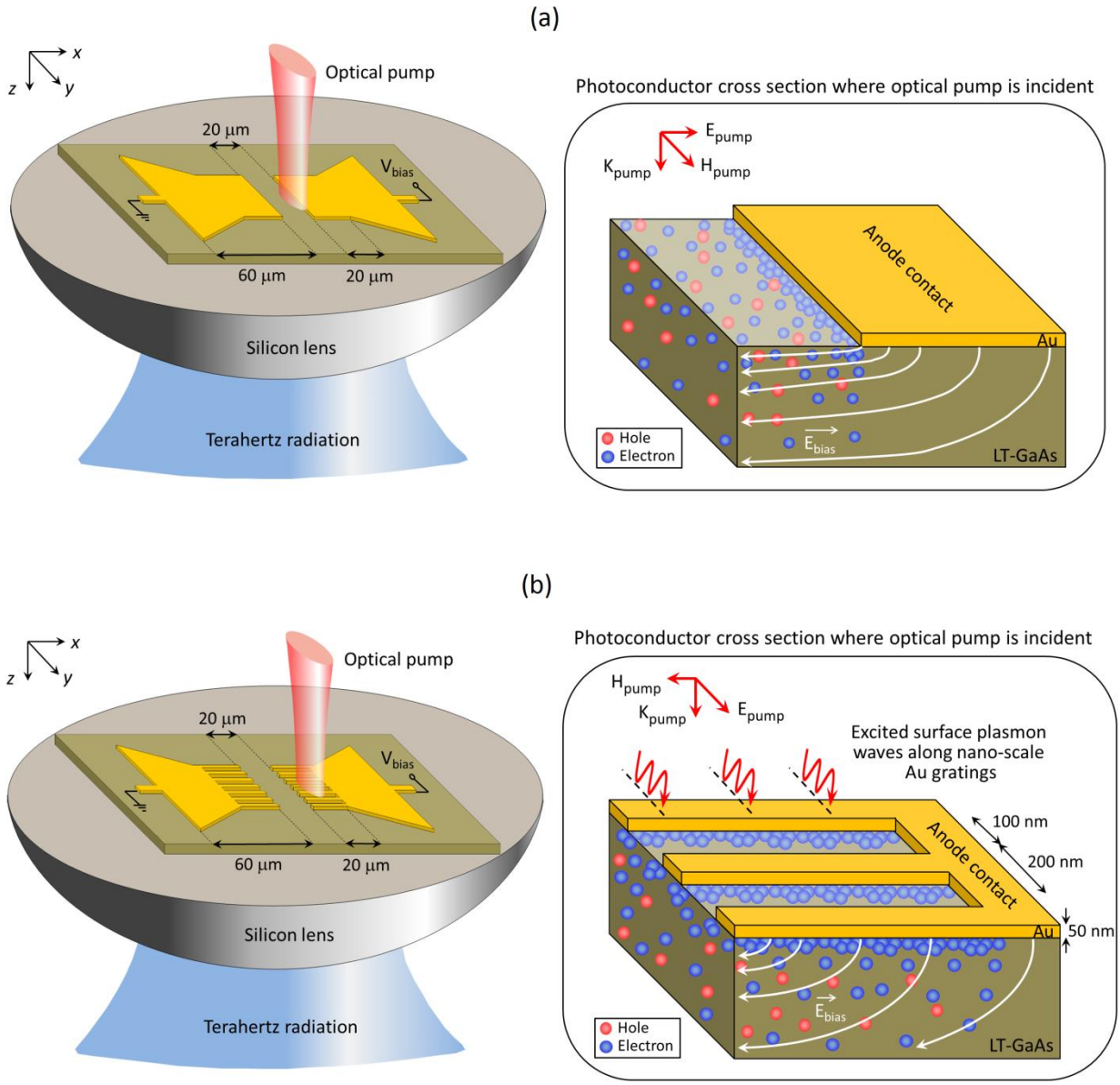

Figure 1. Schematic diagram and operation concept of photoconductive terahertz emitters/detectors. Left panels: An ultrafast photoconductor connected to a bowtie terahertz antenna on a LT-GaAs substrate. The device is mounted on a silicon lens to collect the terahertz radiation from back side of the substrate. An optical pump is incident upon the ultrafast photoconductor, generating electron-hole pairs inside the photo-absorbing substrate. Right panels: In order to operate as a terahertz emitter, a bias voltage is applied to the ultrafast photoconductor, which induces an electric field inside the substrate and drifts the photo-generated electrons and holes toward the anode and cathode contact electrodes, respectively. Upon reaching the contact electrodes, the photocurrent drives the terahertz antenna to produce radiation. In order to operate as a terahertz detector, a zero bias voltage is applied to the ultrafast photoconductor, and the bowtie terahertz antenna connected to the contact electrodes of the ultrafast photoconductor receives the incident terahertz radiation, inducing a terahertz electric field across the photoconductor contact electrodes. The photo-generated electrons and holes are drifted to the photoconductor contact electrodes under the induced terahertz field, generating an output photocurrent which is proportional to the magnitude of the incident terahertz field. (a) A conventional photoconductive terahertz emitter/detector. (b) A plasmonic photoconductive terahertz emitter/detector incorporating plasmonic contact electrodes to reduce photocarrier transport times to the contact electrodes and, thus, increase the photoconductor quantum efficiency.

The grating geometry is designed to excite surface plasmon waves along the periodic metallic grating interface upon incidence of a TM-polarized optical pump [29, 30]. Excitation of surface plasmon waves allows transmission of a large portion of the optical pump through the nanoscale grating into the photo-absorbing substrate. It also significantly enhances the intensity of the optical pump in very close proximity to the contact electrodes. As a result, the average photo-generated electron transport path length to the anode electrode is significantly reduced in comparison with the conventional photoconductive emitter (Fig. 1a). Therefore, the design strategy for the optimum plasmonic grating is maximizing the optical pump transmission into the photo-absorbing substrate while minimizing the electrode spacing to minimize the average photo-generated electron transport path length to the anode electrode.

Incorporating a dielectric passivation layer could reduce the Fresnel reflection at the semiconductor interface and, thus, could enhance optical pump transmission into the photo-absorbing semiconductor for both conventional and plasmonic photoconductors [31, 32]. While optical pump transmission into the photo-absorbing semiconductor of the conventional photoconductor is the result of direct interaction between the pump wave and the semiconductor interface, optical pump transmission into the photo-absorbing semiconductor of the plasmonic photoconductor is through coupling to the excited surface plasmon waves. Because of the differences between the nature of the interacting waves with the semiconductor interface, the optimum passivation layer thicknesses, that maximize optical pump transmission into the photo-absorbing semiconductor, are not the same for the conventional and plasmonic photoconductors. While the passivation layer thickness can be independently optimized for each photoconductor, we have chosen the passivation layer thicknesses to obtain the same optical pump transmission into the photo-absorbing semiconductor for the conventional and plasmonic photoconductors. We used a 150 nm SiO_2 passivation layer for the plasmonic photoconductor with Au contact gratings having a 200 nm pitch, 100 nm spacing, and 50 nm height and no passivation layer for the conventional photoconductor. Both designs offer ~70% optical pump transmission into the photo-absorbing semiconductor at a 800 nm optical pump wavelength.

Using a multi-physics finite-element solver (COMSOL), we have analyzed the interaction of an incident optical pump (λ = 800 nm) with the conventional and plasmonic photoconductors. For maximum optical power enhancement near the photoconductor contact electrodes, we have aligned the optical pump field along the *x*-axis and *y*-axis for the conventional and plasmonic photoconductors, respectively [33]. The optical absorption in the semiconductor substrate for the conventional (*xz* cross section) and plasmonic (*yz* cross section) photoconductors is shown in Fig. 2a. For the conventional photoconductor, the metal contact shadows the substrate from the incident optical pump, allowing for almost all of the optical absorption and photocarrier generation in the gap between the anode and cathode. In the case of the plasmonic photoconductor, the optical pump is transmitted through the nanoscale metallic grating through the coupling with surface plasmons. Since the excited surface plasmon waves exist at the dielectric-metal interface, the highest optical absorption and photocarrier generation occurs in direct proximity to the metal contacts. To better illustrate the impact of the excited surface plasmon waves, we have compared the optical absorption profile in the semiconductor substrate of the photoconductor with nanoscale Au gratings with a similar photoconductor with nanoscale Ni gratings. Figure 2a shows that under the same optical transmission through nanoscale Au and Ni gratings, the highest optical absorption and photocarrier generation regions are more tightly confined at the metal-semiconductor interface of Au gratings in comparison with Ni gratings.

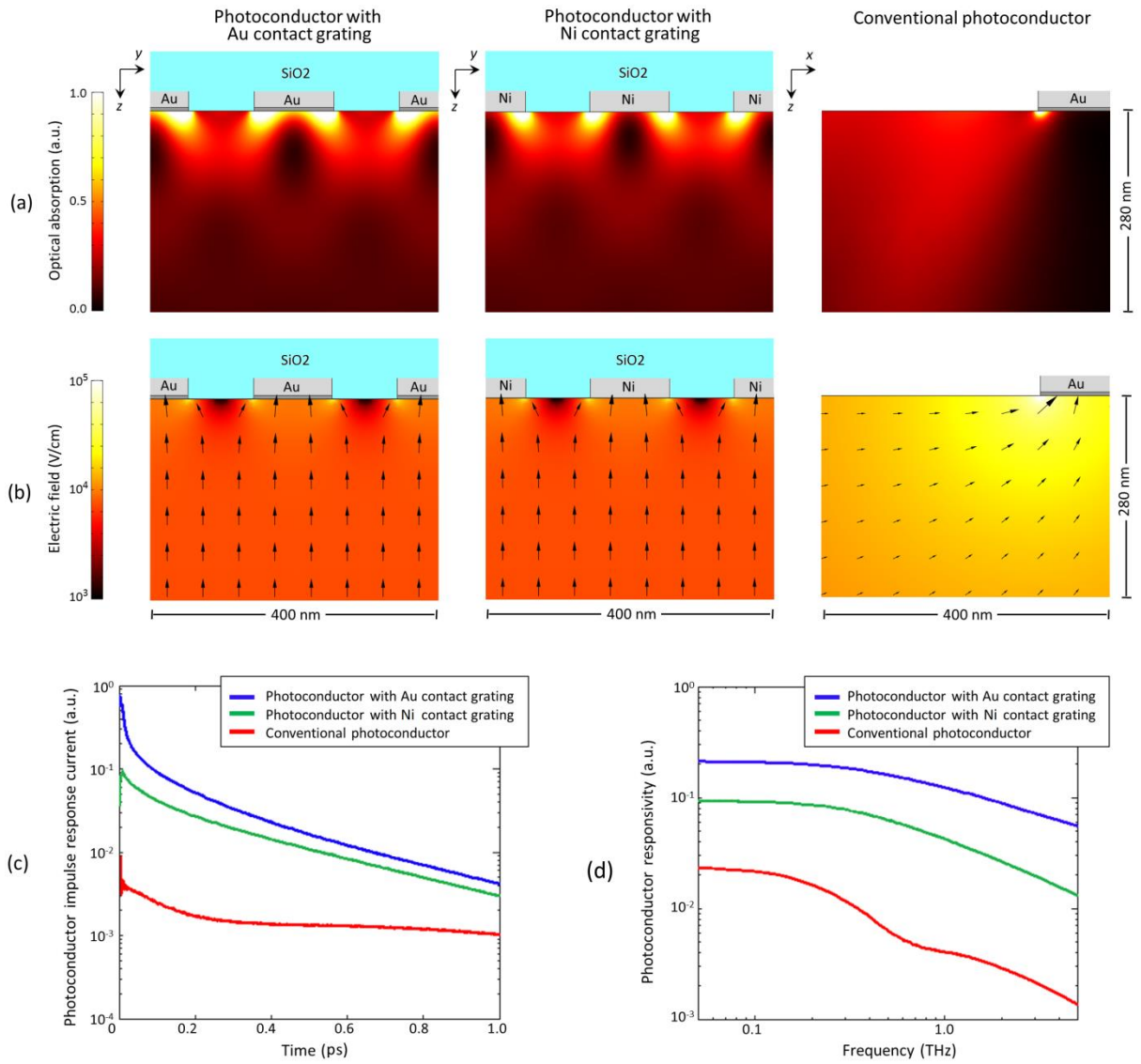

Figure 2. Finite element analysis of optical and electrical interactions in the photoconductor cross sections. Right panel: cross section of the conventional photoconductor (*xz*-plane), Left and center panels: cross sections of the designed plasmonic photoconductor and a similar photoconductor with Ni contact gratings (*yz*-plane). A 5 nm thick Ti adhesion layer is deposited under Au electrodes. A 150 nm thick SiO_2 passivation layer is used for the photoconductors with nanoscale contact gratings and no passivation layer is used for the conventional photoconductor. This allows equal optical transmission to the photo-absorbing substrate (~70%) at 800 nm optical pump wavelength for all three photoconductors. (a) Color plot of optical absorption in GaAs substrate due to an incident optical plane wave (λ = 800 nm). The optical pump field is aligned along the *x*-axis and *y*-axis for the conventional photoconductor and photoconductors with nanoscale contact gratings, respectively. (b) Bias electric field in GaAs substrate. Color map corresponds to electric field magnitude, and arrows denote field direction. Applied voltages in all three cases are set to not exceed electric fields of $1x10^5$ V/cm. The cross sections of the photoconductors with nanoscale contact gratings are shown for a distance 1 µm inset from the tip of the gratings. (c) Estimated impulse response of the analyzed photoconductors with the illustrated cross sections by combining the photogenerated carrier density in the GaAs substrate, the electric field data, and the classical drift-diffusion model in a multi-physics finite-element solver (COMSOL) and calculating the induced photocurrent in response to an optical pump impulse. A carrier lifetime of 400 fs is assumed for the LT-GaAs substrate. (d) Estimated responsivity spectra of the analyzed photoconductors calculated by convolving the impulse response of each photoconductor with the sinusoidal power envelope of two frequency-offset optical beams as a function of optical beat frequency.

This is explained by the weak plasmonic properties of Ni at 800 nm optical wavelength. Using COMSOL, we have analyzed the bias electric field that drifts photo-generated carriers toward the photoconductor contact electrodes (Fig. 2b). For this analysis, the bias voltage is set such that the maximum induced electric field remains below 10^5 V/cm ($1/4^{th}$ of the GaAs breakdown electric field). In the case of the conventional photoconductor, we see elliptical electric field lines beneath the contact electrode with the highest electric field near the corner of the electrodes. In the case of the plasmonic photoconductor, the electric field lines are illustrated at the *yz* cross section 1 μm away from the grating tip. Although relatively lower electric fields are induced in the case of the plasmonic photoconductor compared with the conventional photoconductor, the electric field levels are maintained above 10^3 V/cm (at which electron drift velocity reaches saturation) within 100 nm from photoconductor anode contact electrodes [28]. Moreover, simulation results show that the electric field levels are maintained above 10^3 V/cm within 100 nm from contact electrodes along a 20 μm long plasmonic contact electrode, indicating that the superior performance of the plasmonic photoconductive emitter can be maintained when using relatively large device active areas.

The impulse response of the analyzed photoconductors to an optical pump impulse is estimated by calculating the collected transient photocurrent at the contact electrodes using COMSOL. For this purpose, the photo-generated carrier density is derived from the calculated optical intensity in the GaAs substrate and combined with the electric field data in the classical drift-diffusion model to calculate the induced photocurrent. The results are presented in Fig. 2c, indicating the superior performance of the designed plasmonic photoconductor offering high-quantum efficiency and ultrafast operation simultaneously. The advantage of the designed plasmonic photoconductor is more apparent when comparing its responsivity with the conventional photoconductor and the photoconductor with Ni contact gratings. The responsivity spectra are calculated by convolving the impulse response of the analyzed photoconductors with the sinusoidal power envelope of two frequency-offset optical beams as a function of optical beat frequency. The responsivity spectra (Fig. 2d) show that the designed plasmonic photoconductor offers more than one order of magnitude higher responsivity levels compared with the conventional photoconductor. Moreover, comparing the responsivity spectra of the designed plasmonic photoconductor with the photoconductor with Ni contact gratings indicates the impact of plasmonic optical enhancement in direct proximity to the metal contacts, which offers higher photoconductor responsivity levels especially at higher terahertz frequencies. It should be mentioned that at a given pump power, the radiated power from a photoconductive emitter has a quadratic dependence on the photoconductor responsivity. Therefore, compared with the conventional photoconductor, the designed plasmonic photoconductor is expected to offer two orders of magnitude higher optical-to-terahertz conversion efficiencies.

Figure 3 shows the microscope and SEM images of the fabricated photoconductive emitter prototypes. Fabrication began with the patterning of the nanoscale gratings using electron beam lithography, followed by Ti/Au (5/45 nm) deposition and liftoff to form ohmic photoconductor contacts [34]. A 150 nm thick SiO_2 passivation layer was then deposited using PECVD. Using a plasma etcher, contact vias were then opened, and the antenna and metal contacts were formed using optical lithography followed by Ti/Au (5/400 nm) deposition and liftoff. The fabricated devices were then mounted on a silicon lens and placed on an optical rotation mount, for optical pump polarization adjustments.

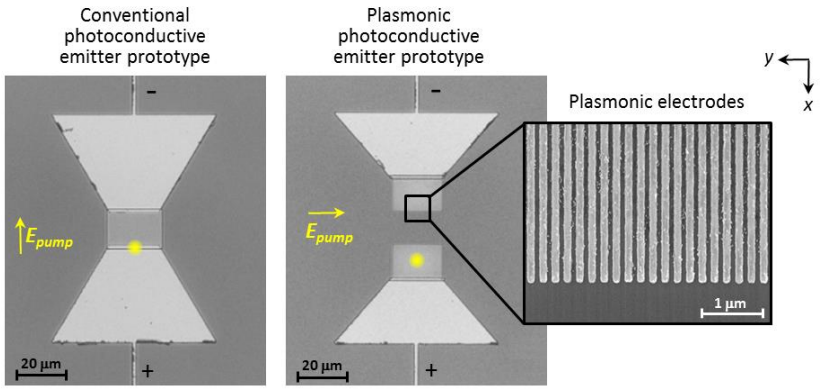

Figure 3. Fabricated device images. Left: microscope image of the conventional terahertz emitter with a 20 µm scale bar. Middle: microscope image of the plasmonic terahertz emitter with a 20 µm scale bar. Right: SEM image of the plasmonic electrodes of the plasmonic terahertz emitter with a 1 µm scale bar. The circular pump spot is positioned on the antenna axis at the anode contact edge and along the anode plasmonic contact electrodes for the conventional and plasmonic photoconductive emitters, respectively.

To evaluate the performance of the photoconductive terahertz emitter with and without the plasmonic gratings, the output power of each device was measured in response to an incident optical pump from a Ti:sapphire mode-locked laser with a central wavelength of 800 nm, 76 MHz repetition rate, and 200 fs pulse width, using a pyroelectric detector (Spectrum Detector, Inc. SPI-A-65 THz). In order to maximize terahertz radiation, the incident optical pump was tightly focused onto each device and the circular pump spot was positioned on the antenna axis at the anode contact edge and along the anode plasmonic contact electrodes for the conventional and plasmonic photoconductive emitters, respectively. Moreover, the device rotation mount was adjusted to align the electric field of the optical pump along the *x*-axis and *y*-axis for the conventional and plasmonic prototypes, respectively. The measured output power of the two prototype devices at a 40 V bias voltage and under various optical pump powers is presented in Fig. 4a. A radiation power enhancement of more than 33 was observed from the plasmonic photoconductive emitter in the 0 - 25 mW optical pump power range. This significant radiation power enhancement is due to the higher photocurrent levels generated when employing plasmonic contact electrodes (Fig. 4a inset), which have a quadratic relation with the radiation power. Another important advantage of the plasmonic emitter compared with the conventional emitter is that the close photocarrier proximity to contact electrodes is satisfied over significantly larger device active areas and, thus, the operation of the plasmonic emitter is more immune from optical pump misalignment. While the radiated power from the conventional emitter drops dramatically as a result of optical pump displacement along the *x*-axis, the plasmonic emitter does not show any noticeable drop in power as a result of the optical pump displacement along the 20 µm long anode plasmonic contact electrodes. To further examine the impact of photocurrent increase on the radiation power enhancement, we compared the radiation power of the two photoconductor devices as a function of their photocurrent under various bias voltages (10 - 40 V) and optical pump powers (5 - 25 mW). The results are presented in Fig. 4b in a logarithmic scale. The data points are all curve-fitted to the same line with a slope of 2, confirming the quadratic dependence of the radiation power on the induced photocurrent and the fact that all other operational conditions (including antenna specifications) are the same for the conventional and plasmonic photoconductive emitter prototypes.

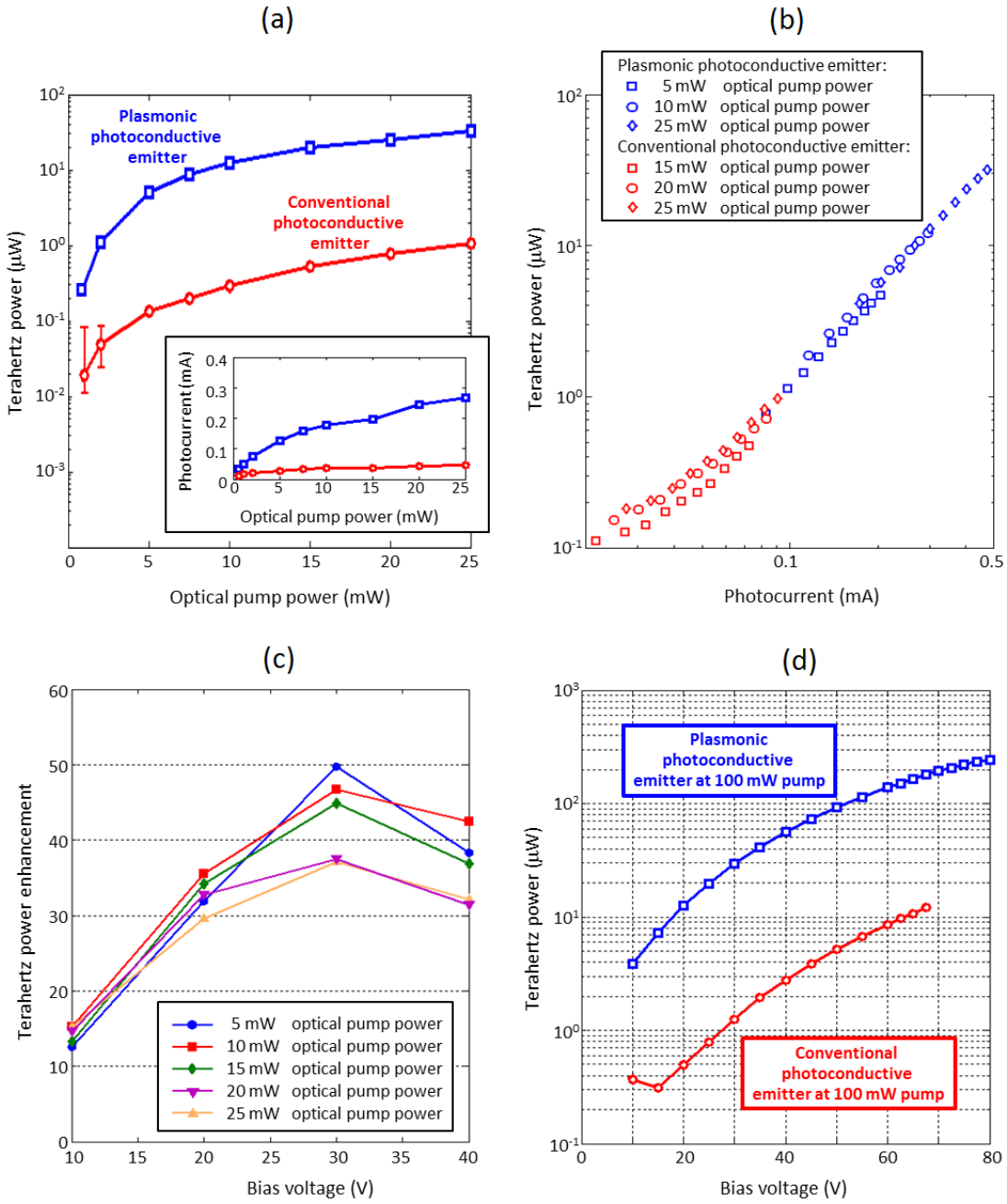

Figure 4. Comparison of the conventional and plasmonic photoconductive terahertz emitter prototypes. (a) Measured terahertz radiation from the plasmonic (blue) and conventional (red) terahertz emitters, electrically biased at 40 V, under various optical pump powers. The inset curve shows the corresponding photocurrent of the plasmonic (blue) and conventional (red) emitters. The error bars are associated with the noise of the Pyroelectric terahertz detector listed in the detector datasheet. (b) Measured terahertz radiation versus collected photocurrent for the plasmonic and conventional terahertz emitters. The data represented in the plot includes various bias voltages (10 – 40 V) under various optical pump powers (5 – 25 mW). (c) Relative terahertz power enhancement defined as the ratio of the terahertz power emitted by the plasmonic terahertz emitter to the conventional terahertz emitter. Maximum enhancement is obtained at low optical powers before the onset of the carrier screening effect. (d) Maximum terahertz power measured from the plasmonic (blue) and conventional (red) terahertz emitters under a 100 mW optical pump. The bias voltage of each device is increased until the point of device failure.

By dividing the output power of the plasmonic photoconductive emitter by the output power of the conventional photoconductive emitter, we define a power enhancement factor. Figure 4c shows the power enhancement factor under various optical pump powers and bias voltages. At low optical pump power levels and a bias voltage of 30 V, output power enhancement factors up to 50 are observed, the same order of magnitude predicted by the theoretical predictions. The enhancement factor decreases slightly at higher optical pump power levels. This can be explained by the carrier screening effect, which affects the plasmonic photoconductor more than the conventional photoconductor, since a larger number of electron-hole pairs are separated in the plasmonic photoconductor. Additionally, the enhancement factor decreases slightly at higher bias voltages. This is because stronger forces separate electron-hole pairs at higher bias voltages. Since a larger number of electron-hole pairs contribute to the induced photocurrent in the plasmonic photoconductor compared to the conventional photoconductor, the relative increase in the induced electric field opposing the bias electric field as a function the bias electric field is higher in the plasmonic photoconductor. It should be also mentioned that the lower enhancement factors at bias voltages below 30 V, are associated with insufficient bias electric field levels along the plasmonic contact electrodes of the plasmonic photoconductor. Finally, the maximum radiated power from each photoconductive terahertz emitter was measured at an optical pump power of 100 mW, up to the point that the devices burned, as shown in Fig. 4d. At maximum, the plasmonic photoconductive emitter produced an average power of 250 µW, compared to the 12 µW of the conventional photoconductive emitter.

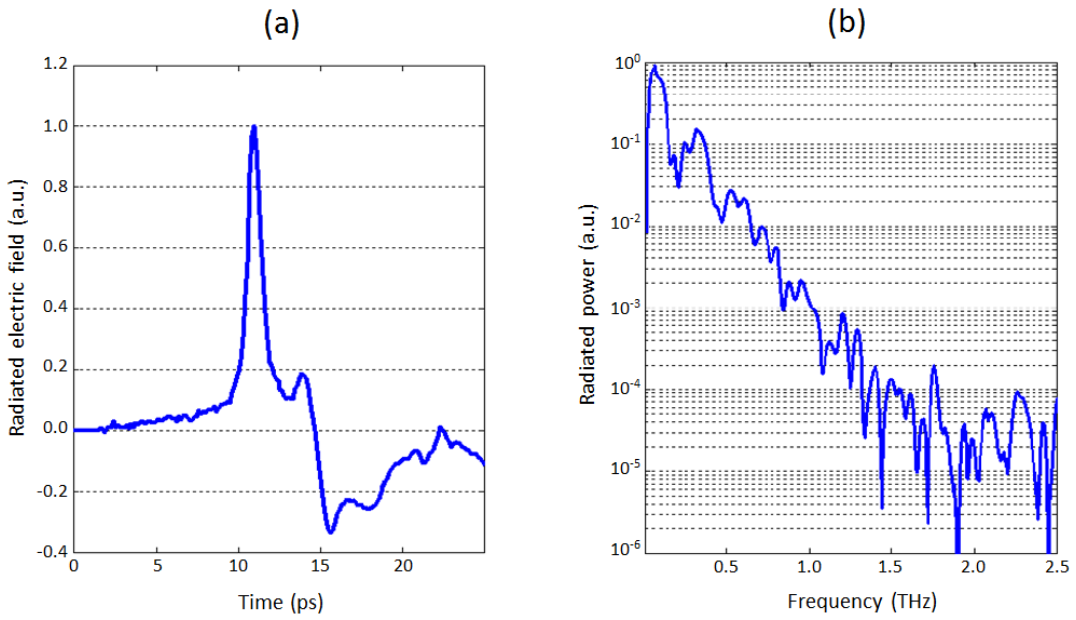

Figure 5. Radiation characteristics of the plasmonic photoconductive emitter. (a) Radiated electric field in the time domain in response to a 200 fs optical pulse from the Ti:sapphire mode-locked laser with 800 nm central wavelength and 76 MHz repetition rate. (b) Radiated power in the frequency domain, obtained by calculating the Fourier transform of the measured time-domain terahertz electric field intensity.

The time-domain (Fig. 5a) and frequency domain (Fig. 5b) radiation of the plasmonic photoconductive emitter in response to a 200 fs optical pump pulse from the Ti:sapphire mode-locked laser was measured using a terahertz time-domain spectroscopy setup with electro-optic

detection [35]. The detailed description of the terahertz time-domain spectroscopy setup used for characterizing the photoconductive terahertz emitter prototypes can be found in the methods section. The radiated power from the plasmonic terahertz source was detected up to 1.5 THz, after which the noise of the system limited the detection. The observed radiation peaks around 0.35 THz and 0.55 THz are associated with the resonance peaks of the employed bowtie antenna, and the radiation peak around 0.1 THz is associated with the resonance peak of the dipole antenna formed by the bowtie antenna bias lines.

Plasmonic photoconductors for terahertz detection

Following the demonstration of terahertz radiation enhancement by use of plasmonic contact electrodes, we evaluated the potential of plasmonic electrodes for enhancing the detection sensitivity of conventional photoconductive terahertz detectors by characterizing the performance of the fabricated proof-of-concept photoconductors in terahertz detection mode. Figure 1a shows the schematic diagram and operation concept of the proof-of-concept photoconductive terahertz detector in the absence of the plasmonic gratings (conventional scheme). Photocarriers are generated inside the active area of the ultrafast photoconductor upon incidence of an optical pump. The terahertz antenna connected to the contact electrodes of the ultrafast photoconductor receives the incident terahertz radiation and induces a terahertz electric field across the photoconductor contact electrodes. The induced terahertz field drifts the photocarriers toward the photoconductor contact electrodes, generating an output photocurrent which is proportional to the magnitude of the incident terahertz field. The responsivity of the conventional photoconductive terahertz detector is directly affected by the number of the photocarriers that reach the photoconductor contact electrodes within a sub-picosecond time-scale. Similar to the conventional photoconductive terahertz emitter, the quantum efficiency of the described conventional photoconductive terahertz detector is limited by the relatively long carrier transport path lengths to the photoconductor contact electrodes. Therefore, even if the optical pump is focused down to a diffraction-limited spot size next to the photoconductor contact electrodes, a small portion of the photocarriers can reach the photoconductor contact electrodes within a sub-picosecond time-scale, limiting the responsivity of the conventional photoconductive terahertz detector. Figure 1b shows the schematic diagram of the proof-of-concept photoconductive terahertz detector that incorporates plasmonic contact electrode gratings (plasmonic scheme). Similar to the plasmonic photoconductive terahertz emitter, the use of plasmonic contact electrodes reduces the average transport path of the photocarriers to the photoconductor contact electrodes considerably. This results in a significant increase in the number of the drifted photocarriers to the photoconductor contact electrodes and, thus the output photocurrent of the plasmonic photoconductive detector in comparison with the conventional photoconductive detector under the same incident terahertz wave intensities.

To evaluate the performance of the photoconductive terahertz detector with and without the plasmonic gratings, the output photocurrent of each device in response to the radiation from a commercially available photoconductive terahertz emitter (iPCA-21-05-1000-800-h) was measured in a time-domain terahertz spectroscopy setup. The detailed description of the terahertz time-domain spectroscopy setup used for characterizing the photoconductive terahertz detector prototypes can be found in the methods section. A Ti:sapphire mode-locked laser with a central wavelength of 800 nm, 76 MHz repetition rate, and 200 fs pulse width was used for pumping the commercially available photoconductive terahertz emitter and the photoconductive terahertz detector prototypes in the terahertz time-domain spectroscopy setup. The optical pump

polarization was set along the *x*-axis and *y*-axis for the conventional and plasmonic photoconductive detectors, respectively, and both photoconductive detector prototypes were characterized under the same optical pump and terahertz radiation intensities. To achieve the highest output photocurrent levels from the photoconductive detector prototypes, the optical pump was tightly focused onto each device and the circular pump spot was asymmetrically positioned onto the photoconductive gap of each device. To have a fair comparison between the performance of the conventional and plasmonic photoconductive terahertz detectors, each measurement was repeated for various optical pump spot positions along the photoconductive gap until the highest output photocurrent level is achieved for each detector prototype (Fig. 6).

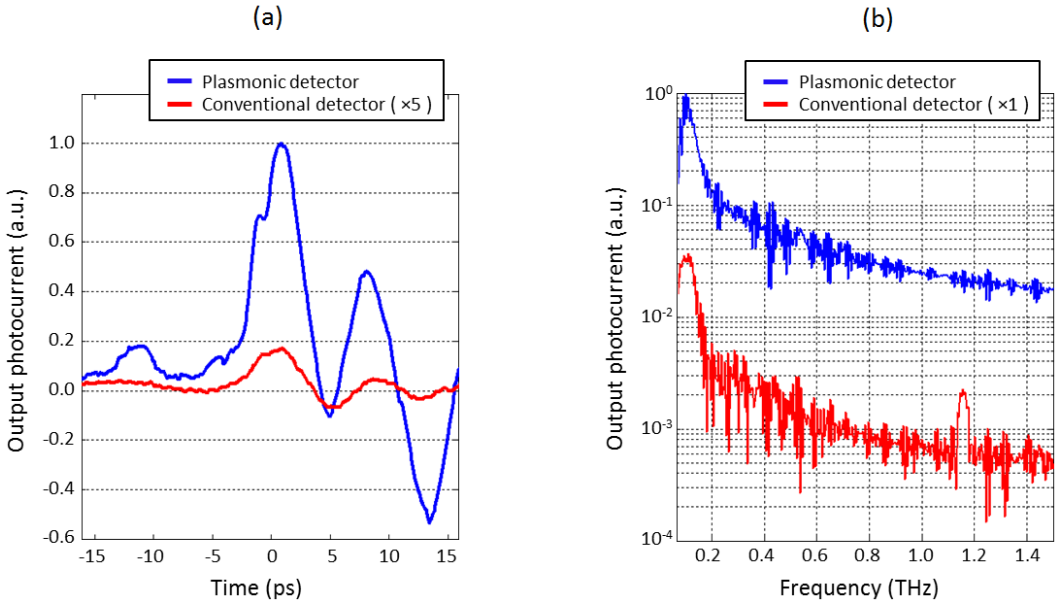

Figure 6. Comparison of the conventional and plasmonic photoconductive terahertz detector prototypes. (a) Time-domain output photocurrent of the conventional photoconductive terahertz detector ×5 (red) and plasmonic photoconductive terahertz detector ×1 (blue), measured in a time-domain terahertz spectroscopy setup under an optical pump power of 50 mW. While the output photocurrent of both photoconductive detectors follow the envelope of the received electric field from the photoconductive terahertz emitter used in the terahertz spectroscopy setup, 30 times higher responsivity levels are offered by the plasmonic photoconductive terahertz detector. (b) Frequency-domain output photocurrent of the conventional (red) and plasmonic (blue) photoconductive terahertz detectors, obtained by calculating the Fourier transform of the measured time-domain output photocurrents. The calculated frequency components of the measured output photocurrents indicate that the 30 fold responsivity enhancement offered by the plasmonic photoconductive terahertz detector is maintained over a 0.1-1.5 THz frequency band.

The measured time-domain output photocurrent of the conventional and plasmonic photoconductive terahertz detectors is shown in Fig. 6a. While the output photocurrent of both photoconductive detectors follow the envelope of the received electric field from the photoconductive terahertz emitter used in the terahertz spectroscopy setup, 30 times higher output photocurrent levels are offered by the plasmonic photoconductive terahertz detector. Additionally, the calculated frequency components of the measured time-domain output photocurrents (Fig. 6b) indicate that the 30 fold output photocurrent enhancement offered by the plasmonic photoconductive terahertz detector is maintained over a 0.1-1.5 THz frequency band.

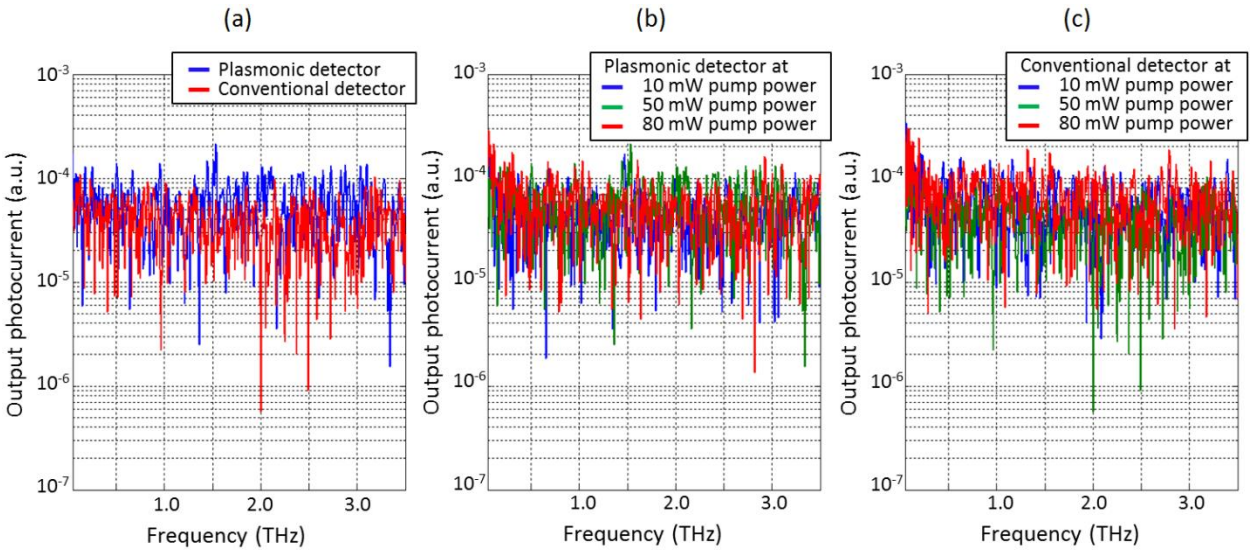

Figure 7. Noise analysis of the plasmonic and conventional photoconductive detector prototypes. (a) Comparison between the output noise current of the conventional and plasmonic photoconductive detector prototypes at 50 mW optical pump power, indicating similar output noise current spectra for the conventional and plasmonic photoconductive detector prototypes. The output noise level of the photoconductive detectors is estimated by measuring the time-domain output photocurrent of each photoconductive detector while blocking the incident terahertz radiation, and calculating the frequency components of the measured time-domain output photocurrents, subsequently. The same output noise level for the conventional and plasmonic photoconductive detector prototypes is due to the fact that the dominant noise source in both photoconductive detector prototypes is the Johnson–Nyquist noise rather than the photoconductor Shot noise. The output noise level of the plasmonic photoconductive detector and (b) the conventional photoconductive detector (c) show no dependence on the optical pump power level over the 10 – 80 mW pump power range, validating the dominance of the Johnson–Nyquist noise (rather than Shot noise) in the device operation regime.

The output noise level of the conventional and plasmonic photoconductive detector prototypes is estimated by measuring the time-domain output photocurrent of each photoconductive detector while blocking the incident terahertz radiation, and subsequently calculating the frequency components of the measured time-domain output photocurrents. The results indicate similar output noise current spectra for the conventional and plasmonic photoconductive detector prototypes (Fig. 7a). This is due to the fact that the dominant noise source in both photoconductive detectors is the Johnson–Nyquist noise rather than the photoconductor Shot noise (Fig. 7b and 7c). Therefore, the 30 fold responsivity enhancement offered by the plasmonic photoconductive detector enables achieving 30 times higher detection sensitivities over the 0.1-1.5 THz frequency band.

Discussion

The ability to excite surface plasmon waves has enabled many unique opportunities for routing and manipulating electromagnetic waves [36]. It has enabled strong light concentration in the near-field, paving the way for higher resolution imaging and spectroscopy [37, 38], deep electromagnetic focusing and beam shaping [39, 40], higher efficiency photovoltaics [41, 42], photodetectors [43, 44], modulators [45, 46], and photoconductors [22]. On the basis of this capability, we have proposed and experimentally demonstrated 50 times radiation power enhancement and 30 times detection sensitivity enhancement by incorporating plasmonic contact

electrodes in a photoconductive terahertz emitter and detector, respectively. Subsequently, the presented plasmonic photoconductive terahertz optoelectronics concept enhances the signal-to-noise ratio of conventional time-domain and frequency-domain terahertz spectroscopy and imaging systems by more than three orders of magnitude. Plasmonic electrodes are designed to significantly reduce the average carrier transport distance to photoconductor contact electrodes over relatively large device active areas and without a considerable increase in the capacitive loading to the terahertz radiating antenna. This enables boosting the maximum terahertz radiation power and detection sensitivity [47-52] by mitigating the carrier screening effect [53], semiconductor bleaching [54], and thermal breakdown [55] at high optical pump powers.

It should be noted that the focus of this study has been the demonstration of the impact of plasmonic electrodes in enhancing the quantum efficiency of ultrafast photoconductors and, thus, the radiation power and detection sensitivity of photoconductive terahertz emitters and detectors, respectively. Hence, the choice of the photoconductive emitter/detector architecture, terahertz radiating/receiving antenna, and bias feed in our study has been arbitrary, and the enhancement concept can be similarly applied to enhance the performance of photoconductive terahertz emitters/detectors with a variety of terahertz antennas with and without interdigitated contact electrodes as well as large-area photoconductive terahertz emitters/detectors in both pulsed and continuous-wave operation. In this regard, the output power and detection sensitivity of our prototype devices can be further enhanced through use of resonance cavities [26, 29] and antennas with higher radiation resistance and bandwidth [56, 57]. Moreover, the use of high aspect ratio plasmonic contact electrodes embedded inside the photo-absorbing semiconductor [58, 59] allows a larger number of carriers generated in close proximity with photoconductor contact electrodes and, thus, enables further terahertz radiation power and detection sensitivity enhancement. In this regard, extending the plasmonic electrode height to dimensions larger than the optical pump absorption depth allows ultrafast transport of the majority of photocarriers to the photoconductor contact electrodes and their efficient contribution to terahertz generation and detection. This eliminates the need for using short carrier lifetime semiconductors, which are used for suppressing the DC current of photoconductive emitters/detectors (in general) and for preventing undesired destructive interferences in continuous-wave photoconductive emitters/detectors (specifically) [60]. Eliminating the need for using short carrier lifetime semiconductors, which have lower carrier mobilities and thermal conductivities [55] compared to high quality crystalline semiconductors, would have an important impact on future high efficiency photoconductive terahertz emitters and detectors.

References

1. Tonouchi, M. Cutting-edge terahertz technology. *Nature Photonics* **1**, 97-105 (2007).
2. Eisele, H. & Haddad, G. Two terminal millimeter-wave sources. *IEEE Trans. Microwave Theory Tech.* **46**, 739-746 (1998).
3. Maestrini, A., Ward, J., Gill, J., Javadi, H., Schlecht, E., Chattopadhyay, G., Maiwald, F., Erickson, N. R. & Mehdi, I. A 1.7-1.9 THz local oscillator source. *IEEE Microwave and Wireless Component Lett*. **14**, 253-255 (2004).
4. Momeni, O. & Afshari, E. High Power Terahertz and Sub-millimeter-Wave Oscillator Design: A Systematic Approach. *IEEE J. Solid-State Circuits* **46**, 583-597 (2011).
5. Gold, S. H. & Nusinovich, G. S. Review of high-power microwave source research. *Rev. Scientific Instruments* **68**, 3945-3974 (1997).

6. Tucek, J., Kreischer, K., Gallagher, D., Vogel, R. & Mihailovich, R. A compact, high power, 0.65 THz source. *Proc. 9th Int. Vacuum Electron. Conf.* 16-17 (2008).
7. Gorshunov, B. P., Volkov, A. A., Prokhorov, A. S. & Spektor, I. E. Methods of terahertz-sub-terahertz BWO spectroscopy of conducting materials. *Physics of the Solid State* **50**, 2001-2012 (2008).
8. Kohler, R., Tredicucci, A., Beltram, F., Beere, H. E., Linfield, E. H., Davies, A. G., Ritchie, D. A., Iotti, R. C. & Rossi, F. Terahertz semiconductor-heterostructure laser. *Nature* **417**, 156-159 (2002).
9. Scalari, G., Walther, C., Fischer, M., Terazzi, R., Beere, H., Ritchie, D. & Faist, J. THz and sub-THz quantum cascade lasers. *Laser Photon. Rev*. **3**, 45-66 (2009).
10. Fathololoumi, S., Dupont, E., Chan, C. W. I., Wasilewski, Z. R., Laframboise, S. R., Ban, D., Mátyás, A., Jirauschek, C., Hu, Q. & Liu, H. C. Terahertz quantum cascade lasers operating up to ~200 K with optimized oscillator strength and improved injection tunneling. *Opt. Express* **20**, 3866-3876 (2012).
11. Chang, G., Divin, C. J., Yang, J., Musheinish, M. A., Williamson, S. L., Galvanauskas, A. & Norris, T. B. GaP waveguide emitters for high power broadband THz generation pumped by Yb-doped fiber lasers. *Opt. Express* **15**, 16308-16315 (2007).
12. Sasaki, Y., Avetisyan, Y., Kawase, K. & Ito, H. Terahertz-wave surface-emitted difference frequency generation in slant-stripe-type periodically poled LiNbO3 crystal. *Appl. Phys. Lett*. **81**, 3323-3325 (2002).
13. Vodopyanov, K. L., Fejer, M. M., Yu, X., Harris, J. S., Lee, Y.-S., Hurlbut, W. C., Kozlov, V. G., Bliss, D. & Lynch, C. Terahertz wave generation in quasi-phase-matched GaAs. *Appl. Phys. Lett*. **89**, 141119 (2006).
14. Stepanov, A., Kuh, J., Kozma, I., Riedle, E., Almási, G. & Hebling, J. Scaling up the energy of THz pulses created by optical rectification. *Opt. Express* **13**, 5762-5768 (2005).
15. Butcher, P. N. & Cotter, D. The elements of nonlinear optics. *Cambridge University Press, Cambridge, U. K*. (1990).
16. Preu, S., Dohler, G. H., Malzer, S., Wang, L. J. & Gossard, A. C. Tunable, continuous-wave terahertz photomixer sources and applications. *J. Appl. Phys.* **109**, 061301 (2011).
17. Bjarnason, J. E., Chan, T. L. J., Lee, A. W. M., Brown, E. R., Driscoll, D. C., Hanson, M., Gossard, A. C. & Muller, R. E. ErAs:GaAs photomixer with two-decade tunability and 12 μW peak output power. *Appl. Phys. Lett.* **85**, 3983-3985 (2004).
18. Peytavit, E., Lepilliet, S., Hindle, F., Coinon, C., Akalin, T., Ducournau, G., Mouret, G. & Lampin, J.-F. Milliwatt-level output power in the sub-terahertz range generated by photomixing in a GaAs photoconductor. *Appl. Phys. Lett.* **99**, 223508 (2011).
19. Upadhya, P. C., Fan, W., Burnett, A., Cunningham, J., Davies, A. G., Linfield, E. H., Lloyd-Hughes, J., Castro-Camus, E., Johnston, M. B. & Beere, H. Excitation-density-dependent generation of broadband terahertz radiation in an asymmetrically excited photoconductive antenna. *Opt. Lett.* **32**, 2297-2299 (2007).
20. Roehle, H., Dietz, R. J. B., Hensel, H. J., Böttcher, J., Künzel, H., Stanze, D., Schell, M. & Sartorius, B. Next generation 1.5 μm terahertz antennas: mesa-structuring of InGaAs/InAlAs photoconductive layers. *Opt. Express* **18**, 2296-2301 (2010).
21. Taylor, Z. D., Brown, E. R. & Bjarnason, J. E. Resonant-optical-cavity photoconductive switch with 0.5% conversion efficiency and 1.0W peak power. *Opt. Lett*. **31**, 1729-1731 (2006).
22. Park, S.-G., Jin, K. H., Yi, M., Ye, J. C., Ahn, J. & Jeong, K.-H. Enhancement of Terahertz Pulse Emission by Optical Nanoantenna. *ACS NANO* **6**, 2026–2031 (2012).
23. Auston, D. H., Cheung, K. P. & Smith P. R. Picosecond photocoducting Hertzian dipoles. *Appl. Phys. Lett*. **45**, 284-286 (1984).
24. van Exter, M. & Grischkowsky, D. Characterization of an optoelectronic terahertz beam system. *IEEE Trans. Microwave Theory and Techniques* **38**, 1684 (1990).
25. Cai, Y., Brener, I., Lopata, J., Wynn, J., Pfeiffer, L., Stark, J. B., Wu, Q., Zhang, X. C. & Federici, J. F. Coherent terahertz radiation detection: Direct comparison between free-space electro-optic sampling and antenna detection. *Appl. Phys. Lett.* **73**, 444 (1998).
26. Ralph, S. E. & Grischkowsky, D. Trap-enhanced electric fields in semi-insulators: The role of electrical and optical carrier injection. *Appl. Phys. Lett.* **59**, 1972 (1991).
27. Berry, C. W. & Jarrahi, M. Principles of impedance matching in photoconductive antennas. *J. Infrared, Millimeter and Terahertz Waves* **33**, 1182-1189 (2012)

28. Pozhela, J. & Reklaitis, A. Electron transport properties in GaAs at high electric fields. *Solid State Electron*. **23**, 927-933 (1980).
29. Berry, C. W. & Jarrahi, M. Plasmonically-enhanced localization of light into photoconductive antennas. *Proc. Conf. Lasers and Electro-Optics*, CFI2 (2010).
30. Berry, C. W. & Jarrahi, M. Ultrafast Photoconductors based on Plasmonic Gratings. *Proc. Int. Conf. Infrared, Millimeter, and Terahertz Waves*, 1-2 (2011).
31. Lloyd-Hughes, J., Merchant, S. K. E., Fu, L., Tan, H. H., Jagadish, C., Castro-Camus, E. & Johnston, M. B. Influence of surface passivation on ultrafast carrier dynamics and terahertz radiation generation in GaAs. *Appl. Phys. Lett*. **89**, 232102 (2006).
32. Headley, C., Fu, L., Parkinson, P., Xu, X. L., Lloyd-Hughes, J., Jagadish, C. & Johnston, M. B. Improved performance of {GaAs}-based terahertz emitters via surface passivation and silicon nitride encapsulation. *J. Sel. Top. Quantum Electron.* **17**, 17-21 (2011).
33. Huggard, P. G., Shaw, C. J., Cluff, J. A. & Andrews, S. R. Polarization-dependent efficiency of photoconducting THz transmitters and receivers. *Appl. Phys. Lett*. **72**, 2069-2071 (1998).
34. Shi, W., Hou, L. & Wang, X. High effective terahertz radiation from semi-insulating-GaAs photoconductive antennas with ohmic contact electrodes. *J. Appl. Phys.* **110**, 023111 (2011).
35. Cai, Y., Brener, I., Lopata, J., Wynn, J., Pfeiffer, L., Stark, J. B., Wu, Q., Zhang, X.-C. & Federici, J. F. Coherent terahertz radiation detection: Direct comparison between free-space electro-optic sampling and antenna detection. *Appl. Phys. Lett*. **73**, 444-446 (1998).
36. Schuller, J. A., Barnard, E. S., Cai, W., Jun, Y. C., White, J. S. & Brongersma, M. L. Plasmonics for extreme light concentration and manipulation. *Nature Materials* **9**, 193-204 (2010).
37. Hartschuh, A., Sanchez, E. J., Xie, X. S. & Novotny, L. High resolution nearfield Raman microscopy of single-walled carbon nanotubes. *Phys. Rev. Lett*. **90**, 095503 (2003).
38. Frey, H., Witt, S., Felderer, K. & Guckenberger, R. High resolution imaging of single fluorescent molecules with the optical nearfield of a metal tip. *Phys. Rev. Lett*. **93**, 200801 (2004).
39. Cubukcu, E., Kort, E. A., Crozier, K. B. & Capasso, F. Plasmonic laser antenna. *Appl. Phys. Lett*. **89**, 093120 (2006).
40. Yu, N., Fan, J., Wang, Q., Pflugl, C., Diehl, L., Edamura, T., Yamanishi, M., Kan, H. & Capasso, F. Small-divergence semiconductor lasers by plasmonic collimation. *Nature Photonics* **2**, 564-570 (2008).
41. Atwater, H. A. & Polman, A. Plasmonics for improved photovoltaic devices. *Nature Materials* **9**, 205-213 (2010).
42. Pala, R. A., White, J., Barnard, E., Liu, J. & Brongersma, M. L. Design of plasmonic thin film solar cells with broadband absorption enhancements. *Adv. Mater*. **21**, 3504-3509 (2009).
43. Ishi, T., Fujikata, T., Makita, K., Baba, T. & Ohashi, K. Si nanophotodiode with a surface plasmon antenna. *Jpn. J. Appl. Phys*. **44**, 364-366 (2005).
44. Tang, L., Kocabas, S. E., Latif, S., Okyay, A. K., Ly-Gagnon, D. S., Saraswat, K. C. & Miller, D. A. B. Nanometre scale germanium photodetector enhanced by a near infrared dipole antenna. *Nature Photon*. **2**, 226-229 (2008).
45. Dintinger, J., Robel, I., Kamat, P. V., Genet, C. & Ebbesen, T. W. Terahertz all-optical molecule-plasmon modulation. *Adv. Mater*. **18**, 1645–1648 (2006).
46. Berry, C. W., Moore, J. & Jarrahi, M. Design of Reconfigurable Metallic Slits for Terahertz Beam Modulation. *Opt. Express* **19**, 1236-1245 (2011).
47. Beck, M., Schafer, H., Klatt, G., Demsar, J., Winnerl, S., Helm, M. & Dekorsy, T. Impulsive terahertz radiation with high electric fields from an amplifier-driven large-area photoconductive antenna. *Opt. Express* **18**, 9251-9257 (2010).
48. Jarrahi, M. & Lee, T. H. High power tunable terahertz generation based on photoconductive antenna arrays. *Proc. IEEE International Microwave Symposium* 391-394 (2008).
49. Jarrahi, M. Terahertz radiation-band engineering through spatial beam-shaping. *Photon. Technol. Lett*. **21**, 2019620 (2009).
50. Hattori, T., Egawa, K., Ookuma, S. I. & Itatani, T. Intense terahertz pulses from large-aperture antenna with interdigitated electrodes. *Jpn. J. Appl. Phys.* **45**, L422-L424 (2006).
51. Kim, J. H., Polley, A. & Ralph, S. E. Efficient photoconductive terahertz source using line excitation. *Opt. Lett*. **30**, 2490-2492 (2005).

52. Dreyhaupt, A., Winnerl, S., Dekorsy, T. & Helm, M. High-intensity terahertz radiation from a microstructured large-area photoconductor. *Appl. Phys. Lett.* **86**, 121114 (2005).
53. Loata, G. C., Thomson, M. D., Löffler, T. & Roskos, H. G. Radiation field screening in photoconductive antennae studied via pulsed terahertz emission spectroscopy. *Appl. Phys. Lett.* **91**, 232506 (2007).
54. Gray, M. B., Shaddock, D. A., Harb, C. C. & Bachor, H.-A. Photodetector designs for low-noise, broadband, and high-power applications. *Rev. Scientific Instruments* **69**, 3755-3762 (1998).
55. Jackson, A. W., Ibbetson, J. P., Gossard, A. C. & Mishra, U. K. Reduced thermal conductivity in low-temperature grown GaAs. *Appl. Phys. Lett.* **74**, 2325-2327 (1999).
56. Brown, E. R., Lee, A. W. M., Navi, B. S. & Bjarnason, J. E. Characterization of a planar self-complementary square-spiral antenna in the THz region. *Microwave Opt. Technol. Lett.* **48**, 524-529 (2006).
57. Huo, Y., Taylor, G. W. & Bansal, R. Planar log-periodic antennas on extended hemishperical silicon lenses for millimeter/submillimeter wave detection applications. *Int. J. Infrared and Millimeter Waves* **23**, 819 (2002).
58. Hsieh, B.-Y. & Jarrahi, M. Analysis of periodic metallic nano-slits for efficient interaction of terahertz and optical waves at nano-scale dimensions. *J. Appl. Phys.* **109**, 084326 (2011).
59. Hsieh, B.-Y., Wang, N. & Jarrahi, M. Toward Ultrafast Pump-Probe Measurements at the Nanoscale. *Special Issue of "Optics in 2011" Optics & Photonics News* **22**, 48 (2011).
60. Berry, C. W. & Jarrahi, M. Terahertz generation using plasmonic photoconductive gratings. *New J. Phys.* **14**, 105029 (2012).

Army Research Office Progress Report

ARO-YIP: Fundamental Properties and Capabilities of Plasmonic Antennas for Efficient Interaction with Nanoelectronics

Contract # W911NF-12-1-0253

Performance Period: 07/01/2013 – 06/30/2014

Program Manager: Dr. James Harvey

Lead Organization: University of Michigan, Ann Arbor

Technical Point of Contact: Mona Jarrahi (mjarrahi@umich.edu)

Administrative Point of Contact: Michelle Chapman (chapman@eecs.umich.edu)

Executive Summary

Here is a list of research activities conducted during the second year of the ARO-YIP program:

- We extended the powerful capabilities of nano-plasmonic antennas that we demonstrated during the first year of the research program to achieve higher efficiencies and radiation powers. In this regard, we presented second generation plasmonic photoconductive terahertz emitters based on three-dimensional nano-plasmonic contact electrodes. We experimentally demonstrated three orders of magnitude terahertz radiation enhancement from a plasmonic photoconductive emitter that incorporates three-dimensional nano-plasmonic contact electrodes in comparison with a conventional photoconductive emitter without plasmonic electrodes. We experimentally demonstrated a record-high optical-to-terahertz conversion efficiency of 7.5% from the second generation photoconductive terahertz emitters based on three-dimensional nano-plasmonic contact electrodes.

- We extended the powerful capabilities of nano-plasmonic antennas that we demonstrated during the first year of the research program to achieve high optical-to-terahertz conversion efficiencies and high terahertz power levels not only for broadband terahertz generation, but also for continuous-wave terahertz generation. We experimentally demonstrate an order of magnitude enhancement in the continuous-wave radiated power from a photomixer with plasmonic contact electrodes in comparison with an analogous conventional photomixer without plasmonic contact electrodes. We have also optimized our plasmonic photoconductive emitters and photomixers for operation at telecommunication wavelengths, where very high power, narrow linewidth, wavelength tunable, compact and cost-effective optical sources are commercially available. For this purpose, we have formed a research partnership with Prof. Arthur Gossard's group at the University of California Santa Barbara, which gives us access to epitaxially grown ErAs:InGaAs substrates with the desired short carrier lifetime and high substrate resistivity properties while operating at 1.55μm pump wavelengths. Following this work, we presented a 1550 nm plasmonic photomixer operating under pumping duty cycles below 10%, which offers significantly higher terahertz radiation power levels compared to previously demonstrated photomixers. The record-high terahertz radiation powers are enabled by enhancing the device quantum efficiency through use of plasmonic contact electrodes, and by mitigating thermal breakdown at high optical pump power levels through use of a low duty cycle optical pump. At an average optical pump power of 150 mW with a pump modulation frequency of 1 MHz and pump duty cycle of 2%, we demonstrate up to 0.8 mW radiation power at 1 THz, within each CW radiation cycle.

- This research in the 07/01/2013 – 06/30/2014 performance period has resulted in 10 peer-reviewed journal papers, 18 peer-reviewed conference papers, 14 peer-reviewed conference abstracts, 24 keynote/plenary/tutorial/invited talks, 1 Ph.D. Dissertation, and 2 provisional patents. Additionally, the PI of this project, Mona Jarrahi, has received the Booker Fellowship from the United States National Committee of the International Union of Radio Science (USNC/URSI), IEEE Nanotechnology Council Early Career Award in Nanotechnology, IEEE Microwave Theory & Techniques Society (MTT-S) Outstanding Young Engineer Award, Presidential Early Career Award for Scientists and Engineers and has been elevated to Senior Membership of Optical Society of America and SPIE. The details are as follows:

Awards and Recognitions

- Booker Fellowship from the United States National Committee of the International Union of Radio Science (USNC/URSI)
- IEEE Nanotechnology Council Early Career Award in Nanotechnology
- IEEE Microwave Theory & Techniques Society (MTT-S) Outstanding Young Engineer Award
- OSA Senior Membership
- Presidential Early Career Award for Scientists and Engineers
- SPIE Senior Membership

Journal Publications

1. M. Unlu, M. R. Hashemi, C. W. Berry, S. Li, S.-H. Yang, M. Jarrahi, "Switchable scattering meta-surfaces for broadband terahertz modulation", *Nature Scientific Reports*, 4, 5708, DOI:10.1038/srep05708, 2014
2. C. W. Berry, M. R. Hashemi, S. Preu, H. Lu, A. C. Gossard, and M. Jarrahi, "High Power Terahertz Generation Using 1550 nm Plasmonic Photomixers," *Applied Physics Letters*, 105, 011121, 2014
3. C. W. Berry, M. R. Hashemi, S. Preu, H. Lu, A. C. Gossard, and M. Jarrahi, "Plasmonics enhanced photomixing for generating continuous-wave frequency-tunable terahertz radiation," *Optics Letters*, 39, 2014
4. S.-H. Yang, M. R. Hashemi, C. W. Berry, M. Jarrahi, "7.5% Optical-to-Terahertz Conversion Efficiency Offered by Photoconductive Emitters with Three-Dimensional Plasmonic Contact Electrodes," *Trans. Terahertz Sci. Tech*., 4, 2014
5. C. W. Berry, M. R. Hashemi, M. Jarrahi, "Generation of High Power Pulsed Terahertz Radiation using a Plasmonic Photoconductive Emitter Array with Logarithmic Spiral Antennas," *Applied Physics Letters*, 104, 081122, 2014
6. M. R. Hashemi, C. W. Berry, E. Merced, N. Sepulveda, M. Jarrahi, "Direct Measurement of Vanadium Dioxide Dielectric Properties in W-band", *Journal of Infrared, Millimeter and Terahertz Waves*, 35, 486-492, 2014
7. S.-H. Yang, M. Jarrahi, "Enhanced light-matter interaction at nanoscale by utilizing high aspect-ratio metallic gratings," *Optics Letters*, 38, 3677-3679, 2013
8. C. W. Berry, M. R. Hashemi, M. Unlu, M. Jarrahi "Design, Fabrication, and Experimental Characterization of Plasmonic Photoconductive Terahertz Emitters," *J. Visualized Experiments*, 77, e50517, doi:10.3791/50517, 2013
9. N. Wang, M. Jarrahi, "Noise Analysis of photoconductive terahertz detectors," *Journal of Infrared, Millimeter and Terahertz Wave*, 34, 519-528, 2013
10. N. Wang, M. R. Hashemi, M. Jarrahi, "Plasmonic photoconductive detectors for enhanced terahertz detection sensitivity," *Optics Express*, 21, 17221–17227, 2013

Conference Publications

1. N. T. Yardimci, S.-H. Yang, C. W. Berry, M. Jarrahi, "Plasmonics Enhanced Terahertz Radiation from Large Area Photoconductive Emitters", *Proc. IEEE Photonics Conference (IPC)*, San Diego, CA, October 12-16, 2014
2. C. W. Berry, M. R. Hashemi, S. Preu, H. Lu, A. C. Gossard, M. Jarrahi, "High Power Terahertz Generation From ErAs:InGaAs Plasmonic Photomixers", *Proc. International Conference on Infrared, Millimeter, and Terahertz Waves*, Tucson, AZ, Sep 14-19, 2014
3. S.-H. Yang, M. R. Hashemi, C. W. Berry, M. Jarrahi, "Three-Dimensional Plasmonic Contact Electrodes for High-Efficiency Photoconductive Terahertz Sources", *Proc. International Conference on Infrared, Millimeter, and Terahertz Waves*, Tucson, AZ, Sep 14-19, 2014
4. S.-H. Yang, M. R. Hashemi, C. W. Berry, M. Jarrahi, "High-Efficiency Photoconductive Terahertz Antennas based on High-Aspect Ratio Plasmonic Electrodes", *Proc. IEEE International Antennas and Propagation Symposium*, Memphis, TN, July 6-12, 2014

5. C. W. Berry, M. R. Hashemi, S. Preu, H. Lu, A. C. Gossard, M. Jarrahi, "Terahertz Radiation Enhancement through Use of Plasmonic Photomixers", *Proc. IEEE International Antennas and Propagation Symposium*, Memphis, TN, July 6-12, 2014
6. S.-H. Yang, M. R. Hashemi, C. W. Berry, M. Jarrahi, "7.5% Optical-to-Terahertz Conversion Efficiency through Use of Three-Dimensional Plasmonic Electrodes", *Proc. Conference of Lasers and Electro-Optics*, San Jose, CA, June 8-13, 2014
7. C. W. Berry, M. R. Hashemi, S. Preu, H. Lu, A. C. Gossard, M. Jarrahi, "Plasmonic Photomixers for Increased Terahertz Radiation Powers at 1550 nm Optical Pump Wavelength", *Proc. Conference of Lasers and Electro-Optics*, San Jose, CA, June 8-13, 2014
8. S.-H. Yang, M. R. Hashemi, C. W. Berry, M. Jarrahi, "High-Efficiency Terahertz Emitters based on Three-Dimensional Metallic Nanostructures", *IEEE Microwave Symposium Digest*, Tampa Bay, FL, June 1-6, 2014
9. S.-H. Yang, C. W. Berry, M. R. Hashemi, M. Jarrahi, "Plasmonic-Enhanced Optical-to-Terahertz Conversion Efficiency", *Proc. 4th European Optical Society Topical Meeting on Terahertz Science & Technology*, Camogli, Italy, May 11-14, 2014
10. C. W. Berry, N. Wang, M. R. Hashemi, M. Jarrahi, "Plasmonic Photoconductive Antennas for High-Power Terahertz Generation and High-Sensitivity Terahertz Detection", *Proc. European Conference on Antennas and Propagation*, Hague, Netherlands, April 6-11, 2014
11. M. Unlu, M. R. Hashemi, C. W. Berry, S. Li, S-H. Yang, M. Jarrahi, "High-performance terahertz spatial light modulators based on reconfigurable diamagnetic meta-surfaces", *Proc. International Congress on Advanced Electromagnetic Materials in Microwaves and Optics*, Bordeaux, France, September 16-21, 2013
12. C. W. Berry, M. R. Hashemi, M. Jarrahi, "Plasmonic Photoconductive Terahertz Emitters Based On Logarithmic Spiral Antenna Arrays", *Proc. International Conference on Infrared, Millimeter, and Terahertz Waves*, Mainz, Germany, September 1-6, 2013
13. M. Unlu, M. R. Hashemi, C. W. Berry, S. Li, S-H. Yang, M. Jarrahi, "Broadband Terahertz Modulation Through Reconfigurable Meta-Surfaces With Diamagnetic Switching Capability", *Proc. International Conference on Infrared, Millimeter, and Terahertz Waves*, Mainz, Germany, September 1-6, 2013
14. N. Wang, C. W. Berry, M. R. Hashemi, M. Jarrahi, "Terahertz Detection Sensitivity Enhancement By Incorporating Plasmonic Gratings In Photoconductive Detectors", *Proc. International Conference on Infrared, Millimeter, and Terahertz Waves*, Mainz, Germany, September 1-6, 2013
15. C. W. Berry, M. R. Hashemi, M. Unlu, M. Jarrahi, "Plasmonics-Enhanced Photoconductive Terahertz Emitters", *Proc. International Microwave and Optoelectronic Conference*, Rio de Janeiro, Brazil, August 4-7, 2013
16. C. W. Berry, M. R. Hashemi, M. Jarrahi, "Plasmonic Photoconductors for High-Efficiency Terahertz Generation", *Proc. Optical Society of Americas Sensors topical meeting*, Rio Grande, Puerto Rico, July 14-19, 2013
17. M. Unlu, C. W. Berry, S. Li, M. R. Hashemi, S-H. Yang, M. Jarrahi, "A Microelectromechanically Reconfigurable Mesh Filter for High-Performance Terahertz Modulation", *Proc. IEEE International Antennas and Propagation Symposium*, Orlando, FL, July 7-12, 2013
18. C. W. Berry, M. R. Hashemi, M. Unlu, M. Jarrahi, "Plasmonic Photoconductive Antennas for Significant Terahertz Radiation Enhancement", *Proc. IEEE International Antennas and Propagation Symposium*, Orlando, FL, July 7-12, 2013

Conference Abstracts

1. M. Jarrahi, "Plasmonic Enhanced Terahertz Imaging and Spectroscopy", *International Symposium on Optomechatronic Technologies*, Seattle, WA, November 5-7, 2014
2. M. Jarrahi, "An Overview of Recent Advances in Plasmonic Photoconductive Terahertz Sources", *Workshop on Terahertz Technologies (in association with European Microwave Conference)*, Rome, Italy, October 5-10, 2014
3. M. Jarrahi, "Nanophotonics and Plasmonics for Advancement of Terahertz Technology", *IEEE International Conference on Nanotechnology*, Toronto, Canada, August 18-21, 2014

4. M. Jarrahi, "Advanced Terahertz Imaging and Spectroscopy Systems based on Plasmonic Terahertz Optoelectronics", *Proc. SPIE Optics and Photonics Conference*, San Diego, CA, August 17-21, 2014
5. M. Jarrahi, "Plasmonics-enabled advancements in terahertz spectroscopy systems", *Days on Diffraction 2014*, St. Petersburg, Russia, May 26-30, 2014
6. S.-H. Yang, C. W. Berry, M. R. Hashemi, M. Jarrahi, "Plasmonic Nanostructures for Terahertz Emission Enhancement", *Proc. 5th International Conference on Metamaterials, Photonic Crystals and Plasmonics*, Singapore, May 20-23, 2014
7. C. W. Berry, M. R. Hashemi, M. Jarrahi, "Plasmonic Terahertz Optoelectronics for Higher Performance Terahertz Imaging Systems", *Proc. SPIE defense and Security Sensing*, Baltimore, MD, May 5-9, 2014
8. M. Jarrahi, "Advanced Terahertz Optoelectronics based on Plasmonic Nanostructures", *Nano and Giga Challenges in Electronics, Photonics and Renewable Energy From Materials to Devices to System Architecture Symposium*, Phoenix, Arizona, March 10-14, 2014
9. C. W. Berry, S.-H. Yang, M. R. Hashemi, M. Jarrahi, "Plasmonic Nanostructures for Enhanced Terahertz Emission", *International Workshop on Terahertz Technology*, Zao, Japan, March 7-10, 2014
10. S.-H. Yang, C. W. Berry, N. Wang, M. R. Hashemi, M. Jarrahi, "Plasmonic Photoconductive Terahertz Optoelectronics", *Proc. SPIE Photonic West*, San Francisco, CA, February 1-6, 2014
11. C. W. Berry, N. Wang, M. R. Hashemi, M. Jarrahi, "Plasmonics-enhanced terahertz spectroscopy", *USNC-URSI National Radio Science Meeting*, Boulder, CO, Jan 8-11, 2014
12. C. W. Berry, N. Wang, M. R. Hashemi, M. Jarrahi, "Plasmonics-Enhanced Photoconductive Terahertz Optoelectronics", *Proc. International Conference and Exhibition on Lasers, Optics & Photonic*, San Antonio, TX, October 7-9, 2013
13. M. Unlu, M. R. Hashemi, C. W. Berry, S. Li, S-H. Yang, M. Jarrahi, "Reconfigurable diamagnetic meta-molecules for broadband terahertz modulation", *Proc. SPIE Optics and Photonics Conference*, San Diego, CA, August 25-29, 2013
14. M. Jarrahi, "Plasmonics-Enhanced Terahertz Imaging and Sensing Systems", *CMOS Emerging Technologies Research Symposium*, Whistler, Canada, July 17-19, 2013

Keynote/Plenary/Tutorial/Invited Talks

1. M. Jarrahi, "Plasmonic Enhanced Terahertz terahertz Imaging and Spectroscopy", *International Symposium on Optomechatronic Technologies*, Seattle, WA, November 5-7, 2014 **(*Plenary talk*)**
2. N. T. Yardimci, S.-H. Yang, C. W. Berry, M. Jarrahi, "Plasmonics Enhanced Terahertz Radiation from Large Area Photoconductive Emitters", *IEEE Photonics Conference (IPC)*, San Diego, CA, October 12-16, 2014
3. M. Jarrahi, "An Overview of Recent Advances in Plasmonic Photoconductive Terahertz Sources", *Workshop on Terahertz Technologies (in association with European Microwave Conference)*, Rome, Italy, October 5-10, 2014
4. M. Jarrahi, "Nanophotonics and Plasmonics for Advancement of Terahertz Technology", *IEEE International Conference on Nanotechnology*, Toronto, Canada, August 18-21, 2014 **(*Keynote talk*)**
5. M. Jarrahi, "Advanced Terahertz Imaging and Spectroscopy Systems based on Plasmonic Terahertz Optoelectronics", *SPIE Optics and Photonics Conference*, San Diego, CA, August 17-21, 2014
6. M. Jarrahi, "Plasmonics-enabled advancements in terahertz spectroscopy systems", *Days on Diffraction 2014*, St. Petersburg, Russia, May 26-30, 2014
7. S.-H. Yang, C. W. Berry, M. R. Hashemi, M. Jarrahi, "Plasmonic Nanostructures for Terahertz Emission Enhancement", *5th International Conference on Metamaterials, Photonic Crystals and Plasmonics*, Singapore, May 20-23, 2014
8. S.-H. Yang, C. W. Berry, M. R. Hashemi, M. Jarrahi, "Plasmonic-Enhanced Optical-to-Terahertz Conversion Efficiency", *4th European Optical Society Topical Meeting on Terahertz Science & Technology*, Camogli, Italy, May 11-14, 2014
9. C. W. Berry, M. R. Hashemi, M. Jarrahi, "Plasmonic Terahertz Optoelectronics for Higher Performance Terahertz Imaging Systems", *SPIE defense and Security Sensing*, Baltimore, MD, May 5-9, 2014

10. M. Jarrahi, "Advanced Terahertz Optoelectronics based on Plasmonic Nanostructures", *Nano and Giga Challenges in Electronics, Photonics and Renewable Energy From Materials to Devices to System Architecture Symposium*, Phoenix, Arizona, March 10-14, 2014 **(*tutorial lecture*)**
11. C. W. Berry, S.-H. Yang, M. R. Hashemi, M. Jarrahi, "Plasmonic Nanostructures for Enhanced Terahertz Emission", *International Workshop on Terahertz Technology*, Zao, Japan, March 7-10, 2014
12. M. Jarrahi, "Pushing the Limits of Terahertz Optoelectronics", *IEEE Coastal Los Angeles Section Seminar*, Los Angeles, CA, February 2014
13. M. Jarrahi, "Panel on THz Wireless Communication", *IEEE Radio and Wireless Week*, Newport Beach, CA, Jan 19-22, 2014
14. C. W. Berry, N. Wang, M. R. Hashemi, M. Jarrahi, "Plasmonics-enhanced terahertz spectroscopy", *USNC-URSI National Radio Science Meeting*, Boulder, CO, Jan 8-11, 2014
15. M. Jarrahi, "Pushing the Limits of Terahertz Optoelectronics", *Physics Department, Oakland University*, Rochester, MI, December 2013
16. M. Jarrahi, "Pushing the Limits of Terahertz Optoelectronics", *Electrical and Computer Engineering Department, Rice University*, Houston, TX, October 2013
17. C. W. Berry, N. Wang, M. R. Hashemi, M. Jarrahi, "Plasmonics-Enhanced Photoconductive Terahertz Optoelectronics", *International Conference and Exhibition on Lasers, Optics & Photonic*, San Antonio, TX, October 7-9, 2013
18. M. Jarrahi, "Plasmonic photoconductive emitters and detectors", *Workshop on Terahertz Technologies (in association with European Microwave Conference)*, Nuremberg, Germany, October 6-11, 2013
19. M. Unlu, M. R. Hashemi, C. W. Berry, S. Li, S-H. Yang, M. Jarrahi, "High-performance terahertz spatial light modulators based on reconfigurable diamagnetic meta-surfaces", *International Congress on Advanced Electromagnetic Materials in Microwaves and Optics*, Bordeaux, France, September 16-21, 2013
20. M. Unlu, M. R. Hashemi, C. W. Berry, S. Li, S-H. Yang, M. Jarrahi, "Broadband Terahertz Modulation Through Reconfigurable Meta-Surfaces With Diamagnetic Switching Capability", *International Conference on Infrared, Millimeter, and Terahertz Waves*, Mainz, Germany, September 1-6, 2013
21. M. Unlu, M. R. Hashemi, C. W. Berry, S. Li, S-H. Yang, M. Jarrahi, "Reconfigurable diamagnetic meta-molecules for broadband terahertz modulation", *SPIE Optics and Photonics Conference*, San Diego, CA, August 25-29, 2013
22. C. W. Berry, M. R. Hashemi, M. Unlu, M. Jarrahi, "Plasmonics-Enhanced Photoconductive Terahertz Emitters", *International Microwave and Optoelectronic Conference*, Rio de Janeiro, Brazil, August 4-7, 2013 **(*Plenary talk*)**
23. M. Jarrahi, "Plasmonics-Enhanced Terahertz Imaging and Sensing Systems", *CMOS Emerging Technologies Research Symposium*, Whistler, Canada, July 17-19, 2013
24. C. W. Berry, M. R. Hashemi, M. Jarrahi, "Plasmonic Photoconductors for High-Efficiency Terahertz Generation", *Optical Society of Americas Sensors topical meeting*, Rio Grande, Puerto Rico, July 14-19, 2013

Ph.D. Dissertation

1. C. W. Berry, "Plasmonic Enhanced Terahertz Imaging and Spectroscopy Plasmonic Photoconductors for Higher Performance Terahertz Radiation Sources", *Electrical Engineering and Computer Science Department*, University of Michigan, Ann Arbor, August 2013

Patents

1. M. Jarrahi, "Low-Duty-Cycle Continuous-Wave Photoconductive Terahertz Imaging and Spectroscopy Systems," Provisional Patent Application No. 62011848, filed 06/13/14
2. M. Jarrahi, M. Unlu, M. R. Hashemi, C. W. Berry, and S. Li, "Reconfigurable Device for Terahertz and Infrared Filtering and Modulation," Provisional Patent Application No. 61862730, filed 08/06/13

Detailed Research Summary

Terahertz Emitters Based on Three-dimensional Nano-Plasmonic Photoconductors:
Terahertz technology has attracted extensive attention because of its unique applications in environmental monitoring[1,2], chemical identification, material inspection[3], and biological sensing[4-6]. However, the practical feasibility of many terahertz systems is still limited by the low power, low efficiency, and bulky nature of existing terahertz radiation sources. Terahertz generation through photoconduction has demonstrated very promising performance for both pulsed and continuous-wave terahertz radiation[7,8], which offers relatively high radiation powers at room temperature and a compact solution for portable terahertz systems. A photoconductive terahertz emitter is mainly composed of an ultrafast photoconductor connected to a terahertz antenna and driven by an external optical pump. For narrowband/broadband terahertz radiation generation a heterodyning/pulsed optical pump beam is incident on the ultrafast photoconductor, generating photocarriers in the active region of the photoconductor. When a bias voltage is applied to the photoconductor, the bias electric field drifts the photocarriers to the photoconductor contact electrodes, inducing a photocurrent that feeds the terahertz antenna and generates terahertz radiation. Compared to other optically-assisted terahertz emitters based on nonlinear optical processes, a photoconductive terahertz emitter can reach much higher optical-to-terahertz conversion efficiencies since each optical pump photon can generate several terahertz photons. Therefore, the optical-to-terahertz conversion efficiency of a photoconductive terahertz emitter can be orders of magnitude higher than the optical-to-terahertz conversion efficiency of a terahertz emitter based on nonlinear optical processes, which is limited by the Manley–Rowe limit.

In spite of their great promise, the performance of existing photoconductive terahertz emitters is severely limited by poor quantum efficiency of ultrafast photoconductors. This limitation is mainly caused by inefficient collection of the majority of the photocarriers in sub-picosecond time scales. In order to efficiently contribute to terahertz radiation, the transit time of the photocarriers to the photoconductor contact electrodes should be within a fraction of the terahertz oscillation period. Considering the carrier transportation dynamics inside semiconductors, only the photocarriers which are generated within distances of ~100 nm from the contact electrode can efficiently contribute to terahertz radiation, even under sufficient bias electric fields. Since the minimum spot size of the optical pump beam is diffraction limited, the majority of photocarriers cannot efficiently contribute to terahertz generation.

Recent studies have shown that incorporating plasmonic contact electrodes in photoconductive terahertz emitters can significantly enhance the photoconductor quantum efficiency by concentrating a larger fraction of the incident pump photons within nano-scale distances from the contact electrodes[9-12]. This enhancement mechanism has been widely used in various photoconductive terahertz emitters with a variety of device architectures and in various operational settings, demonstrating significant optical-to-terahertz conversion efficiency enhancements as high as two-orders of magnitude. Up to date, the existing photoconductive terahertz emitters that utilize plasmonic contact electrodes have been all based on two-dimensional plasmonic contact electrodes fabricated on the surface of the photo-absorbing semiconductor substrate. By use of two-dimensional plasmonic contact electrodes, the concentration of the photocarriers near photoconductive contact electrodes is enhanced for the

photocarriers that are generated near the surface of the photo-absorbing semiconductor substrate. However, the optical-to-terahertz efficiency of the photoconductive emitter would be still limited by the photocarriers generated deeper than ~100 nm in the photo-absorbing substrate. To address this limitation, we present a novel photoconductive terahertz emitter based on three-dimensional plasmonic contact electrodes embedded inside the photo-absorbing substrate. By use of three-dimensional plasmonic contact electrodes the majority of the photocarriers absorbed within the absorption depth of the optical pump will be localized within ~100 nm distance from the photoconductor contact electrodes. Hence, the majority of the photocarriers can be drifted to the photoconductor contact electrodes and the terahertz antenna within a fraction of the terahertz oscillation period, further enhancing the optical-to-terahertz conversion efficiency of the photoconductive terahertz emitter. Here, we present, for the first time, a photoconductive terahertz emitter based on three-dimensional plasmonic contact electrodes that extends the optical-to-terahertz conversion efficiency of the photoconductive terahertz emitters based on two-dimensional plasmonic contact electrodes by another order of magnitude, offering the highest reported optical-to-terahertz conversion efficiency of 7.5%.

In order to demonstrate the significant optical-to-terahertz conversion efficiency enhancement through use of three-dimensional plasmonic contact electrodes, a photoconductive terahertz emitter with three-dimensional plasmonic contact electrodes is implemented and its performance is compared with a comparable photoconductive emitter with two-dimensional plasmonic contact electrodes. Figure 1 shows the schematic diagram of the plasmonic photoconductive terahertz emitters fabricated on the same low temperature grown (LT) GaAs substrate with a carrier lifetime of ~400 fs. Both plasmonic photoconductive emitters utilize the same logarithmic spiral terahertz antenna, well-suited for pulsed terahertz generation. The logarithmic spiral antennas are designed to offer a broadband radiation resistance of 70-100 Ω while maintaining a reactance value near 0 Ω over the 0.1-2 THz frequency range[10]. The plasmonic photoconductive emitters are mounted on identical hyper-hemispherical silicon lenses, used for collecting and collimating the generated terahertz radiation from the back-side of the LT-GaAs substrate. The plasmonic contact electrodes of both photoconductive emitters cover a 15 μm × 15 μm area for the cathode and anode contacts. The end-to-end spacing between the anode and cathode plasmonic contact electrodes is 5 μm. The geometry and spacing of the anode and cathode contacts are selected to provide high bias electric field for the entire device active area such that the photocarriers within ~100 nm distance from the contact electrodes travel with saturation velocity of ~10^7 cm/s.

The plasmonic photoconductive emitter with two-dimensional plasmonic contact electrodes on the surface of the LT-GaAs substrate (Fig. 1a) incorporates Au gratings with 200 nm pitch, 100 nm spacing, 50 nm height, and 150 nm thick SiO_2 anti-reflection coating. This design allows excitation of surface plasmon waves along the Au gratings and transmission of 70% of the optical pump power into the substrate in response to a transverse magnetic (TM)-polarized optical pump at 800 nm wavelength[11]. When a TM-polarized incident optical pump at 800 nm wavelength is incident on the two-dimensional plasmonic contact electrodes, the bias electric field separates the cluster of the photo-generated electrons and holes and drifts them toward the anode and cathode contact electrodes, respectively. The induced photocurrent is then fed to the logarithmic spiral antenna, generating terahertz radiation. The use of two-dimensional plasmonic contact electrodes on the surface of the LT-GaAs substrate significantly enhances the concentration of the photocarriers near the photoconductor contact electrodes, enhancing the number of the photocarriers that are drifted to the contact electrodes in a sub-picosecond time-

scale to efficiently contribute to terahertz radiation. However, since the plasmonic contact electrodes are located on the surface of the substrate, a large fraction of the photocarriers generated within depths of more than ~100 nm from the surface of the substrate cannot be drifted to the contact electrodes within a sub-picosecond time-scale to efficiently contribute to terahertz radiation. Use of three-dimensional plasmonic contact electrodes embedded inside the LT-GaAs substrate mitigates this limitation and further enhances the ultrafast photocurrent by significantly increasing light-matter interaction in the close proximity to the contact electrodes.

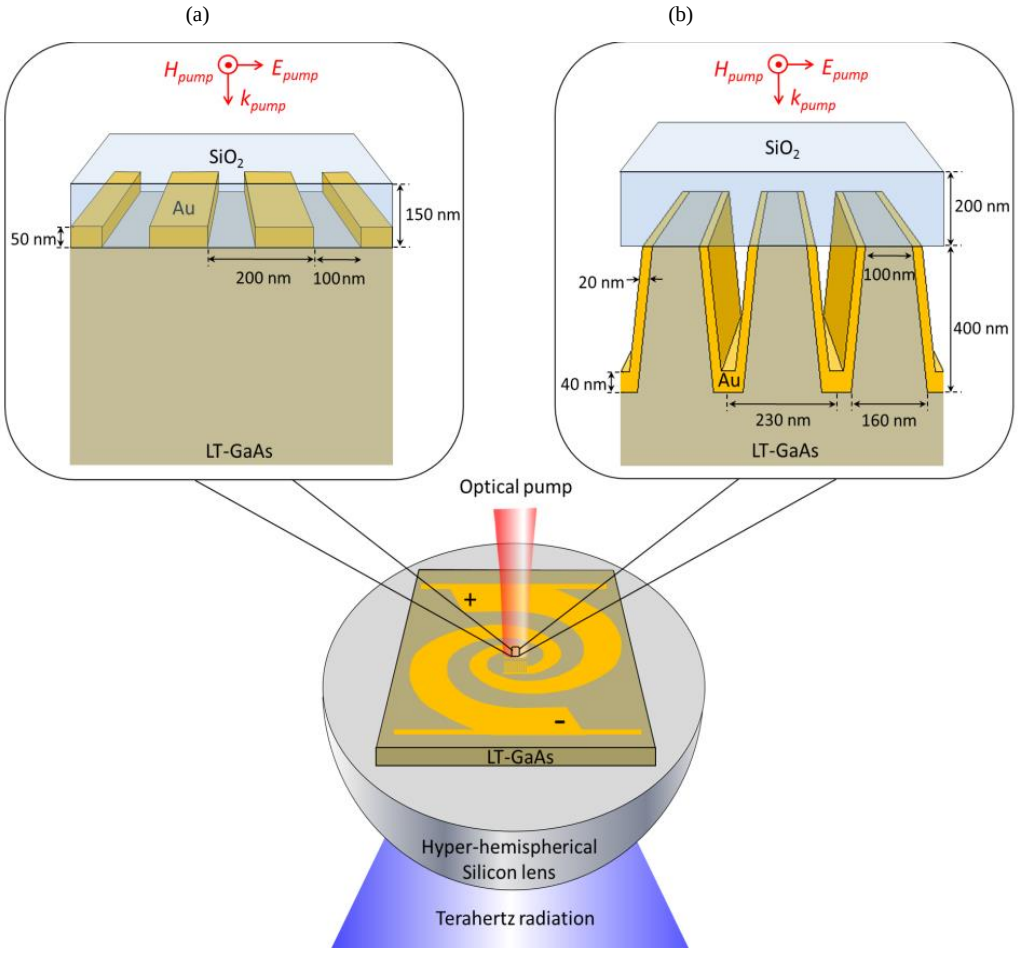

Fig. 1. Schematic diagram of plasmonic photoconductive terahertz emitters with (a) two-dimensional plasmonic contact electrodes on the surface of the LT-GaAs substrate, (b) three-dimensional plasmonic contact electrodes embedded inside the LT-GaAs substrate.

The plasmonic photoconductive emitter with three-dimensional plasmonic contact electrodes embedded inside the substrate (Fig. 1b) incorporates high-aspect ratio metallic gratings that cover the side-walls of nanoscale LT-GaAs device active regions sandwiched between the metallic gratings. Utilizing a periodic arrangement of nanoscale metallic gratings allows excitation of surface plasmonic waves along the gratings, which enables efficient coupling of a TM-polarized incident optical wave into the TEM guided modes of subwavelength slab waveguides formed by the metallic gratings[14-16]. The height of the LT-GaAs nanostructures determines the excited modes inside the subwavelength slab waveguides formed by the metallic gratings. Therefore, by extending the metallic grating height, higher order TEM guided mode can

be excited by the incident optical beam, resulting in strong light-matter interaction inside the LT-GaAs nanostructures.

For our presented three-dimensional plasmonic contact electrodes (Fig. 1b), the high-aspect ratio metallic gratings are designed to excite the 4th order TEM guided mode of the subwavelength slab waveguides formed by the metallic gratings in response to a TM-polarized optical pump at 800 nm wavelength. This design allows efficient coupling of 70% of the 800 nm optical pump into the LT-GaAs nanostructures with 400 nm height. To reduce the Fresnel reflection losses a 200 nm SiO_2 anti-reflection coating layer is used on the top of the LT-GaAs nanostructures. By use of the designed high-aspect ratio metallic gratings, the majority of the incident photons are localized inside LT-GaAs nanostructures. Therefore, the photocarriers are generated within distances of less than 50 nm from the photoconductor contact electrodes. Since the majority of the photons are guided and absorbed inside the LT-GaAs nanostructures sandwiched between the contact electrodes, the number of the photocarriers drifted to the contact electrodes within a sub-picosecond time-scale is significantly increased. Consequently, the optical-to-terahertz conversion efficiency of the photoconductive emitter is dramatically enhanced.

We have fabricated prototypes of the presented plasmonic photoconductive emitters based on the two-dimensional plasmonic contact electrodes and three-dimensional plasmonic contact electrodes on a LT-GaAs substrate. For the photoconductive emitter with two-dimensional plasmonic contact electrodes, the fabrication process starts with patterning the plasmonic contact electrodes using electron-beam lithography, followed by deposition of Ti/Au (50/450 Å) and liftoff. Next, the 150 nm thick SiO_2 anti-reflection coating is deposited using plasma enhanced chemical vapor deposition. Contact vias are then opened by etching the SiO_2 coating. Finally, the bias lines and antennas are patterned using optical lithography followed by Ti/Au (10/400 nm) deposition and liftoff.

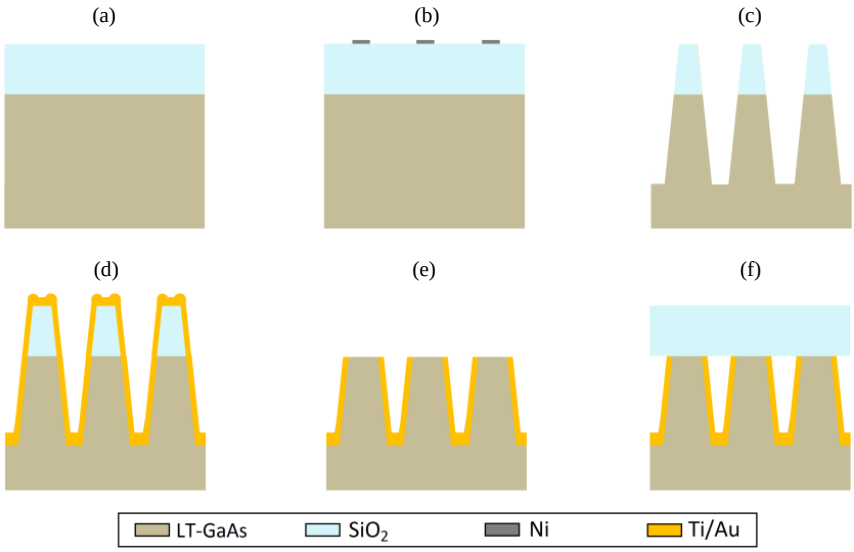

Fig. 2. Fabrication process of the three-dimensional plasmonic contact electrodes based on high aspect-ratio metallic gratings embedded inside the LT-GaAs substrate: (a) Deposition of a SiO_2 layer, (b) pattering a Ni hard mask, (c) etching the SiO_2 layer and the underlying LT-GaAs substrate, (d) Ti/Au sputtering, (e) liftoff, and (f) Deposition of a SiO_2 anti-reflection coating.

For the photoconductive emitter with three-dimensional plasmonic contact electrodes, the fabrication process starts with deposition of a 200 nm thick SiO_2 film by plasma enhanced chemical vapor deposition (Fig. 2a). Next, nanoscale Ni gratings, which serve as a hard mask for etching the underlying SiO_2 layer, are patterned on the surface of the SiO_2 film using electron beam lithography followed by Ni deposition and liftoff (Fig. 2b). By using inductively coupled plasma reactive ion etching (ICP-RIE), nanoscale SiO_2 gratings with 200 nm height are then formed to serve as a hard mask for shaping the high-aspect ratio LT-GaAs nanostructures (Fig. 2c). Metallic gratings are then formed by sputtering Ti/Au (2/20 nm) on the sidewall of LT-GaAs nanostructures (Fig. 2d). In order to maintain high-uniformity metal coverage on the sidewalls of the LT-GaAs nanostructures, the slope of the SiO_2 and LT-GaAs sidewalls are specifically controlled by adjusting the ICP-RIE etch parameters. The SiO_2 hard mask is then removed by a wet etching process (Fig. 2e). A 200 nm thick SiO_2 anti-reflection coating is then deposited to cover the top of the LT-GaAs nanostructures (Fig. 2f). Finally, the logarithmic spiral terahertz antennas and bias lines are formed using optical lithography followed by Ti/Au (20/400 nm) deposition and liftoff. The fabricated device are then mounted and centered on a high resistivity hyper-hemispherical silicon lens.

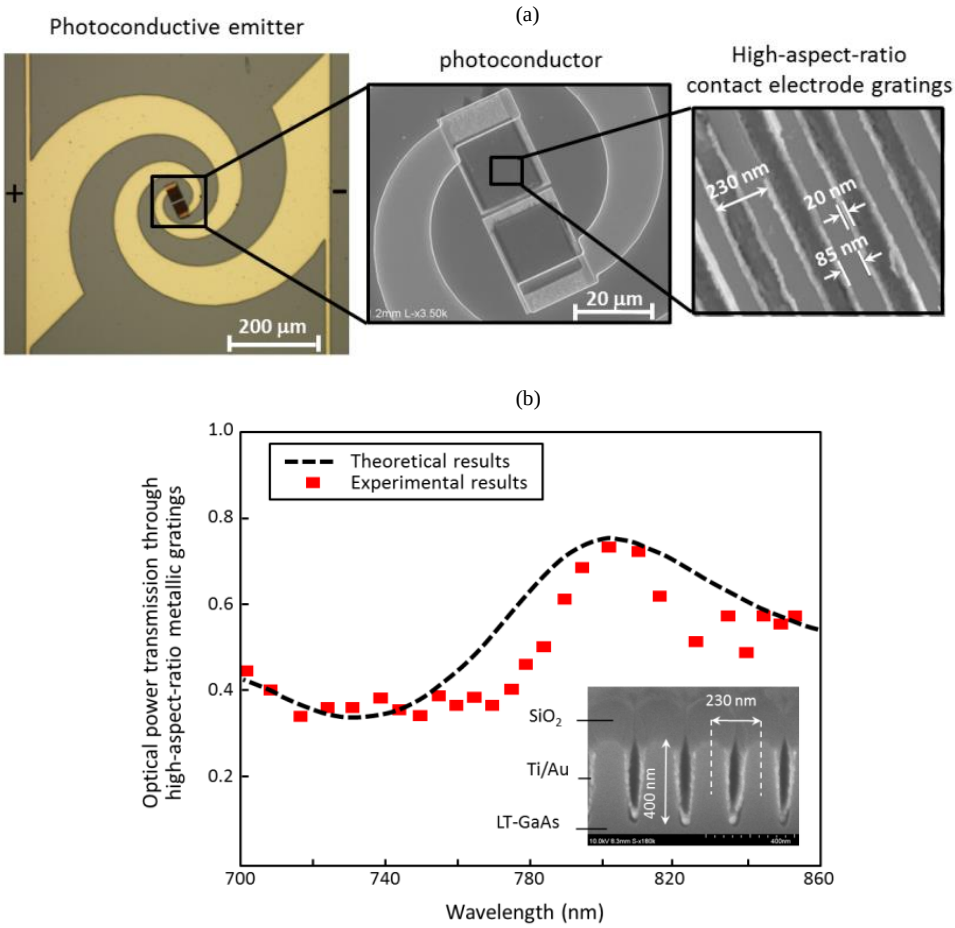

Fig. 3. (a) Microscope image of the photoconductive emitter based on three-dimensional plasmonic contact electrodes and the SEM image of the three-dimensional plasmonic contact electrodes based on high-aspect-ratio metallic gratings, (b) Transmission of a TM-polarized optical beam through the high-aspect-ratio metallic gratings. Inset shows the cross sectional SEM image of the high-aspect-ratio metallic gratings.

Figure 3a shows the optical microscope and scanning electron microscope (SEM) top-view images of the fabricated plasmonic photoconductive emitter incorporating three-dimensional plasmonic contact electrodes. The cross-sectional SEM image of the high-aspect ratio metallic gratings is shown in Fig. 3b inset, illustrating the configuration of the LT-GaAs nanostructures and the complete metallic coverage on the sidewalls of the LT-GaAs nanostructures. Transmission of a TM-polarized optical beam through the high-aspect-ratio metallic gratings into the LT-GaAs substrate is measured in the range of 700-860 nm wavelength range, indicating more than 70% optical power transmission into the LT-GaAs nanostructures (Fig. 3b). The measurement results are in agreement with the theoretical calculations based on excitation of the 4^{th} order TEM guided mode of the subwavelength slab waveguides formed by the metallic gratings, predicting the majority of the photocarriers to be localized within ~100 nm distance from the three-dimensional plasmonic contact electrodes.

In order to characterize the terahertz radiation performance of the photoconductive terahertz emitter prototypes based on two-dimensional and three-dimensional plasmonic contact electrodes, a TM-polarized optical beam from a Ti:sapphire mode-locked laser with a pulse width of 200 fs and wavelength of 800 nm is used to pump the photoconductive emitters. The optical pump is asymmetrically focused on the anode plasmonic contact electrodes to maximize the induced ultrafast photocurrent feeding the terahertz antenna and to offer the optimum impedance loading to the terahertz antenna[17,18]. The photocurrent characteristics of the photoconductors based on the two-dimensional and three-dimensional plasmonic contact electrodes are shown in Fig. 4a and Fig. 4b, respectively. At the same optical pump power and bias voltage, the induced ultrafast photocurrent in the photoconductor with three-dimensional plasmonic contact electrodes is significantly higher than the induced ultrafast photocurrent in the photoconductor with two-dimensional plasmonic contact electrode. This verifies the predicted quantum-efficiency enhancement as the result of using the three-dimensional plasmonic contact electrodes, which accumulates a significantly larger number of photocarriers in close proximity to the contact electrodes. By accumulating larger number of photocarriers in ~ 100 nm distances from the contact electrodes, a larger number of the photocarriers can travel to the contact electrodes before recombination in the LT-GaAs substrate.

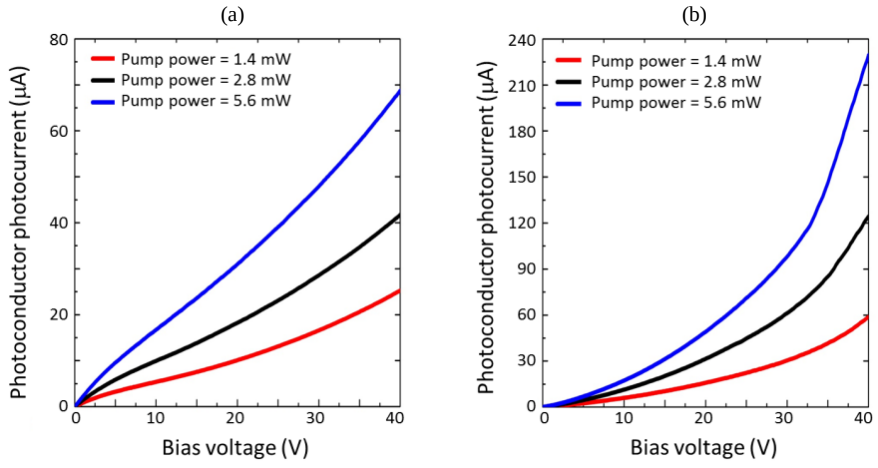

Fig. 4. Output photocurrent of the photoconductors based on (a) two-dimensional plasmonic contact electrodes, and (b) three-dimensional plasmonic contact electrodes as a function of the bias voltage and optical pump power.

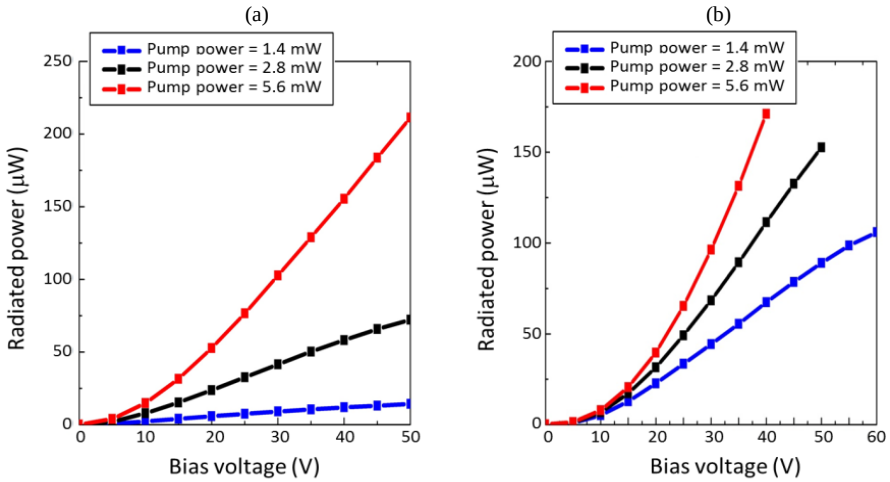

Fig. 5. Radiated power from the photoconductors based on (a) two-dimensional plasmonic contact electrodes, and (b) three-dimensional plasmonic contact electrodes as a function of the bias voltage and optical pump power.

A pyroelectric detector is used to measure the radiated power from the plasmonic photoconductive terahertz emitters in response to the optical pump. Figures 5a and 5b show the radiated power from the photoconductive emitters with the two-dimensional and three-dimensional plasmonic contact electrodes, respectively. Terahertz radiation powers up to 105 μW are measured from the photoconductive emitter with three-dimensional plasmonic contact electrodes at the optical pump power of 1.4mW, exhibiting the record-high optical-to-terahertz power conversion efficiency of 7.5%. Moreover, the radiated terahertz power from the photoconductive emitter based on three-dimensional plasmonic contact electrodes is ~6 times higher than the radiated terahertz power from the comparable photoconductive emitter based on two-dimensional plasmonic contact electrodes at the optical pump power of 1.4 mW. The observed optical-to-terahertz conversion efficiency enhancement is due to the impact of the three-dimensional plasmonic contact electrodes embedded inside the LT-GaAs substrate, which enhances the photoconductor quantum-efficiency by accumulating the majority of the photocarriers in close proximity to the contact electrodes.

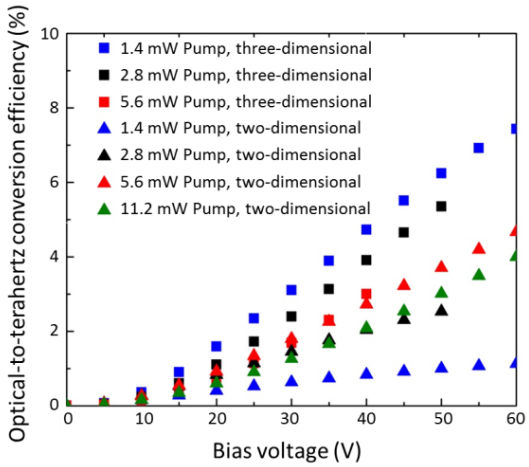

Fig. 6. Optical-to-terahertz conversion efficiency of the photoconductive emitters based on the two-dimensional and three-dimensional plasmonic contact electrodes as a function of the optical pump power and bias voltage.

While the output power of the plasmonic photoconductive emitters increase as a function of the optical pump power, their optical-to-terahertz conversion efficiency is slightly degraded at higher optical pump powers (Fig. 6). This is due to the carrier screening effect, decreasing the bias electric field when a large number of electro-hole pairs are separated from each other. It should be noted that the optical-to-terahertz conversion efficiency degradation at higher optical pump powers is more pronounced for the photoconductive emitter based on the three-dimensional plasmonic contact electrodes. This is because a larger number of photocarriers are localized in close proximity to the contact electrodes in the design with three-dimensional plasmonic contact electrodes. Therefore, separating a larger number of electron-hole pairs in the three-dimensional design induces a larger electric field in the opposite direction to the bias electric field.

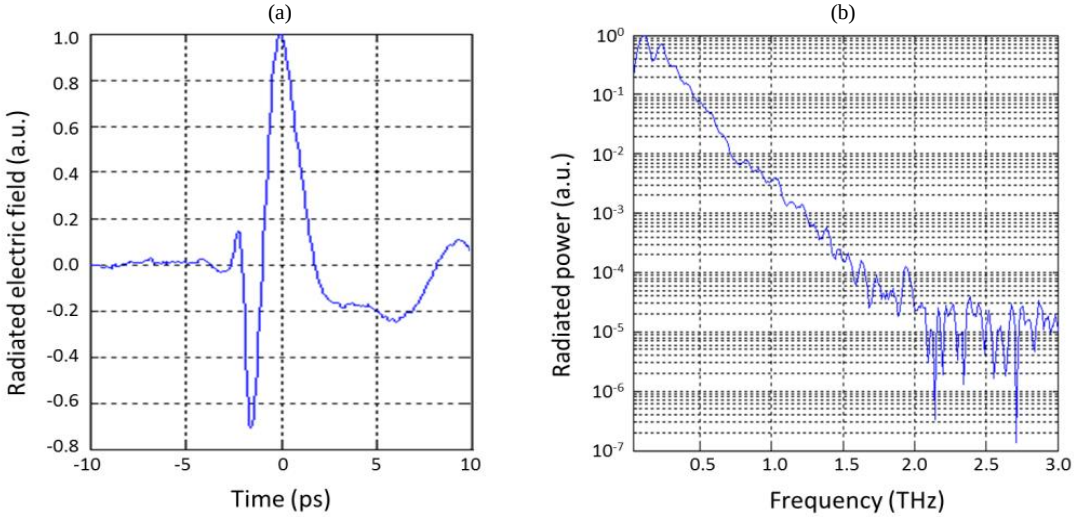

Fig. 7. Measured radiated electric field in the time-domain (a) and radiated power in frequency-domain (b) for the plasmonic photoconductive emitters with the two-dimensional and three-dimensional plasmonic contact electrodes.

Finally, the radiated field from the plasmonic photoconductive emitters is characterized in a time-domain terahertz spectroscopy setup with electro-optic detection in a 1 mm thick ZnTe crystal[19]. Figures 7a and 7b show the time-domain radiated field and frequency-domain radiated power from the photoconductive emitter with three-dimensional plasmonic contact electrodes, indicating a radiation bandwidth of more than 2 THz. It should be mentioned that the measured time-domain and frequency-domain radiation properties are identical for both photoconductive emitters based on two-dimensional and three-dimensional plasmonic contact electrodes in the 0.1-3 THz frequency range. This is because of the fact that the plasmonic contact electrodes are deep subwavelength and the radiated field is mainly affected by the spectral properties of the terahertz radiating antenna, which is identical for both photoconductive sources.

In summary, a novel plasmonic photoconductive terahertz emitter based on three-dimensional plasmonic contact electrodes integrated with a logarithmic spiral antenna on a LT-GaAs substrate is presented. The three-dimensional plasmonic contact electrodes are based on high-aspect-ratio metallic gratings embedded inside the LT-GaAs substrate. The use of the three-dimensional plasmonic contact electrodes manipulates the three-dimensional spatial distribution of photocarriers in the substrate and enhances the number of the photocarriers in close proximity to the contact electrodes. Therefore, efficient transport of the majority of the photocarriers to the

contact electrodes in a sub-picosecond time-scale in achieved, mitigating the tradeoff between high quantum-efficiency and ultrafast operation and offering high optical-to-terahertz conversion efficiencies. In order to evaluate the performance of the photoconductive emitter with three-dimensional plasmonic contact electrodes, a comprehensive characterization of the device performance in comparison with a comparable photoconductive emitter with two-dimensional plasmonic contact electrodes is presented. By use of the three-dimensional plasmonic contact electrodes, we experimentally demonstrate a record-high optical-to-terahertz conversion efficiency of 7.5% at an optical pump power of 1.4 mW. This optical-to-terahertz conversion efficiency is ~6 times higher than the optical-to-terahertz conversion efficiency offered by the two-dimensional plasmonic contact electrodes. The unprecedented power efficiency enhancement offered by the three-dimensional plasmonic contact electrodes can be further extended to offer higher optical-to-terahertz conversion efficiencies through use of higher aspect ratio three-dimensional contact electrodes and use of larger device active areas to mitigate carrier screening effect.

Plasmonic Photomixers Operating at Standard Telecommunication Wavelengths:

Photomixers are one of the most promising sources of continuous wave (CW) terahertz radiation with excellent frequency tunability and high spectral purity while operating at room temperature[20-24]. Photomixing, or photoconductive mixing, involves pumping a high-speed photoconductor integrated with a terahertz antenna with two frequency-offset pump lasers. The frequency offset of the two pump lasers and, thus, the frequency of generated photocurrent and terahertz radiation, are set to be at the desired terahertz frequency. Technological breakthroughs in fiber optic communications and availability of high power, widely tunable, narrow linewidth and compact fiber lasers and amplifiers have made telecommunication wavelengths the most desired wavelength for pumping photomixers.

The main challenge toward developing high-performance photomixers operating at telecommunication pump wavelengths is the high conductivity nature of photo-absorbing semiconductors in this wavelength range (e.g. InGaAs). This is because efficient acceleration of photocarriers inside high conductivity substrates requires sufficient biasing accompanied by high dark current levels, which could lead to thermal breakdown especially at high pump power levels. Various techniques have been explored to overcome the high conductivity limitation of photo-absorbing semiconductors at telecom wavelengths [25-28]. Among them, use of a superlattice of monolayers of ErAs in InGaAs has proven to be very effective in offering low substrate conductivity and short carrier lifetime levels simultaneously [28].

In this work, we present an ErAs:InGaAs photomixer pumped at 1550 nm pump wavelength that incorporates plasmonic contact electrodes to offer significantly higher terahertz radiation powers compared to previously demonstrated ErAs:InGaAs photomixer [28]. This is because incorporating plasmonic contact electrodes enhances the concentration of photocarriers generated in close proximity to the photomixer contact electrodes [29-35]. By reducing the average transport path length of the photocarriers to the photomixer contact electrodes, a larger number of photocarriers are drifted to the terahertz radiating element in a sub-picosecond time scale and, thus, significantly higher radiation powers are achieved [36-38].

Additionally, in order to achieve high terahertz radiation power levels, the optical pump is

modulated with a duty cycle below10%. This allows us to increase the optical pump power within each CW radiation cycle, while pushing the thermal breakdown onset to higher optical pump powers. At an average optical pump power of 150 mW with a pump modulation frequency of 1 MHz and pump duty cycle of 2%, we demonstrate up to 0.8 mW radiation power at 1 THz, within each CW radiation cycle.

Figure 8a shows the microscope image of the plasmonic photomixer fabricated on an ErAs:InGaAs substrate, with a carrier lifetime of ~0.85 ps. In order to achieve a broad radiation frequency range, a logarithmic spiral antenna is used as the terahertz radiating element. The logarithmic spiral antenna is designed to offer a broadband radiation resistance of 70-100 Ω while maintaining a reactance value near 0 Ω over the 0.1-2.5 THz frequency range [19-40]. Figure 8b shows the scanning electron microscope (SEM) image of the plasmonic contact electrodes. Each contact electrode of the plasmonic photomixer is a plasmonic grating covering a 15×15 μm^2 area, with 200 nm pitch, 100 nm metal width, 5/45 nm Ti/Au height, and a 250 nm thick Si_3N_4 anti-reflection coating. The plasmonic contact electrodes are designed to maximize device quantum efficiency at optical pump wavelength of 1550 nm [36, 37, 41]. The end-to-end spacing between the anode and cathode contact electrodes is set to 10 μm to maintain the highest photocarrier drift velocity across the entire 15×15 μm^2 plasmonic contact electrode area [35, 42].

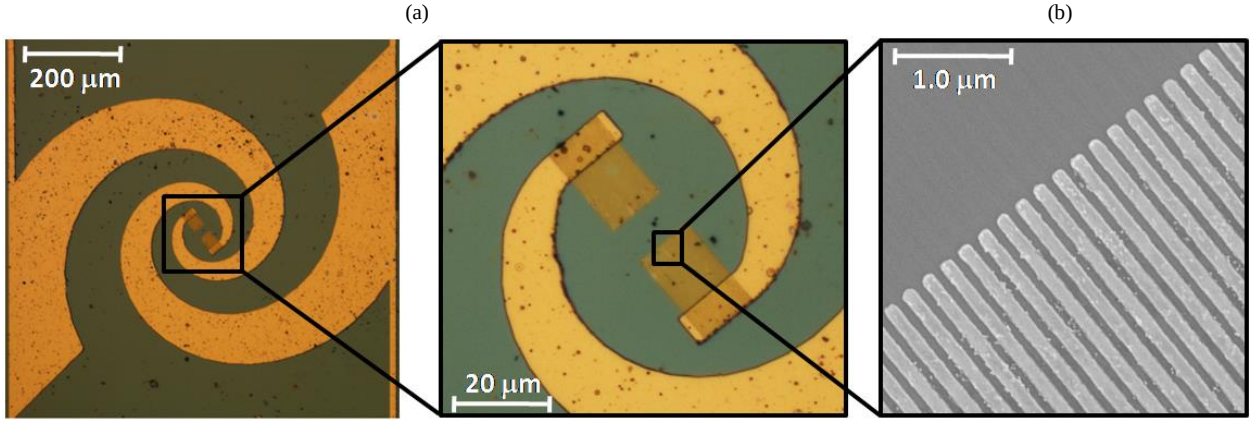

Fig. 8. (a) Microscope image of the fabricated plasmonic photomixer with a logarithmic spiral antenna integrated with plasmonic contact electrodes on an ErAs:InGaAs substrate. (b) SEM image of the plasmonic contact electrodes.

The fabrication process starts with patterning plasmonic contact electrode gratings using electron-beam lithography followed by deposition of Ti/Au (5/45 nm) and liftoff. A 250 nm Si_3N_4 anti-reflection coating is then deposited using plasma-enhanced chemical vapor deposition. Next, contact vias are patterned using optical lithography and formed using dry plasma etching. Finally, the logarithmic spiral antennas and bias lines are patterned using optical lithography, followed by deposition of Ti/Au (10/400 nm) and liftoff.

The fabricated plasmonic photomixers are then mounted on a hyper-hemispherical silicon lens and characterized using two frequency-offset pump lasers in the 1550 nm wavelength range. In order to mitigate thermal breakdown, which is the ultimate limit for device failure at high optical pump powers, the optical pump is modulated with a duty cycle below10%. Using short optical pump duty cycles allows increasing the optical pump power within each CW radiation cycle,

while pushing the thermal breakdown onset to higher optical pump powers. In this work, the CW optical beam from the wavelength-tunable optical sources is modulated at 1 MHz and then amplified using a pulsed fiber amplifier. The photomixers are characterized at 2%, 4%, 6%, and 8% pump duty cycles, generating terahertz waves over 20, 40, 60, and 80 ns CW radiation cycles, respectively.

Figure 9 shows the experimental setup used for characterizing the plasmonic photomixers. It consists of two fiber-coupled CW lasers, one with a fixed wavelength at 1545.4 nm (QPhotonics QDFBLD-1550-10) and the other one with a tunable wavelength (Santec TSL-510). The output of the two lasers are combined in a 2:1 fiber combiner and modulated by an acousto-optic modulator (NEOS Technologies 15200-.2-1.55-LTD-GaP-FO). The pulsed laser beam is then amplified using a pulse amplifier (Optilab APEDFA-C-10) and focused onto the plasmonic photomixer. For optimal photomixing efficiency, the incident light from two laser sources should be linearly polarized with equal power levels. For this purpose, a quarter waveplate is used to convert the polarization of the laser light to circular polarization and convert it back to a linear polarization using a linear polarizer. In order to adjust the two laser beams to have equal power levels, a pellicle is used to separate a ~8% of the laser beam to be monitored by an optical spectrum analyzer.

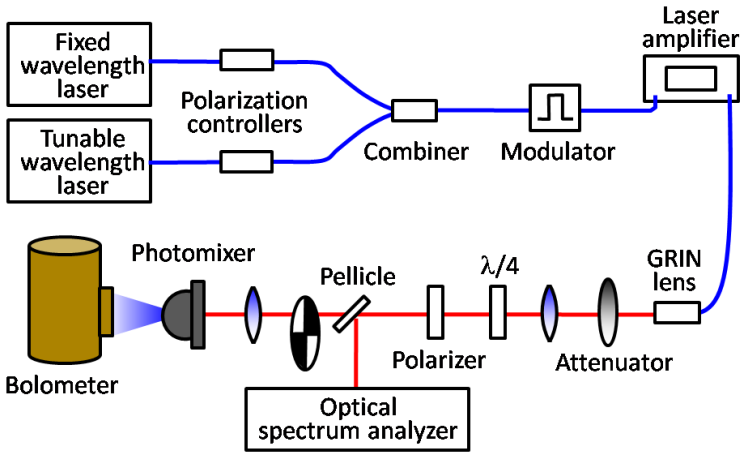

Fig. 9. Experimental setup for characterizing the ErAs:InGaAs plasmonic photomixer prototypes

Finally, the generated terahertz radiation is measured via a silicon bolometer, while tuning the wavelength of the tunable laser. In order to achieve the highest photomixing efficiency, the focus spot size and position of the incident optical pump is adjusted to maximize the induced photocurrent level. The optimum focus spot of the pump overlaps with both anode and cathode plasmonic contact electrodes and is positioned closer to the edge of the contact electrodes.

Figure 10a shows the radiated terahertz power within each CW radiation cycle as a function of the average optical pump power, for a radiation duty cycle of 2% and photomixer bias voltage of 10 V. The radiated terahertz power within each CW radiation cycle increases quadratically as a function of the average pump power (Fig. 10b). At an average optical pump power of 150 mW, terahertz radiation powers as high as 0.8 mW are achieved at 1 THz over 20 ns CW radiation cycles, corresponding to a spectral linewidth broadening of 50 MHz.

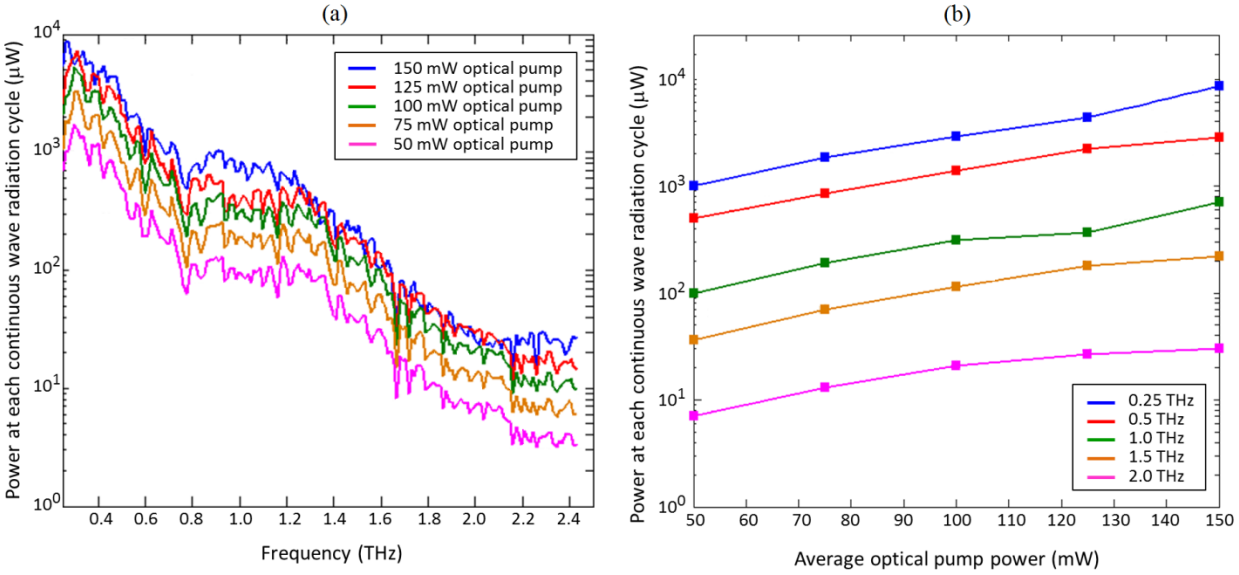

Fig. 10. (a) Radiated terahertz power from the plasmonic photomixer as a function of frequency for a radiation duty cycle of 2%, photomixer bias voltage of 10 V, and average optical pump power ranging from 50 mW to 150 mW. (b) Radiated terahertz power from the plasmonic photomixer as a function of the average optical pump power for a radiation duty cycle of 2%, photomixer bias voltage of 10 V, and 0.25 THz, 0.5 THz, 1 THz, 1.5 THz, and 2 THz radiation frequency.

Figure 11 shows the tradeoff between the radiated terahertz power and spectral linewidth as a function of the pump duty cycle. The terahertz power measurements are taken at an average optical pump power of 100 mW and a pump modulation frequency of 1 MHz. At the optical pump duty cycles of 2%, 4%, 6%, and 8%, radiation power levels as high as 300 μW, 75 μW, 35 μW, and 20 μW are measured at 1 THz over 20, 40, 60, and 80 ns CW radiation cycles (Fig. 11a), corresponding to 50, 25, 16, and 12.5 MHz linewidth broadening, respectively (Fig. 11b). The radiation linewidth broadening is estimated using the Fourier theory.

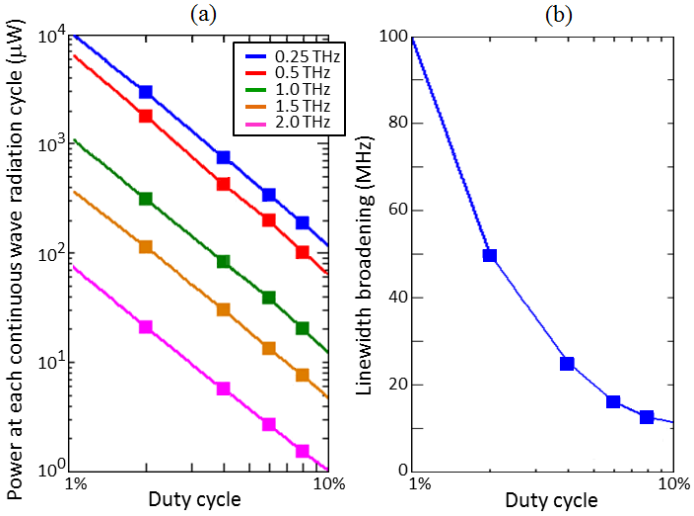

Fig. 11. (a) Radiated terahertz power from the plasmonic photomixer as a function of pump duty cycle for a photomixer bias voltage of 10 V and average optical pump power of 100 mW. (b) Estimated spectral broadening of the radiated terahertz wave from the plasmonic photomixer as a function of pump duty cycle for a pump modulation frequency of 1 MHz.

As expected, use of shorter optical pump duty cycles allows increasing the optical pump power within each CW radiation cycle, while pushing the thermal breakdown onset to higher optical pump powers. Since the terahertz radiation power from the photomixer has a quadratic relation with the optical pump power, reducing the optical pump duty cycle dramatically increases the optical-to-terahertz conversion efficiency and the maximum radiated power from a photomixer before thermal breakdown. In the meantime, use of shorter CW radiation cycles results in broader radiation linewidths. Therefore, the duty cycle and repetition rate of the optical pump should be carefully selected to satisfy the spectral linewidth requirements of the specific application the photomixer is used for. In this regard, reducing the pump modulation frequency in our measurements would reduce the radiation linewidth while offering the same terahertz radiation power levels at a given optical pump duty cycle.

In summary, we present an ErAs:InGaAs plasmonic photomixer operating at 1550 nm optical pump wavelength, which offers significantly higher terahertz radiation power levels compared to previously demonstrated photomixers. Similar to previously demonstrated plasmonic photoconductive terahertz emitters, the presented plasmonic photomixer takes advantage of the enhanced device quantum efficiency enabled by the enhanced photocarrier concentration near the plasmonic contact electrodes. Moreover, the photomixer takes advantage of pump duty cycles below 10% to push the thermal breakdown onset to higher optical pump powers and achieve higher terahertz radiation powers. At an average optical pump power of 150 mW with a pump modulation frequency of 1 MHz and pump duty cycle of 2%, we demonstrate up to 0.8 mW radiation power at 1 THz within each CW radiation cycle. The enhanced terahertz radiation powers offered by the presented 1550 nm plasmonic photomixer would have a big impact on next generation terahertz imaging and spectroscopy systems.

References

[1] M. Tonouchi, Nat. Photon. 1, 97-105, 2007.
[2] D. Van der Weide, J. Murakowski, and F. Keilmann, IEEE Trans. Microwave Theory and Techniques 48, 740-743, 2000.
[3] N. Nagai, T. Imai, R. Fukasawa, K. Kato, and K. Yamauchi, Appl. Phys. Lett. 85, 4010, 2004.
[4] L. Van Zandt and V. Saxena, Phys. Rev. A 39, 2672-2674, 1989.
[5] P. Siegel, IEEE Trans. Microwave Theory and Techniques 52, 2438-2447, 2004.
[6] M. Nagel, M. Forst, and H. Kurz, J. Phys. Condensed Matter 18, S601-S618, 2006.
[7] D. H. Auston, K. P. Cheung, and P. R. Smith, Appl. Phys. Lett, 45, 284, 1984.
[8] S. Preu, G. H. Dohler, S. Malzer, L. J. Wang, and A. C. Gossard, J. Appl. Phys. 109, 061301, 2011.
[9] S.-G. Park, K. H. Jin, M. Yi, J. C. Ye, J. Ahn, and K.-H. Jeong, ACS Nano 6, 2026-2031, 2012.
[10] C. W. Berry, M. R. Hashemi, M. Jarrahi, Proc. International Conference on Infrared, Millimeter, and Terahertz Waves, Mainz, Germany, September 1-6, 2013.
[11] C. W. Berry, N. Wang, M. R. Hashemi, M. Unlu, and M. Jarrahi, Nat. Commun. 4, 1622, 2013.
[12] C. W. Berry, M. Jarrahi, New J. Phys. 14, 105029, 2012.
[13] C. W. Berry, M. Jarrahi, Proc. International Conference on Infrared, Millimeter, and Terahertz Waves, Houston, TX, Oct 2-7, 2011.
[14] P. B. Catrysse, G. Veronis, H. Shin, J. T. Shen, and S. Fan, Appl. Phys. Lett. 88, 031101, 2006.
[15] B-Y. Hsieh, M. Jarrahi, J. Appl. Phys. 109, 084326, 2011.
[16] S.-H. Yang, M. Jarrahi, Opt. Lett. 38, 3677-3679, 2013.
[17] P. C. Upadhya et. al., Opt. Lett. 32, 2297-2299, 2007.
[18] C. W. Berry, M. Jarrahi, J. Infrared, Millimeter and Terahertz Waves 33, 1182-1189, 2012.
[19] C. W. Berry, M. R. Hashemi, M. Unlu, M. Jarrahi, J. Vis. Experiments 77, e50517, doi:10.3791/50517, 2013.
[20] S. Preu, G. H. Dohler, S. Malzer, L. J. Wang and A. C. Gossard, J. Appl. Phys. 109, 061301, 2011.
[21] E. R. Brown, F. W. Smith, K. A. McIntosh, Appl. Phys. Lett. 73, 1480, 1993.

[22] J. Bjarnason, J. Chan, A. W. M. Lee, E. R. Brown, D. C. Driscoll, M. Hanson, A. C. Gossard and R. E. Muller, Appl. Phys. Lett. 85, 3983-3985, 2004.
[23] E. Peytavit, S. Lepilliet, F. Hindle, C. Coinon, T. Akalin, G. Ducournau, G. Mouret and J.-F. Lampin, Appl. Phys. Lett. 99, 223508, 2011.
[24] E. A. Michael, B. Vowinkel, R. Schieder, M. Mikulics, M. Marso, and P. Kordos, Apl. Phys. Lett. 86, 111120, 2005.
[25] J. R. Middendorf and E. R. Brown, Opt. Express 20, 16504-16509, 2012.
[26] M. Suzuki and M. Tonouchi, Appl. Phys. Lett. 86, 051104, 2005.
[27] A. Takazato, M. Kamakura, T. Matsui, J. Kitagawa and Y. Kadoya, Appl. Phys. Lett. 90, 101119, 2007.
[28] M. Sukhotin, E. R. Brown, A. C. Gossard, D. Driscoll, M. Hanson, P. Maker and R. Muller, Appl. Phys. Lett. 82, 3116, 2003.
[29] S.-G. Park, K. H. Jin, M. Yi, J. C. Ye, J. Ahn and K.-H. Jeong, ACS Nano 6, 2026, 2012.
[30] S. Liu, X. Shou and A. Nahata, IEEE Trans. Terahertz Sci. Technol. 1, 412, 2011.
[31] S.-G. Park, Y. Choi, Y.-J. Oh and K.-H. Jeong, Opt. Express 20, 25530, 2012.
[32] N. Wang, M. R. Hashemi and M. Jarrahi, Opt. Express 21, 17221, 2013.
[33] B. Heshmat, H. Pahlevaninezhad, Y. Pang, M. Masnadi-Shirazi, R. B. Lewis, T. Tiedje, R. Gordon and T. E. Darcie, Nano Lett. 12, 6255, 2012.
[34] S.-H. Yang and M. Jarrahi, Opt. Lett. 38, 3677, 2013.
[35] B.-Y. Hsieh and M. Jarrahi, J. Appl. Phys. 109, 084326, 2011.
[36] C. W. Berry and M. Jarrahi, New J. Physics 14, 105029, 2012.
[37] C. W. Berry, N. Wang, M. R. Hashemi, M. Unlu and M. Jarrahi, Nat. Commun. 4, 1622, 2013.
[38] C. W. Berry, M. R. Hashemi and M. Jarrahi, Appl. Phys. Lett. 14, 081122, 2014.
[39] Y. Huo, G. W. Taylor and R. Bansal, J. Infrared, Millimeter and Terahertz Waves 23, 819-839, 2002.
[40] E. R. Brown, A. W. M. Lee, B. S. Navi and J. E. Bjarnason, Microwave Opt. Technol. Lett. 48, 524-529, 2006.
[41] P. B. Catrysse, G. Veronis, H. Shin, J.-T. Shen, and S. Fan, Appl. Phys. Lett. 88, 031101, 2006.
[42] C. W. Berry and M. Jarrahi, J Infrared, Millimeter and Terahertz Waves 33, 1182, 2012.

Army Research Office Progress Report

ARO-YIP: Fundamental Properties and Capabilities of Plasmonic Antennas for Efficient Interaction with Nanoelectronics

Contract # W911NF-12-1-0253

Performance Period: 07/01/2014 – 06/30/2015

Program Manager: Dr. James Harvey

Lead Organization: University of Michigan, Ann Arbor

Technical Point of Contact: Mona Jarrahi (mjarrahi@umich.edu)

Administrative Point of Contact: Michelle Chapman (chapman@eecs.umich.edu)

Executive Summary

Here is a list of research activities conducted during the third year of the ARO-YIP program:

- We extended the powerful capabilities of the nano-plasmonic antennas that we demonstrated during the first two years of the research program to achieve record-high power terahertz radiation pulses. In this regard, we presented a novel design of large area photoconductive emitters which incorporates plasmonic contact electrodes to offer significantly higher optical-to-terahertz conversion efficiencies compared to conventional designs. The presented terahertz emitter can offer high power terahertz radiation because of its capacity to handle relatively high optical powers without suffering from the carrier screening effect and thermal breakdown. Additionally, it can offer broadband terahertz radiation due to the fact that terahertz radiation is generated by dipole nano-plasmonic antennas embedded within the device active area with dipole lengths much smaller than terahertz radiation wavelength. Moreover, use of plasmonic contact electrodes enables a more efficient separation and acceleration of photocarriers, enhancing the effective dipole moment induced within the device active area in response to an incident optical pump. We demonstrate broadband, pulsed terahertz radiation with record-high radiation power levels as high as 3.8 mW over 0.1-5 THz frequency range, exhibiting an order of magnitude higher optical-to-terahertz conversion efficiency compared to conventional designs.

- We extended the powerful capabilities of the nano-plasmonic antennas that we demonstrated during the first two years of the research program to develop advanced heterodyne receivers for terahertz spectrometry. The heterodyne receiver is based on plasmonic photomixers, which employs optical beams from two wavelength-tunable CW lasers with a terahertz frequency difference as the local oscillator. By coupling the optical local oscillator and terahertz signal into specifically-designed semiconductor plasmonic nanostructures, photo-generated carriers can be drifted to the contact electrodes by the incident terahertz electric field and the mixing process can occur directly. The induced IF current is then collected from the nanostructure contact electrodes, coupled to a microwave transmission line, and routed to successive amplifier, filter and detector stages for final processing. First generation heterodyne receivers are based on nano-plasmonic dipole antennas and offer significantly higher signal-to-noise ratio levels and dynamic ranges, as well as broader frequency operation ranges compared to existing heterodyne receivers based on terahertz local oscillators and SIS/HEB/Schottky diode mixers, making them a very promising candidate for future terahertz spectrometers for advanced chemical sensing.

- This research in the 07/01/2014 – 06/30/2015 performance period has resulted in 8 peer-reviewed journal papers, 15 peer-reviewed conference papers, 14 peer-reviewed conference abstracts, 35 keynote/plenary/tutorial/invited talks, 1 Ph.D. Dissertation, 3 pending and 1 provisional patents. The results of our research have been also highlighted in many science and technology news outlets including Laser Focus World and SPIE Newsroom. Additionally, the PI of this project, Mona Jarrahi, has received the IEEE Antennas and Propagation Society (AP-S) Lot Shafai Mid-Career Distinguished Achievement Award, has been named a Kavli Fellow by the National Academy of Sciences, and has been selected as an IEEE Microwave Theory and Techniques Society Distinguished Lecture. Moreover, the students working on this project have received IEEE Antennas and Propagation Society

Doctoral Research Award, Optical Terahertz Science & Technology Conference Best Poster Prize (2nd place), University of Michigan Rackham Summer Award, SPIE Scholarship in Optics and Photonics, Taiwanese Government Studying Abroad Scholarship. The details are as follows:

PI Awards and Recognitions

- IEEE Antennas and Propagation Society (AP-S) Lot Shafai Mid-Career Distinguished Achievement Award (2015)
- IEEE Microwave Theory and Techniques Society Distinguished Lecturer (2015)
- Kavli Fellow by the National Academy of Sciences (2014)

Student Awards and Recognitions

- SPIE Scholarship in Optics and Photonics received by Nezih Tolga Yardimci (2015)
- Taiwanese Government Studying Abroad Scholarship received by Shang-Hua Yang (2015)
- University of Michigan Rackham Summer Award received by Shang-Hua Yang (2015)
- Optical Terahertz Science & Technology Conference Best Poster Prize (2nd place) by Ning Wang (2015)
- IEEE Antennas and Propagation Society Doctoral Research Award received by Shang-Hua Yang (2014)

Journal Publications

1. S.-H. Yang, M. Jarrahi, "Frequency-Tunable Continuous-Wave Terahertz Sources based on GaAs Plasmonic Photomixers," *Applied Physics Letters*, 2015 (in press)
2. S.-H. Yang, M. Jarrahi, "Spectral Characteristics of Terahertz Radiation from Plasmonic Photomixers," *Optics Express*, 2015 (in press)
3. M. Jarrahi, "Advanced Photoconductive Terahertz Optoelectronics based on Nano-Antennas and Nano-Plasmonic Light Concentrators," *IEEE Transactions on Terahertz Science and Technology*, 5, 391-397, 2015
4. N. T. Yardimci, S.-H. Yang, C. W. Berry, M. Jarrahi, "High Power Terahertz Generation Using Large Area Plasmonic Photoconductive Emitters," *IEEE Transactions on Terahertz Science and Technology*, 5, 223-229, 2015
5. M. Unlu, M. Jarrahi, "Miniature Multi-Contact MEMS Switch for Broadband Terahertz Modulation," *Optics Express*, 22, 32245–32260, 2014
6. M. Unlu, M. Hashemi, C. W. Berry, S. Li, S.-H. Yang, M. Jarrahi, "Fully Integrated Broadband Terahertz Modulators," *SPIE Newsroom, International Society for Optics and Photonics*, DOI:10.1117/2.1201410.005657, 2014
7. M. Jarrahi, I. Mehdi, "Emerging technologies for next generation terahertz systems," *IEEE Microwave Magazine*, 15, 30-32, 2014
8. C.W. Berry, N. T. Yardimci, M. Jarrahi, "Responsivity Calibration of Pyroelectric Terahertz Detectors," arXiv:1412.6878v1, 2014

Conference Publications

1. N. T. Yardimci, S.-H. Yang, M. Jarrahi, "High Power Pulsed Terahertz Radiation From Large Area Photoconductive Emitters," *Proc. International Conference on Infrared, Millimeter, and Terahertz Waves*, Hong Kong, August 23-28, 2015
2. M. R. M. Hashemi, S.-H. Yang, T. Wang, N. Sepúlveda, M. Jarrahi, "Fully-Integrated and Electronically-Controlled Millimeter-Wave Phase Modulator," *Proc. International Conference on Infrared, Millimeter, and Terahertz Waves*, Hong Kong, August 23-28, 2015

3. M. Jarrahi, "Plasmonics Enabled Advances in Photoconductive Terahertz Radiation Sources," *Proc. International Conference on Infrared, Millimeter, and Terahertz Waves,* Hong Kong, August 23-28, 2015
4. N. T. Yardimci, M. Jarrahi, "3.8 mW Terahertz Radiation Generation through Plasmonic Nano-Antenna Arrays," *Proc. IEEE International Antennas and Propagation Symposium*, Vancouver, Canada, July 19-25, 2015
5. M. R. Hashemi, S.-H. Yang, T. Wang, N. Sepulveda, M. Jarrahi, "Millimeter-Wave Phase Modulator Based on Vanadium Dioxide Meta-Surfaces," *Proc. IEEE International Antennas and Propagation Symposium*, Vancouver, Canada, July 19-25, 2015
6. N. T. Yardimci, M. Jarrahi, "3.8 mW Terahertz Radiation Generation over a 5 THz Radiation Bandwidth through Large Area Plasmonic Photoconductive Antennas," *IEEE Microwave Symposium Digest*, Phoenix, AZ, May 17-22, 2015
7. M. Jarrahi, "High-Efficiency Terahertz Sources based on Plasmonic Contact Electrodes," *IEEE Microwave Symposium Digest*, Phoenix, AZ, May 17-22, 2015
8. N. T. Yardimci, S.-H. Yang, C. W. Berry, M. Jarrahi, "Terahertz Radiation Enhancement in Large-Area Photoconductive Sources by Using Plasmonic Nanoantennas," *Proc. Conference of Lasers and Electro-Optics*, San Jose, CA, May 10-15, 2015
9. M. R. Hashemi, S.-H. Yang, T. Wang, N. Sepulveda, M. Jarrahi, "Efficient Terahertz Phase Modulation Using Vanadium Dioxide Meta-Surfaces ," *Proc. Conference of Lasers and Electro-Optics*, San Jose, CA, May 10-15, 2015
10. N. T. Yardimci, S.-H. Yang, C. W. Berry, M. Jarrahi, "Large Area Plasmonic Photoconductive Emitters for Generating High Power Broadband Terahertz Radiation ," *Proc. Frontiers in Optics*, Tucson, AZ, October 19-23, 2014
11. N. T. Yardimci, S.-H. Yang, C. W. Berry, M. Jarrahi, "Plasmonics Enhanced Terahertz Radiation from Large Area Photoconductive Emitters," *Proc. IEEE Photonics Conference,* San Diego, CA, October 12-16, 2014
12. C. W. Berry, M. R. Hashemi, S. Preu, H. Lu, A. C. Gossard, M. Jarrahi, "High Power Terahertz Generation From ErAs:InGaAs Plasmonic Photomixers," *Proc. International Conference on Infrared, Millimeter, and Terahertz Waves,*Tucson, AZ, Sep 14-19, 2014
13. S.-H. Yang, M. R. Hashemi, C. W. Berry, M. Jarrahi, "Three-Dimensional Plasmonic Contact Electrodes for High-Efficiency Photoconductive Terahertz Sources," *Proc. International Conference on Infrared, Millimeter, and Terahertz Waves,*Tucson, AZ, Sep 14-19, 2014
14. S.-H. Yang, M. R. Hashemi, C.W. Berry, M. Jarrahi, "High-Efficiency Photoconductive Terahertz Antennas based on High-Aspect Ratio Plasmonic Electrodes," *Proc. IEEE International Antennas and Propagation Symposium,* Memphis, TN, July 6-12, 2014
15. C. W. Berry, M. R. Hashemi, S. Preu, H. Lu, A. C. Gossard, M. Jarrahi, "Terahertz Radiation Enhancement through Use of Plasmonic Photomixers," *Proc. IEEE International Antennas and Propagation Symposium*, Memphis, TN, July 6-12, 2014

Conference Abstracts

1. M. Jarrahi, "Plasmonics-Enabled Advancements in Terahertz Imaging and Spectroscopy Systems," *International Symposium on Frontiers in THz Technology*, Hamamatsu, Japan, August 30 - September 2, 2015
2. M. Jarrahi, "New Frontiers in Terahertz Technology," *8th Global Symposium on Millimeter-Waves*, Montreal, Canada, May 25-27, 2015
3. M. Jarrahi, "Plasmonics Enabled High Power Terahertz Sources," *Proc. International Workshop on Optical Terahertz Science and Technology*, San Diego, CA, March 8-13, 2015
4. N. Wang, M. Jarrahi, "Heterodyne Terahertz Receiver Based on Plasmonic Photomixers," *Proc. International Workshop on Optical Terahertz Science and Technology*, San Diego, CA, March 8-13, 2015

5. M. R. Hashemi, S.-H. Yang, T. Wang, N. Sepúlveda, M. Jarrahi, "Voltage-Controlled Terahertz Phase Modulator based on Vanadium Dioxide," *Proc. International Workshop on Optical Terahertz Science and Technology*, San Diego, CA, March 8-13, 2015
6. S.-H. Yang , C. W. Berry, N. T. Yardimci, M. R. Hashemi, M. Jarrahi, "High-Aspect Ratio Plasmonic Photoconductive Terahertz Sources," *Proc. International Workshop on Optical Terahertz Science and Technology*, San Diego, CA, March 8-13, 2015
7. N. T. Yardimci , S.-H. Yang, C. W. Berry, M. Jarrahi, "Significant Terahertz Radiation Enhancement in Large Area Photoconductive Emitters by Incorporating Plasmonic Contact Electrode Gratings," *Proc. International Workshop on Optical Terahertz Science and Technology*, San Diego, CA, March 8-13, 2015
8. C. W. Berry, M. R. Hashemi, S. Preu, H. Lu, A. Gossard, M. Jarrahi, "Plasmonic Photomixers for High-Power Continuous-Wave Terahertz Generation," *Proc. SPIE Photonic West*, San Francisco, CA, February 7-12, 2015
9. N. T. Yardimci, S.-H. Yang, C. W. Berry, M. Jarrahi, "High-power and broadband terahertz generation through large-area plasmonic photoconductive emitters," *Proc. SPIE Photonic West*, San Francisco, CA, February 7-12, 2015
10. S.-H. Yang, N. T. Yardimci, M. Jarrahi, "Compensating the carrier screening effect in plasmonic photoconductive terahertz sources," *Proc. SPIE Photonic West*, San Francisco, CA, February 7-12, 2015
11. M. Jarrahi, "Plasmonic Terahertz Optoelectronics," *SPIE Photonic West*, San Francisco, CA, February 7-12, 2015
12. M. Jarrahi, "Plasmonic Terahertz Sources for High Performance Terahertz Imaging and Spectroscopy," *Proc. 5th International Symposium on Terahertz Nanoscience*, Martinique, December 1-5, 2014
13. M. Jarrahi, "Game-Changing Terahertz Sensor Technologies for Large-Scale Consumer Market," *Trillion Sensors Summit*, San Diego, CA, November 12-13, 2014
14. M. Jarrahi, "Advanced Terahertz Imaging and Spectroscopy Systems based on Plasmonic Terahertz Optoelectronics," *Proc. SPIE Optics and Photonics Conference*, San Diego, CA, August 17-21, 2014

Keynote/Plenary/Tutorial/Invited Talks

1. M. Jarrahi, "New Frontiers in Terahertz Technology," *15th Mediterranean Microwave Symposium*, Lecce, Italy, November 30- December 2, 2015 (Keynote talk)
2. M. Jarrahi, "New Frontiers in Terahertz Technology," *IEEE Santa Clara Chapter*, Santa Clara, CA, November 2015
3. M. Jarrahi, "New Frontiers in Terahertz Technology," *Electrical Engineering Department California Institute of Technology*, Pasadena, CA, October 2015
4. M. Jarrahi, "New Frontiers in Terahertz Technology," *24th International Conference on Optical Fiber Sensors*, Curitiba, Brazil, September 28 - October 2, 2015 (Plenary talk)
5. M. Jarrahi, "New Frontiers in Terahertz Technology," *IEEE MTT-S International Microwave Workshop on RF and Wireless Technologies for Biomedical and Healthcare Applications*, Taipei, Taiwan, September 21-23, 2015 (Keynote talk)
6. M. Jarrahi, "New Frontiers in Terahertz Technology," *Department of Electrical Engineering National Taiwan University*, Taipei, Taiwan, September 2015
7. M. Jarrahi, "New Frontiers in Terahertz Technology," *MIT Lincoln Laboratory*, Lexington, MA, September 2015
8. M. Jarrahi, "New Frontiers in Terahertz Technology," *IEEE Buenaventura Communications Society Chapter*, Newbury Park, CA, September 2015
9. M. Jarrahi, "High performance terahertz radiation sources based on plasmonic photoconductors," *Workshop on Terahertz Technologies (in association with European Microwave Conference)*, Paris, France, September 6-11, 2015

10. M. Jarrahi, "Plasmonics-Enabled Advancements in Terahertz Imaging and Spectroscopy Systems," *International Symposium on Frontiers in THz Technology*, Hamamatsu, Japan, August 30 - September 2, 2015
11. M. Jarrahi, "New Frontiers in Terahertz Technology," *Department of Electronic Engineering City University of Hong Kong*, Hong Kong, August 2015
12. N. T. Yardimci, S.-H. Yang, M. Jarrahi, "High Power Pulsed Terahertz Radiation From Large Area Photoconductive Emitters," *International Conference on Infrared, Millimeter, and Terahertz Waves*, Hong Kong, August 23-28, 2015 (Keynote talk)
13. M. Jarrahi, "Plasmonics Enabled Advances in Photoconductive Terahertz Radiation Sources," *International Conference on Infrared, Millimeter, and Terahertz Waves*, Hong Kong, August 23-28, 2015 (Keynote talk)
14. M. Jarrahi, "Plasmonic Terahertz Optoelectronics for Advanced Imaging and Sensing Applications," *Women in Optics Summer School: The Castle Meeting*, August 3-6, Ebsdorfergrund, Germany, 2015
15. M. Jarrahi, "New Frontiers in Terahertz Technology," *University of Queensland, The School of School of Information Technology and Electrical Engineering*, Brisbane Australia, July 2015
16. M. Jarrahi, "New Frontiers in Terahertz Technology," *University of Adelaide, The School of Electrical and Electronic Engineering*, Adelaide Australia, July 2015
17. M. Jarrahi, "New Frontiers in Terahertz Technology," *Georgia Institute of Technology, The School of Electrical and Computer Engineering*, Atlanta, GA, June 2015
18. M. Jarrahi, "New Frontiers in Terahertz Technology," *8th Global Symposium on Millimeter-Waves*, Montreal, Canada, May 25-27, 2015
19. M. Jarrahi, "High-Efficiency Terahertz Sources based on Plasmonic Contact Electrodes," *IEEE International Microwave Symposium*, Phoenix, AZ, May 17-22, 2015
20. M. Jarrahi, "Plasmonics Enabled High Power Terahertz Sources," *International Workshop on Optical Terahertz Science and Technology*, San Diego, CA, March 8-13, 2015
21. M. Jarrahi, "New Frontiers in Terahertz Technology," *Department of Electrical and Computer Engineering Purdue University*, West Lafayette, IN, March 2015
22. M. Jarrahi, "New Frontiers in Terahertz Technology," *Department of Physics and Optical Engineering Rose-Hulman Institute of Technology*, Terre Haute, IN, March 2015
23. M. Jarrahi, "Plasmonic Terahertz Optoelectronics for Advanced Terahertz Imaging and Sensing," *Department of Electrical and Computer Engineering Lehigh University*, Bethlehem, PA, March 2015
24. M. Jarrahi, "New Frontiers in Terahertz Technology," *College of Optical Sciences, University of Arizona*, Tucson, AZ, March 2015
25. M. Jarrahi, "New Frontiers in Terahertz Technology," *Raytheon*, Albuquerque, NM, February 2015
26. C. W. Berry, M. R. Hashemi, S. Preu, H. Lu, A. Gossard, M. Jarrahi, "Plasmonic Photomixers for High-Power Continuous-Wave Terahertz Generation," *SPIE Photonic West*, San Francisco, CA, February 7-12, 2015
27. M. Jarrahi, "Plasmonic Terahertz Optoelectronics," *SPIE Photonic West*, San Francisco, CA, February 7-12, 2015 (Keynote talk)
28. M. Jarrahi, "Plasmonic Terahertz Sources for High Performance Terahertz Imaging and Spectroscopy," *5th International Symposium on Terahertz Nanoscience*, Martinique, December 1-5, 2014
29. M. Jarrahi, "Game-Changing Terahertz Sensor Technologies for Large-Scale Consumer Market," *Trillion Sensors Summit*, San Diego, CA, November 12-13, 2014
30. M. Jarrahi, "Plasmonic Enhanced Terahertz Imaging and Spectroscopy," *International Symposium on Optomechatronic Technologies*, Seattle, WA, November 5-7, 2014 (Plenary talk)
31. M. Jarrahi, "Pushing the Limits of Terahertz Optoelectronics", *IEEE Photonics Society UCLA Chapter Seminar*, Los Angeles, CA, October 2014

32. N. T. Yardimci, S.-H. Yang, C. W. Berry, M. Jarrahi, "Plasmonics Enhanced Terahertz Radiation from Large Area Photoconductive Emitters," *IEEE Photonics Conference,* San Diego, CA, October 12-16, 2014
33. M. Jarrahi, "An Overview of Recent Advances in Plasmonic Photoconductive Terahertz Sources," *Workshop on Terahertz Technologies (in association with European Microwave Conference),* Rome, Italy, October 5-10, 2014
34. M. Jarrahi, "Nanophotonics and Plasmonics for Advancement of Terahertz Technology," *IEEE International Conference on Nanotechnology*, Toronto, Canada, August 18-21, 2014 (Keynote talk)
35. M. Jarrahi, "Advanced Terahertz Imaging and Spectroscopy Systems based on Plasmonic Terahertz Optoelectronics," *SPIE Optics and Photonics Conference,* San Diego, CA, August 17-21, 2014

Ph.D. Dissertation

1. N.Wang, "High Sensitivity Terahertz Receivers Based on Plasmonic Photoconductors", *Electrical Engineering and Computer Science Department*, University of Michigan, Ann Arbor, 2015

Patents

1. M. Jarrahi, "Terahertz Endoscopy through Laser-Driven Terahertz Sources and Detectors," Provisional Patent Application No. 62167201, filed 05/27/15
2. M. Jarrahi, "Low-Duty-Cycle Continuous-Wave Photoconductive Terahertz Imaging and Spectroscopy Systems," Pending International Patent Application No. PCT/US2015/035685, filed 06/12/15
3. M. Jarrahi, M. Unlu, M. R. Hashemi, C. W. Berry, and S. Li, "Reconfigurable Device for Terahertz and Infrared Filtering and Modulation," Pending International Patent Application No. PCT/US14/49866, filed 08/06/14
4. M. Jarrahi, C. W. Berry, N. Wang, S.-H. Yang, and M. R. Hashemi, "Photoconductive Device with Plasmonic Electrodes," Pending International Patent Application No. PCT/US2013/022776, filed 01/23/13 (US Serial No. 14/372,779) (European Application number is 13741491.8) (Japanese Application number is 2014-553536)

Detailed Research Summary

Terahertz Emitters Based on Large Area Nano-Plasmonic Photoconductors:

Time domain terahertz spectroscopy systems have provided unique advantages for various applications including chemical identification, material characterization, biological sensing, medical imaging, and security screening [1-14]. However, the scope and potential use of time-domain terahertz spectroscopy systems are still limited by their relatively low signal-to-noise ratio levels and the low radiation power of their pulsed terahertz emitters. Among various terahertz generation techniques, photoconduction has been one of the most commonly used techniques for generating pulsed terahertz radiation [15-22]. Specifically, large area photoconductive emitters have been very promising candidates for time-domain terahertz spectroscopy systems since they can offer relatively high power and broadband pulsed terahertz radiation [23-27]. When the active area of a large area photoconductive emitter is illuminated by an optical pump beam, photo-generated electrons and holes are accelerated in opposite directions by an external bias electric field. The acceleration and separation of photo-carriers induce a time-varying dipole moment within the device active area which generates terahertz radiation. Large area photoconductive emitters can offer high power terahertz radiation because of their capacity to handle relatively high optical powers without suffering from the carrier screening effect and

thermal breakdown. Additionally, the capability of large area photoconductive emitters in offering broadband terahertz radiation is due to the fact that terahertz radiation is generated by time-varying dipole moments induced within the device active area with dipole lengths much smaller than terahertz radiation wavelength. Despite their great promise for generating high power pulsed terahertz radiation, the optical-to-terahertz conversion efficiency of conventional large area photoconductive emitters is limited by the weak effective dipole moments induced within the device active area. This is mainly due to carrier scattering inside the semiconductor substrate, limiting the carrier acceleration and transport velocity.

To address the optical-to-terahertz conversion efficiency limitation of large area photoconductive emitters, we present a novel design based on plasmonic contact electrodes. Plasmonic contact electrodes have proven to be very effective in enhancing the optical-to-terahertz conversion efficiency of photoconductive antennas by reducing the transport path length of the photocarriers to the device contact electrodes [28-37]. By incorporating plasmonic contact electrodes in large area photoconductive emitters, most of the photocarriers are generated in close proximity to the contact electrodes. Therefore, the majority of the photocarriers are drifted to the contact electrodes within a sub-picosecond time-scale. Since the contact electrodes accommodate photocurrent propagation velocities much higher than that of semiconductor substrates, a much stronger time-varying dipole moment is induced in response to an incident optical pump and, thus, a greatly enhanced optical-to-terahertz conversion efficiency is achieved compared to conventional large area photoconductive emitters. We experimentally demonstrate that much higher optical-to-terahertz conversion efficiencies and higher terahertz power levels are achieved by use of plasmonic contact electrode gratings [23]. We demonstrate broadband, pulsed terahertz radiation with radiation power levels as high as 3.8 mW at an optical pump power level of 240 mW over 0.1-5 THz frequency range.

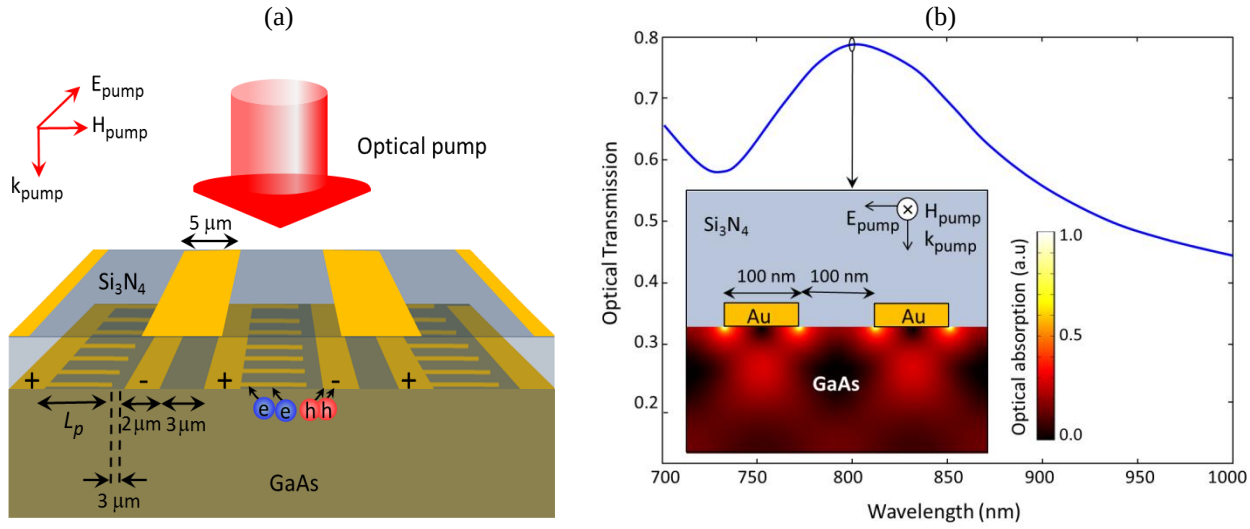

Fig. 1. (a) Schematic diagram and operation principle of the large area plasmonic photoconductive emitter fabricated on a GaAs substrate. (b) Power transmission of a TM-polarized optical beam into the GaAs substrate as a function of optical wavelength. Inset shows color plot of optical absorption in the GaAs substrate in response to a TM-polarized optical beam at 800 nm wavelength.

Schematic diagram of the presented large area plasmonic photoconductive emitter is illustrated in Fig. 1a. The device is fabricated on a GaAs substrate and has an active area of 1×1 mm^2

comprised of a set of interdigitated bias lines. Arrays of plasmonic contact electrode gratings are connected to anode bias lines of the photoconductive emitter within every other gap between the anode and cathode bias lines. The other gaps between the anode and cathode bias lines are shadowed by a second metal layer deposited on top of a Si_3N_4 antireflection coating to block light transmission into the GaAs substrate and induce uni-directional dipole moment in the substrate [25].

Dimensions of the plasmonic contact electrode gratings and thickness of the Si_3N_4 antireflection coating are chosen to transmit the majority of the incident optical pump photons through the plasmonic gratings into the GaAs substrate [38]. A finite-element solver (COMSOL) is used to analyze the interaction of a TM-polarized optical beam with the designed plasmonic gratings. The analysis shows that use of Au gratings with a 200 nm periodicity, 100 nm metal width, and 50 nm metal height and a 350 nm thick Si_3N_4 antireflection coating offers 79% optical transmission into the GaAs substrate at 800 nm pump wavelength (Fig. 1b). Since transmission of the incident optical pump into the GaAs substrate is through excitation of surface plasmon waves and through 100 nm gaps between the plasmonic grating fingers, a large portion of the photocarriers is generated in close proximity to the plasmonic gratings [28, 29]. Therefore, a large portion of the photo-generated electrons is drifted to the plasmonic gratings (anode contact electrodes) in a sub-picosecond timescale and radiate through effective Hertzian dipoles formed by the plasmonic gratings. In order to achieve a broad radiation bandwidth and prevent destructive photocurrent interference along the plasmonic gratings, the length of the plasmonic gratings, L_p, is selected to be much shorter than the effective terahertz radiation wavelength. It should be noted that the photocurrent propagation velocity along plasmonic gratings is not limited by the carrier scattering inside the semiconductor substrate lattice. Therefore, the Hertzian dipole antennas formed by the plasmonic gratings offer significantly higher radiation resistance and better impedance matching to free space compared with the radiating dipoles induced within the semiconductor substrate of conventional large area photoconductive emitters [16, 39].

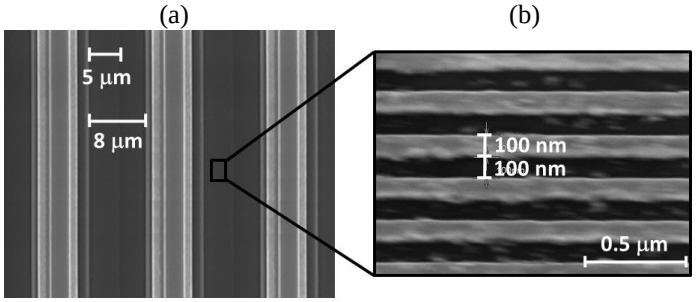

Fig. 2. SEM image of a fabricated large area plasmonic photoconductive emitter with 5 μm long plasmonic contact electrodes, (b) SEM image of the plasmonic contact electrode gratings with 200 nm periodicity and 100 nm width.

Prototypes of large area plasmonic photoconductive emitters are fabricated and characterized to show the key role of plasmonic contact electrodes in offering high power terahertz radiation with significantly enhanced optical-to-terahertz conversion efficiencies. Plasmonic grating lengths of 5 μm and 10 μm are chosen for the fabricated device prototypes to demonstrate the impact of the grating length on terahertz radiation bandwidth and efficiency. A gap of 3 μm is chosen between the tip of the anode contact electrode gratings and the cathode contact electrodes in all device prototypes. This will limit the operation of all device prototypes to the same breakdown bias

voltage levels. The prototypes of large area plasmonic photoconductive emitters are fabricated on semi-insulating (SI) and low-temperature grown (LT) GaAs substrates. The fabrication process begins with patterning the plasmonic contact electrodes using electron-beam lithography, followed by 5/45 nm Ti/Au deposition and liftoff. An optical lithography step with a bi-layer photoresist is used to pattern the bias lines, which is followed by 50/550 nm Ti/Au deposition and liftoff. The 350 nm Si_3N_4 anti-reflection coating is deposited using plasma-enhanced chemical vapor deposition (PECVD). The shadow metals are patterned through optical lithography, followed by 10/90 nm Ti/Au deposition and liftoff. The contact vias are patterned using optical lithography and opened by etching the Si_3N_4 layer using reactive ion etching (RIE). Finally, the device prototypes are mounted on hyper-hemispherical silicon lenses and placed on an optical rotation mount to adjust the polarization of the optical pump with respect to the plasmonic gratings. Figure 2 shows the scanning electron microscope (SEM) images of a fabricated large area plasmonic photoconductive emitter prototype with a 5 μm plasmonic grating length (Fig. 2a) and the plasmonic contact electrode gratings incorporated inside the device active area (Fig. 2b).

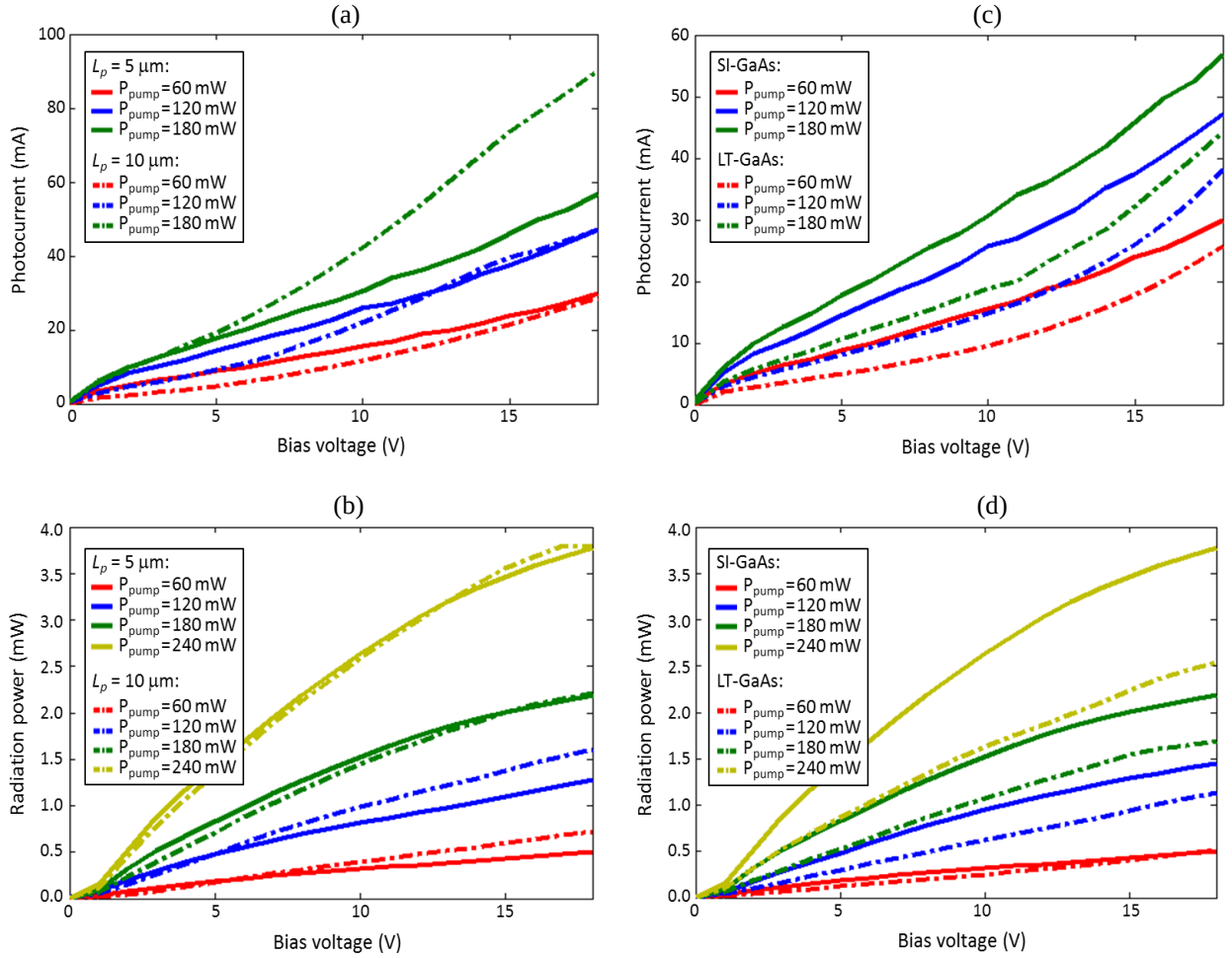

Fig. 3. Measured photocurrent and radiated power for the large area plasmonic photoconductive emitters with 5 μm and 10 μm plasmonic grating lengths fabricated on the SI-GaAs substrate are shown in (a) and (b), respectively. Measured photocurrent and radiated power for the large area plasmonic photoconductive emitters with 5 μm plasmonic grating length fabricated on the SI-GaAs and LT-GaAs substrates are shown in (c) and (d), respectively. Measured dark current of all fabricated emitters is in the 1-10 μA range at 18 V bias voltage.

Terahertz radiation from the large area plasmonic photoconductive emitter prototypes is characterized in response to an optical pump beam from a Ti:sapphire mode-locked laser at 800 nm wavelength, with a repetition rate of 76 MHz and a pulse width of 200 fs. Spot size of the optical pump beam is adjusted to ~ 600 μm to illuminate the entire device active area and polarization of the optical pump beam is set to be normal to the plasmonic contact electrode gratings. A calibrated pyroelectric detector (Spectrum Detector, Inc. SPI-A-65 THz) is used to measure the radiated power from the fabricated large area plasmonic photoconductive emitter prototypes as a function of the bias voltage and optical pump power (P_{pump}) [40]. In order to quantify potential contribution of thermal power to the measured terahertz power levels by the pyroelectric detector, power measurements are repeated under a continuous-wave optical pump beam at 800 nm wavelength. Comparisons between the measured power levels under continuous-wave and mode-locked pump beams indicate that thermal power constitutes a negligible portion (less than 1%) of the measured terahertz power by the pyroelectric detector.

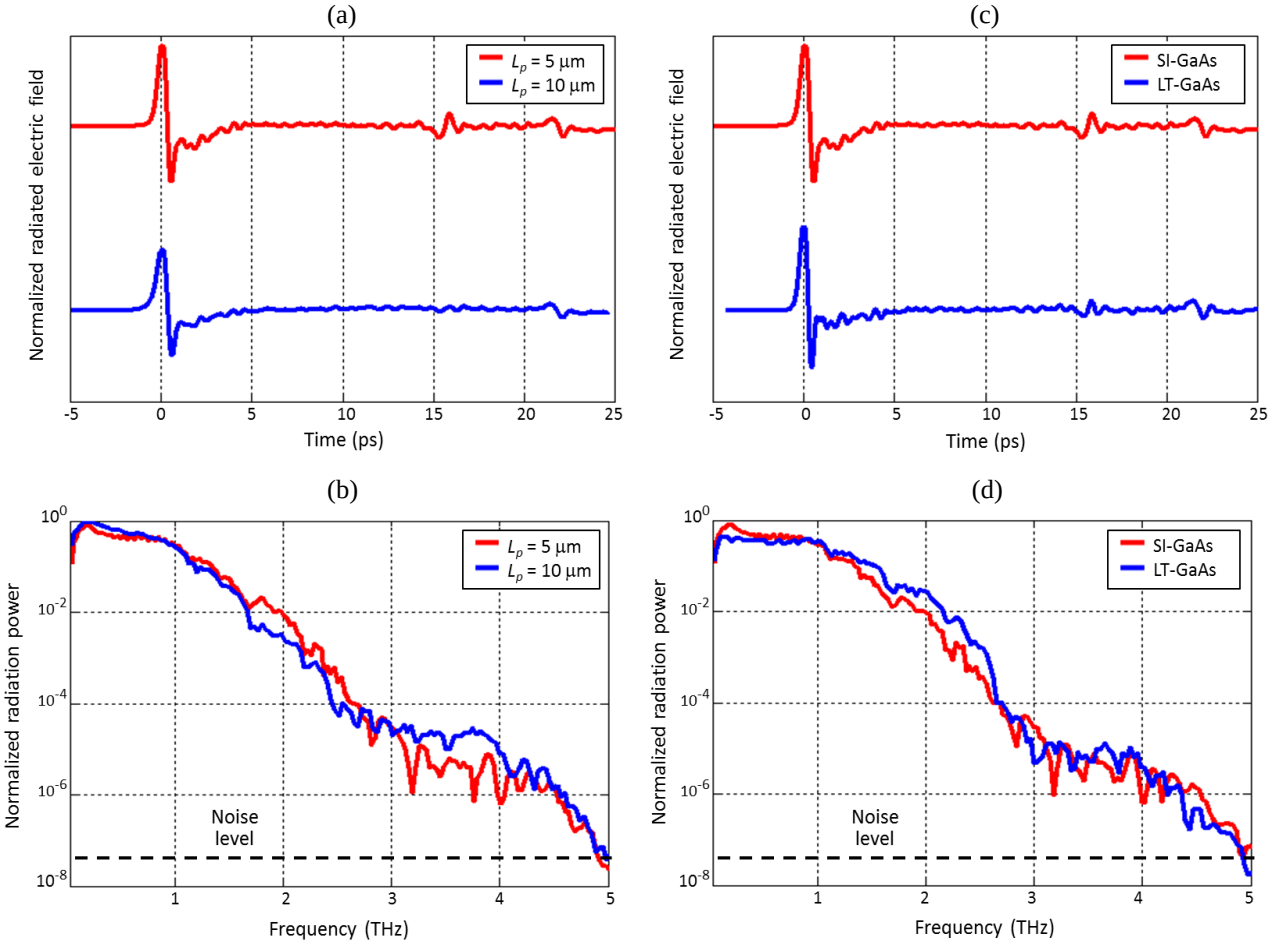

Fig. 4. Measured radiated electric field in the time domain and radiated power in the frequency domain for the large area plasmonic photoconductive emitters with 5 μm and 10 μm plasmonic grating lengths fabricated on the SI-GaAs substrate are shown in (a) and (b), respectively. Measured radiated electric field in the time domain and radiated power in the frequency domain for the large area plasmonic photoconductive emitters with 5 μm plasmonic grating length fabricated on the SI-GaAs and LT-GaAs substrates are shown in (c) and (d), respectively.

Figure 3 shows the impact of the plasmonic grating length and device substrate on the performance of the large area plasmonic photoconductive emitter prototypes. Measured

photocurrent of the large area plasmonic photoconductive emitters with 5 μm and 10 μm plasmonic grating lengths fabricated on the SI-GaAs substrate is shown in Fig. 3a. At low optical pump powers and low bias voltage levels, the emitter prototype with 5 μm plasmonic grating length exhibits higher photocurrent levels compared to the emitter prototype with 10 μm plasmonic grating length. This is because of a larger bias electric field reduction along the 10 μm long plasmonic gratings in comparison with the 5 μm long plasmonic gratings. Increasing the bias voltage level compensates the bias electric field reduction along the 10 μm long plasmonic gratings, leading to a smaller difference between the photocurrent of the emitters with 5 μm and 10 μm plasmonic grating lengths.

While the bias electric field reduction along the 10 μm long plasmonic gratings becomes less effective as the bias voltage is increased further, the emitter prototype with 10 μm plasmonic grating length starts exhibiting higher photocurrent levels compared to the emitter prototype with 5 μm plasmonic grating length. This trend, which is more obvious at higher optical pump power levels, is due to the fact that the shadowed area in the emitter with 10 μm plasmonic grating length covers a smaller portion of the whole device area compared to the emitter with 5 μm plasmonic grating length. Therefore, a larger number of photocarriers is generated within the active area of the emitter with 10 μm plasmonic grating length, leading to higher photocurrent levels under sufficient bias electric field levels. The radiated power from the large area plasmonic photoconductive emitters with 5 μm and 10 μm plasmonic grating lengths fabricated on the SI-GaAs substrate is shown in Fig. 3b. At lower optical pump power levels and sufficient bias voltage levels, the emitter with 10 μm plasmonic grating length offers higher radiation power levels compared to the emitter with 5 μm plasmonic grating length. This is predicted since a larger number of photocarriers contributes to terahertz radiation when a smaller portion of the device active area is shadowed. At higher optical pump power levels, the emitter with 10 μm plasmonic grating length becomes less efficient in offering higher radiation power levels. This is because the emitter with 10 μm plasmonic grating length is more susceptible to suffer from the carrier screening effect compared to the emitter with 5 μm plasmonic grating length. At an optical pump power of 240 mW and bias voltage of 18 V, both large area plasmonic photoconductive emitters with 5 μm and 10 μm plasmonic grating lengths offer 3.8 mW of terahertz radiation power. This is the highest reported terahertz radiation power from large area photoconductive emitters with one order of magnitude enhancement in optical-to-terahertz conversion efficiency compared to conventional designs [23].

Measured photocurrent of the large area plasmonic photoconductive emitters with 5 μm plasmonic grating length fabricated on the SI-GaAs and LT-GaAs substrates is shown in Fig. 3c. As expected, the emitter fabricated on the LT-GaAs substrate exhibits smaller photocurrent levels compared to the emitter fabricated on the SI-GaAs substrate due to shorter carrier lifetime of excess carriers in the LT-GaAs substrate [41]. It should be noted that Fig. 3c shows the DC photocurrent levels of the emitter prototypes fabricated on the SI-GaAs and LT-GaAs substrates. Therefore, it cannot be directly used to predict the radiated terahertz power of the emitter prototypes, especially since the lifetime of the photocarriers is considerably different in the SI-GaAs and LT-GaAs substrates. In fact, the dominant portion of the generated terahertz radiation from the presented large area plasmonic photoconductive emitters is the result of the photocarriers generated in close proximity to the plasmonic contact electrodes, which are drifted to the plasmonic contact electrodes within a fraction of the oscillation period of the terahertz radiation. Therefore, since the concentration of the photocarriers is the same within the active

area of the plasmonic emitters fabricated on the SI-GaAs and LT-GaAs substrates and since higher carrier mobility levels are accommodated in the SI-GaAs substrate compared to the LT-GaAs substrate, a larger number of photocarriers is drifted to the plasmonic contact electrodes within a fraction of the oscillation period of the terahertz radiation. Therefore, higher radiation power levels are offered by the emitter prototypes fabricated on the SI-GaAs substrate (Fig. 3d).

The radiated electric field from the fabricated large area plasmonic photoconductive emitters is measured in a time-domain terahertz spectroscopy setup with electro-optic detection in a 1 mm ZnTe crystal. For this measurement, all the fabricated emitters are characterized at 18 V bias voltage and 150 mW optical pump power. The radiated electric field in the time domain and the radiated power in the frequency domain for the large area plasmonic photoconductive emitters with 5 μm and 10 μm plasmonic grating lengths fabricated on the SI-GaAs substrate are shown in Fig. 4a and Fig. 4b, respectively. At lower frequencies (f_{THz} < 1 THz), the emitter with 10 μm plasmonic grating length radiates higher terahertz power levels compared to the emitter with 5 μm plasmonic grating length. This is because a larger number of photocarriers is generated in close proximity to the plasmonic gratings of the emitter with 10 μm plasmonic grating length since a smaller portion of the device active area is shadowed. Therefore, a larger number of photocarriers is drifted to the plasmonic contact electrodes within a fraction of the oscillation period of the terahertz radiation. The number of the photocarriers drifted to the plasmonic contact electrodes of the emitter with 10 μm plasmonic grating length within a fraction of the oscillation period of the terahertz radiation is not larger than that of the emitter with 5 μm plasmonic grating length at higher terahertz frequencies. This is because the emitter with 10 μm plasmonic grating length is more susceptible to suffer from the carrier screening effect and bias electric field reduction along the plasmonic gratings, which prevent ultrafast drift of the photocarriers to the plasmonic contact electrodes. Therefore, the emitter with 5 μm plasmonic grating length offers higher radiation power levels compared to the emitter with 10 μm plasmonic grating length at higher frequencies (f_{THz} > 1 THz). It should be noted that the higher terahertz radiation power levels offered by the emitter with 10 μm grating length within 3-4 THz is due to the resonant behavior of the 10 μm long plasmonic gratings, which behave like quarter-wave monopole antennas in this frequency range.

The radiated electric field in the time domain and the radiated power in the frequency domain for the large area plasmonic photoconductive emitters with 5 μm plasmonic grating length fabricated on the SI-GaAs and LT-GaAs substrates are shown in Fig. 4c and Fig. 4d, respectively. At lower frequencies (f_{THz} < 1 THz), the emitter fabricated on the SI-GaAs substrate radiates higher terahertz power levels compared to the emitter fabricated on the LT-GaAs substrate. This is because of the lower excess carrier recombination rates and higher carrier mobility levels in the SI-GaAs substrate compared to the LT-GaAs substrate, which result in a larger number of drifted photocarriers to the plasmonic contact electrodes of the emitter fabricated on the SI-GaAs substrate within a fraction of the oscillation period of the terahertz radiation. Despite the larger excess carrier recombination rates and lower carrier mobility levels in the LT-GaAs substrate, the emitter fabricated on the LT-GaAs substrate offers higher terahertz radiation power levels compared to the emitter fabricated on the SI-GaAs at higher frequencies (f_{THz} > 1 THz). This is because of a stronger carrier screening effect in the emitter fabricated on the SI-GaAs substrate, which results in a more severe reduction in the photocarrier drift velocity and device quantum efficiency at high frequencies. It should be noted that the use of ZnTe in the utilized time-domain terahertz spectroscopy setup introduces significant terahertz signal attenuation at frequencies

above 3 THz. Therefore, the actual radiation spectrum of the fabricated large area plasmonic photoconductive emitters is broader than that shown in Fig. 4b and Fig. 4d.

In summary, a novel large area photoconductive terahertz emitter based on plasmonic contact electrode gratings is presented. Incorporating plasmonic contact electrodes within the device active area offers significantly stronger time-varying dipole moments in response to an incident optical pump. Therefore, greatly enhanced optical-to-terahertz conversion efficiencies are achieved compared to conventional large area photoconductive emitters. In order to evaluate the impact of plasmonic contact electrodes on the performance of large area plasmonic photoconductive emitters, a comprehensive characterization of device performance and its relation to the plasmonic electrode geometry and device substrate properties is presented. We demonstrate broadband, pulsed terahertz radiation with radiation power levels as high 3.8 mW at an optical pump power of 240 mW (1.6% optical-to-terahertz conversion efficiency) over 0.1-5 THz frequency range. This is the highest reported terahertz radiation power from large area photoconductive emitters with one order of magnitude enhancement in optical-to-terahertz conversion efficiency compared to conventional designs. Moreover, the optical-to-terahertz conversion efficiency and the maximum radiated power from large area plasmonic photoconductive emitters can be further enhanced by use of larger device active areas and by use of high-aspect ratio plasmonic contact electrodes embedded inside the photo-absorbing substrate [30, 42]. Therefore, the presented large area plasmonic photoconductive emitter could have a significant impact on the scope and potential use of future time-domain terahertz spectroscopy systems.

High Performance Heterodyne terahertz Receivers based on Plasmonic Photomixers:
Figure 5 shows the schematic diagram and operation concept of the first-generation plasmonic heterodyne receiver based on the plasmonic nano-antennas developed during this research program. It consists of a dipole terahertz antenna connected to plasmonic photoconductive grating electrodes. Plasmonic electrodes enable high quantum efficiency operation by enhancing light-matter interaction at nanoscale. Low-temperature grown GaAs (LT-GaAs) is used as the device substrate to allow device operation at 800 nm optical pump wavelengths, while offering a short carrier lifetime needed for ultrafast and low noise device operation.

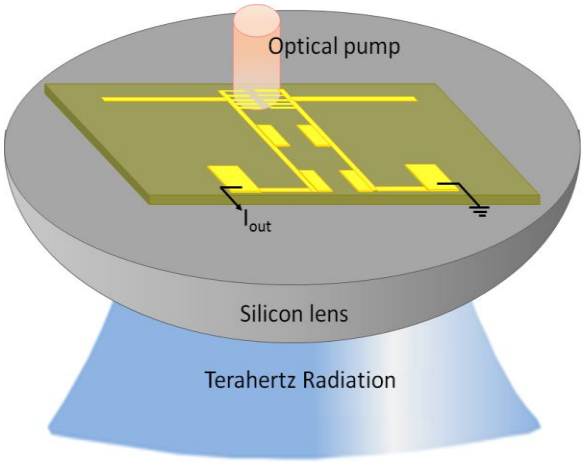

Fig. 5. Schematic diagrams of the designed plasmonic heterodyne terahertz receiver.

A heterodyned optical pump beam with the frequency difference f_{opt} is used to pump the plasmonic heterodyne receiver. The frequency difference f_{opt} is set to be within the frequency range of the terahertz wave that needs to be detected. For the first generation device, the heterodyne receiver is optimized for operation specifically around f_{THz} = 0.1 THz frequency range. With the optical pump incident on the plasmonic electrodes, photo carriers are generated inside the photoconductor and the time-varying photo-carrier density will have an AC component at f_{opt}. In the meantime, the incident terahertz wave is received by the dipole antenna, inducing a terahertz electric field across the plasmonic contact electrodes. The induced terahertz electric field, which has a magnitude envelope at frequency f_{THz}, drives the photocarriers towards the electrodes and forms an output photocurrent which carries an intermediate component at frequency $f_{IF} = | f_{opt} - f_{THz} |$. By measuring the intermediate frequency component signal and tuning the heterodyned optical pump frequency difference f_{opt}, the spectrum of the incident terahertz wave is measured.

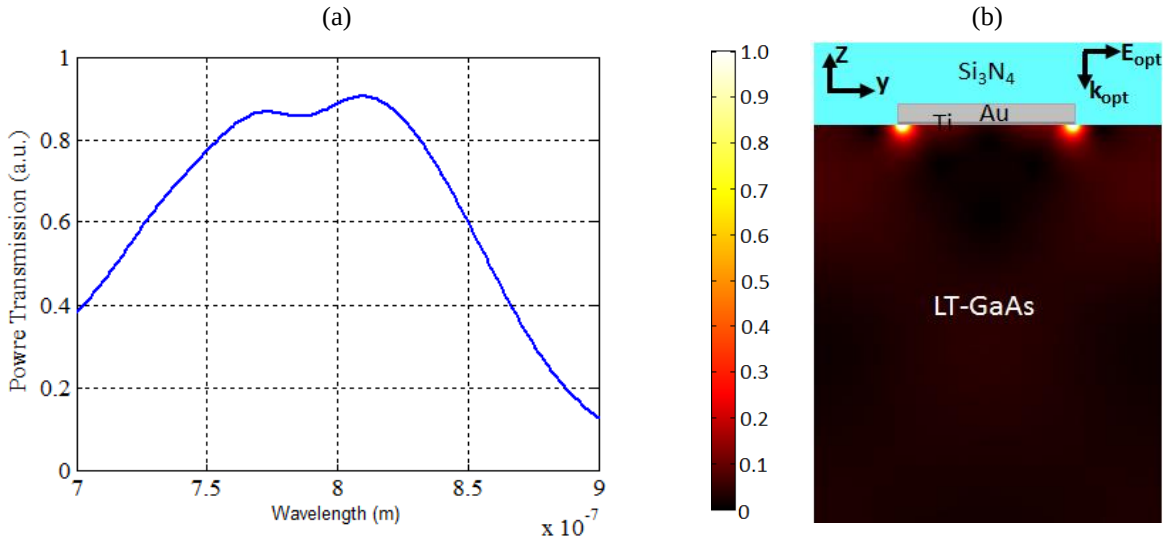

Fig. 6. COMSOL simulation results of (a) optical power transmission through plasmonic electrodes at different wavelengths, (b) optical pump power absorption inside the photo-absorbing substrate.

The plasmonic gratings are designed to allow maximum optical pump power transmission into the device active area where the induced terahertz field drives the induced photocarriers into the plasmonic contact electrodes. Figure 6 shows the optical pump power transmission through the designed plasmonic contact electrodes as a function of the optical pump wavelengths (Fig. 6a) and the optical pump power absorption inside the photo-absorbing substrate at 785 nm optical pump wavelength (Fig. 6b). Silicon nitride (Si_3N_4) is used as an anti-reflection coating to maximize the optical power transmission. COMSOL simulation results show that with a 200 nm periodicity, 100 nm spacing, 5 nm thick Titanium, 45 nm thick gold, and 300 nm thick silicon nitride, the plasmonic gratings can offer a broadband optical power transmission of 85% at 785 nm pump wavelength. To receive the incident terahertz wave, a terahertz antenna needs to be integrated with the plasmonic gratings. A full-wavelength dipole antenna with a resonant frequency at around 95 GHz is designed to be the terahertz antenna in the first generation terahertz heterodyne receiver. To have an efficient use of the optical pump, the dimension of each plasmonic grating electrodes region is designed to be 30 um x 30 um. To induce the maximum terahertz electric field between anode and cathode of the terahertz dipole antenna, the

gap between anode and cathode electrodes should be as small as possible (designed to be 1 um). To minimize current leakage from the antenna to the substrate, the antenna is placed on top of the 300 nm thick silicon nitride layer. The generated photocurrent at intermediate frequency (IF) is guided out through feeding lines of the dipole antenna and monitored by a spectrum analyzer. Another matter that needs to be considered during the antenna design process is that some of the induced terahertz current on the antenna could leak through the feeding lines and, thus, could reduce the antenna efficiency.

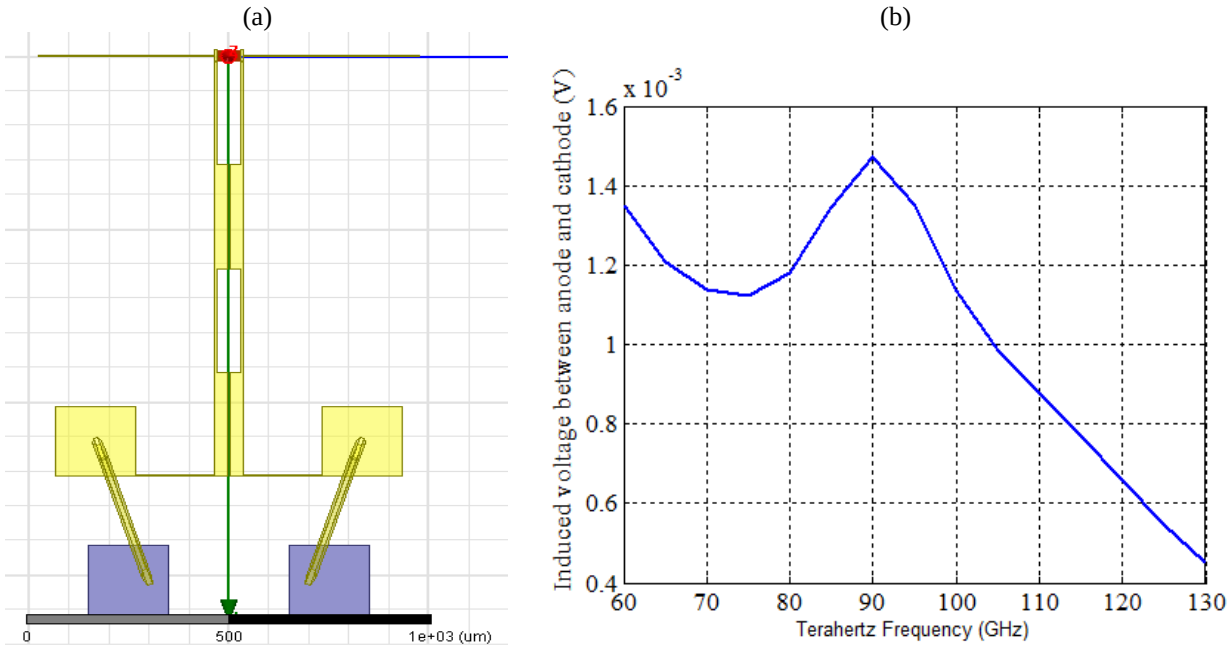

Fig. 7. HFSS simulation of the dipole antenna integrated with plasmonic grating electrodes, low-pass filter, transmission lines and bonding pads, (a) structure layout top view in HFSS, and (b) induced voltage between the anode and cathode electrodes for a 1V/m terahertz plane wave incident from the back side of the substrate. The polarization of the terahertz is set to be along the dipole antenna.

To solve this problem, a low-pass filter is designed and integrated with the feeding lines of the antenna to allow efficient transmission of the IF current, while blocking the terahertz current. HFSS simulator is used to design and simulate the terahertz dipole antenna integrated with the plasmonic gratings, low-pass filter transmission lines and the bonding pads. Figure 7 shows the estimated induced voltage across the gap between the anode and cathode electrodes with a 1 V/m terahertz plane wave incident from the backside of the substrate. In order to induce maximum terahertz electric field and voltage in the gap between the anode and cathode electrodes, the total length of the dipole antenna including the plasmonic gratings is designed to be 900 um, the width of the dipole antenna arm is designed to be 5 um and the thickness of the antenna arm is designed to be 50 nm Titanium and 400 nm gold. The low-pass filter is composed of two 300 um long high-impedance transmission lines and two 300 um long low-impedance transmission lines in alternating turns. Each high-impedance transmission line consists of two 5 um wide traces of 50 nm thick Titanium and 400 nm thick gold with a 61 um separation from each other and each low-impedance transmission line consists of two 33 um wide traces of 50 nm thick Titanium and 400 nm thick gold with a 5 um separation from each other.

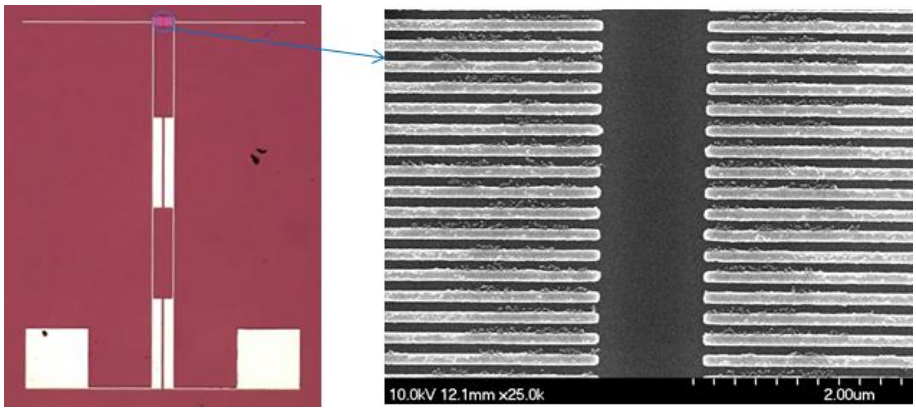

Fig. 8. Microscope and SEM images of a plasmonic heterodyne terahertz receiver fabricated on LT-GaAs substrate.

A prototype of the designed plasmonic heterodyne receiver is fabricated on a LT-GaAs substrate (Fig. 8). The fabrication process starts with patterning plasmonic contact electrode gratings using electron-beam lithography followed by deposition of Ti/Au (5/45 nm) and liftoff. The Si_3N_4 anti-reflection coating is then deposited using plasma-enhanced chemical vapor deposition on the entire piece of substrate. Next, contact vias are patterned using optical lithography and formed by using dry plasma etching. Finally, the dipole antenna, low-pass filter, transmission lines and bonding pads are patterned using optical lithography, followed by deposition of Ti/Au (50/400 nm) and liftoff.

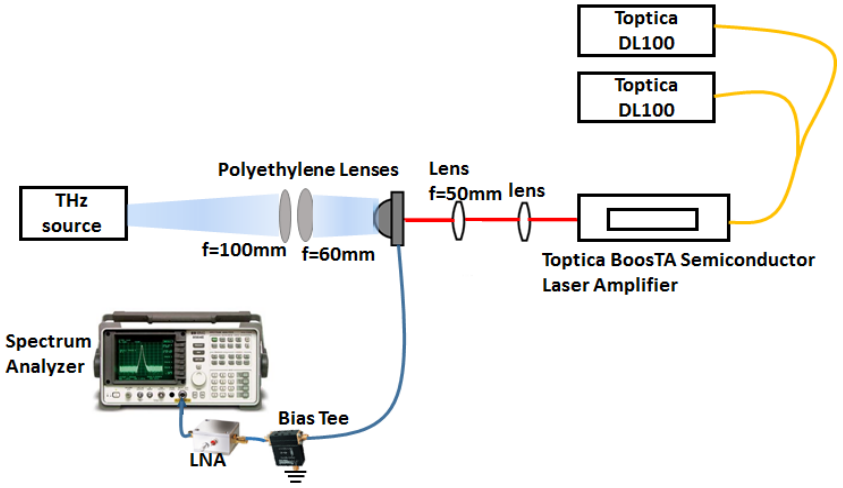

Fig. 9. The experimental setup used for characterizing the plasmonic heterodyne receiver

The fabricated plasmonic heterodyne terahertz receiver prototype is then characterized in the experimental setup shown in Figure 9. Two Toptica Photonics DL100 Grating Stabilized Tunable Single-Mode Diode Lasers (wavelength ~785 nm) are used as the optical pump lasers. The Toptica DL100 lasers can offer two optical pumps with a beating frequency from 0 to 2 THz at equal power levels. The output of these two lasers are combined in a 2:1 fiber combiner and amplified by a Toptica BossTA Semiconductor Laser Amplifier, which can offer an output power as high as 3 W. A Gunn oscillator is used to provide the terahertz signal at around 95 GHz. The terahertz beam is coupled to free space by a WR10 horn antenna and then collimated by two polyethylene lenses, and then focused to the dipole antenna through the silicon lens used for mounting the device prototype. The generated photocurrent at intermediate frequency (IF) is

then coupled to a SMA cable followed by a bias tee (Picosecond, Model 5541A), to maintain a zero DC voltage between the anode and cathode contacts. Finally, the IF signal is amplified by a low-noise amplifier (Mini-circuits, ZFL-1000LN+) and monitored through a spectrum analyzer (HP 8566B).

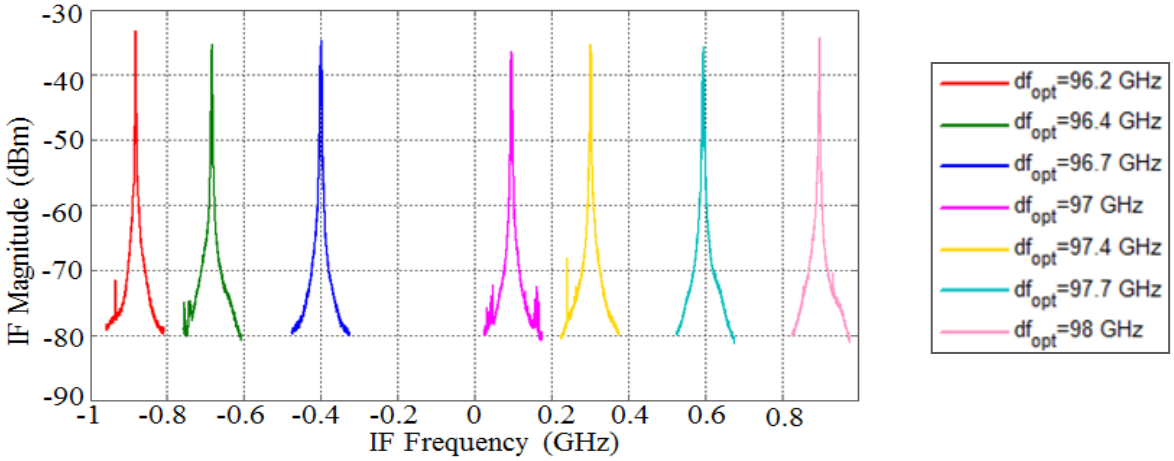

Fig. 10. Measured IF signal from the fabricated plasmonic heterodyne receiver prototype at different beating frequencies and at a 300 mW optical pump power.

Figure 10 shows the observed IF spectrum at 300 mW optical pump power, while tuning the beating frequency of the optical pump lasers from 96 GHz to 98 GHz, illustrating the simplicity of frequency scanning through the designed plasmonic heterodyne receiver. Figure 11 shows the details of one of the measured IF spectral lines for an optical pump beating frequency of 97.5 GHz, indicating a signal-to-noise ratio of 50 dB. It should be mentioned that the utilized amplifier in our experimental setup has a noise figure of 3 dB. Therefore, the actual signal-to-noise ratio of the plasmonic heterodyne receiver prototype is estimated to be 53 dB.

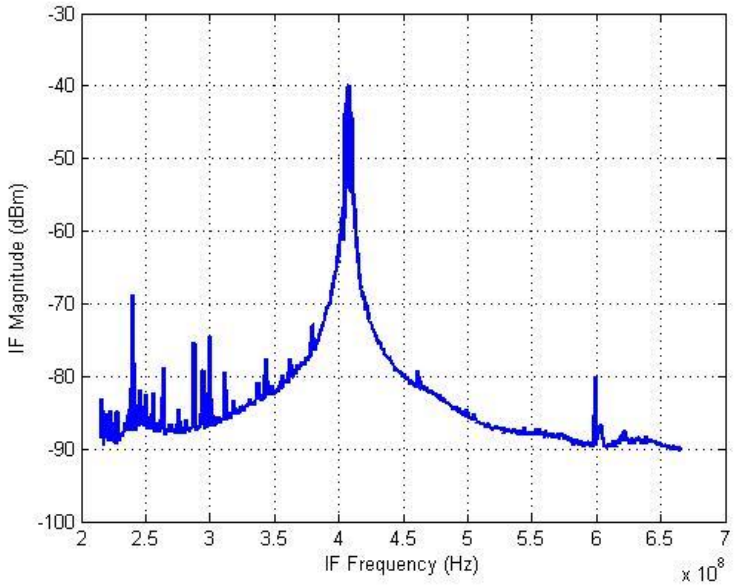

Fig. 11. Measured IF signal from the fabricated plasmonic heterodyne receiver prototype at an optical pump beating frequency of 97.5 GHz and an optical pump power of 300 mW.

Figure 12 shows the relation between the IF signal and the optical pump power. As expected, there is a linear relation between the receiver responsivity and the optical pump power. This is because the pump power level directly affects the number of the photocarriers drifted by the incident terahertz field. Therefore, higher receiver responsivity levels are achieved at higher optical pump power levels and unprecedented dynamic ranges are offered by the demonstrated plasmonic heterodyne terahertz receiver.

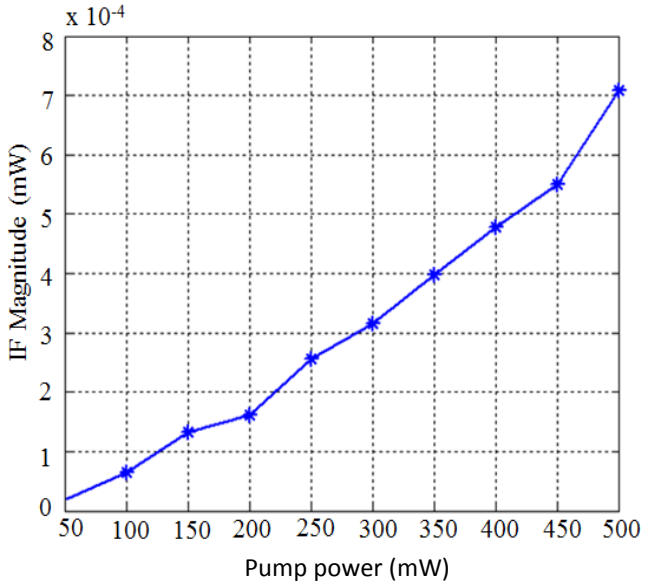

Fig. 12. Receiver responsivity as a function of the optical pump power level.

One of the ways to improve the performance of the plasmonic heterodyne receiver is to modulate the optical pump beam with low duty cycles, so that high pump peak powers can offer high responsivity levels, while low average pump powers can maintain low noise operation. Figure 13 shows the comparison between two IF measurements before and after optical pump modulation with a 5% duty cycle (Figs 13a and 13b, respectively). The results show that at the same average optical pump power (100 mW), the modulated optical pump with 5% duty cycle offers 13 dB higher signal to noise ratio levels.

(a)

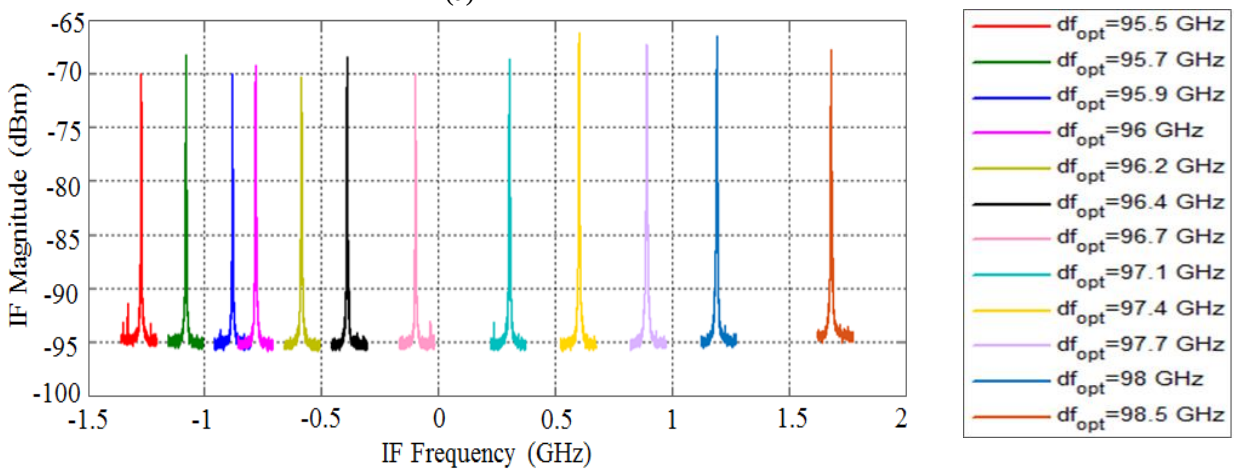

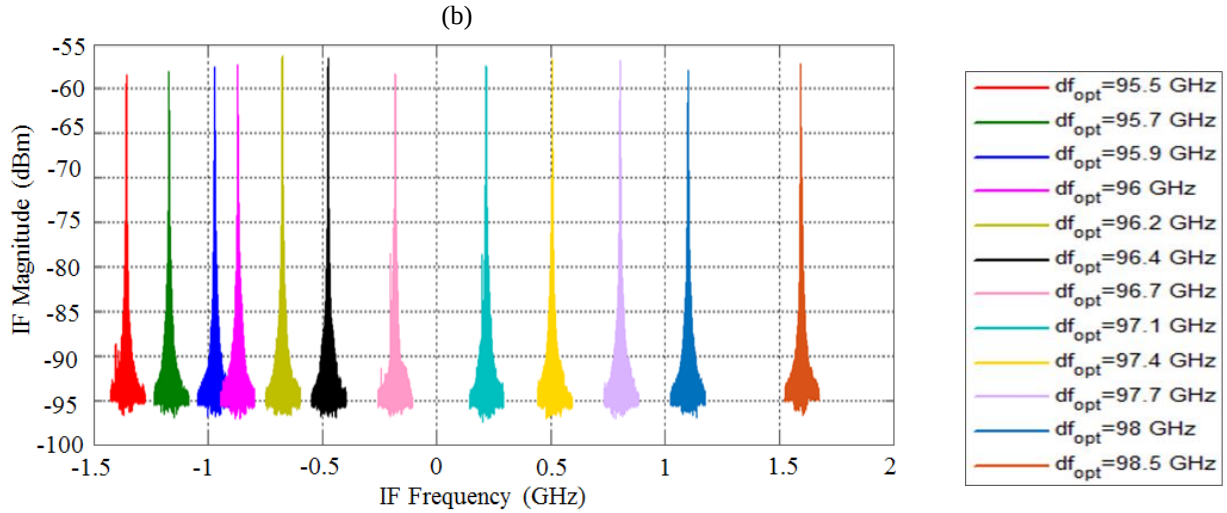

Fig. 13. Comparison between the measured IF spectrum at an average optical pump power of 100 mW, (a) before optical pump modulation, and (b) after pump modulation with a 5% duty cycle.

By combining the high signal-to-noise ratio operation of the plasmonic heterodyne receiver prototype at 300 mW pump power (53 dB) with the significant impact of 5% optical pump duty cycle, 66 dB signal-to-noise ratio and dynamic range is achieved at 0.1 THz. Although the achieved 66 dB signal-to-noise ratio level and dynamic range are already much higher than what can be offered by existing heterodyne terahertz receivers, we plan to further enhance the signal-to-noise ratio and dynamic range of plasmonic heterodyne terahertz receivers by use of smaller pump duty cycles and utilizing lower noise amplifiers and filters for minimizing the device noise level. We also plan to extend the unprecedented performance of plasmonic heterodyne terahertz receivers to a broad range of terahertz frequencies by utilizing broadband antennas (e.g. logarithmic spiral antennas and large area nano-antenna arrays) and utilize three-dimensional plasmonic contact electrodes for a more efficient interaction between the optical pump beam and incident terahertz radiation to extend the plasmonic receiver sensitivity to quantum-level sensitivities for future chemical sensing applications.

References

[1] M. Tonouchi, "Cutting-edge terahertz technology," *Nature Photonics*, vol. 1, pp. 97-105, 2007.

[2] D. G. Rowe, "Terahertz takes to the stage," *Nature Photonics*, vol. 1, pp. 75-77, Feb. 2007.

[3] D. Grischkowsky, Søren Keiding, Martin van Exter, and Ch. Fattinger, "Far-infrared time-domain spectroscopy with terahertz beams of dielectrics and semiconductors," *J. Opt. Soc. Am. B* 7, 2006, 1990.

[4] D.M. Mittleman, R.H. Jacobsen, R. Neelamani, R.G. Baraniuk, M.C. Nuss, "Gas Sensing using terahertz time-domain spectroscopy,"*J. Appl. Phys. B*, vol. 67, 3, 1998.

[5] K. Kawase, Y. Ogawa, Y. Watanabe, H. Inoue, "Non-destructive terahertz imaging of illicit drugs using spectral fingerprints," *Optics Express*, vol. 11, no. 20, pp. 2549-2554, Oct. 2003.

[6] R.M. Woodward, V.P. Wallace, D.D. Arnone, E.H. Linfield, M. Pepper, "Terahertz pulsed imaging of skin cancer in the time and frequency domain," *J Biol Phys*, vol. 29, pp. 257-261, Jun. 2003.

[7] D. D. Arnone, C. Ciesla, M. Pepper, "Terahertz imaging comes into view," *Physics World*, pp. 35-40, Apr. 2000.

[8] L. L. Van Zandt, V. K. Saxena, "Millimeter-microwave spectrum of DNA: Six predictions for spectroscopy," *Phys. Rev. A*, vol. 39, pp. 2672-2674, Mar. 1989.

[9] J. F. Federici, B. Schulkin, F. Huang, D. Gary, R. Barat, F. Oliveira, D. Zimdars, "THz imaging and sensing for security applications-explosives, weapons and drugs," *Semicond. Sci. Technol*, vol. 20, pp. S266–S280, Jul. 2005.

[10] M. C. Kemp, P. F. Taday, B. E. Cole, J. A. Cluff, A. J. Fitzgerald, W. R. Tribe, "Security applications of terahertz technology," *Proceedings of. SPIE*, vol. 5070, pp. 44-52, Jul. 2003.
[11] M. Nagel, M. Forst, H. Kurz, "THz biosensing devices: fundamentals and technology," *J. Phys. Condensed Matter*, vol. 18, no. 18, pp. S601-S618, Apr. 2006.
[12] D. Van der Weide, J. Murakowski, F. Keilmann, "Gas-Absorption Spectroscopy with Electronic Terahertz Techniques," *IEEE Trans. Microwave Theory and Techniques*, vol. 48, no. 4, pp. 740-743, Apr. 2000.
[13] N. Nagai, T. Imai, R. Fukasawa, K. Kato, K. Yamauchi, "Analysis of the intermolecular interaction of nanocomposites by THz spectroscopy,"*Appl. Phys. Lett*., vol. 85, pp. 4010-4012, Nov. 2004.
[14] P. Siegel, "Terahertz Technology in Biology and Medicine," *IEEE Trans. Microwave Theory and Techniques*, vol. 52, no. 10, pp. 2438-2447, Oct. 2004.
[15] D. H. Auston, K. P. Cheung, P. R. Smith, "Picosecond photoconducting Hertzian dipoles,"*Appl. Phys. Lett*., vol. 45, pp. 284-286, May 1984.
[16] S. Preu, G. H. Dohler, S. Malzer, L. J. Wang, A. C. Gossard, "Tunable, continuous-wave Terahertz photomixer sources and applications," *J. Appl. Phys.*, vol. 109, 061301, Mar. 2011.
[17] J. E. Bjarnason, T. L. J. Chan, A. W. M. Lee, E. R. Brown, D. C. Driscoll, M. Hanson, A. C. Gossard, R. E. Muller, "ErAs:GaAs photomixer with two-decade tunability and 12uW peak output power,"*Appl. Phys. Lett.*, vol. 85, pp. 3983-3985, Nov. 2004.
[18] M. Jarrahi, T. H. Lee, "High power tunable terahertz generation based on photoconductive antenna arrays," in *IEEE Microwave Symposium Digest*, 2008, pp. 391-394.
[19] E. Peytavit, S. Lepilliet, F. Hindle, C. Coinon, T. Akalin, G. Ducournau, G. Mouret, J. -F. Lampin, "Milliwatt-level output power in the sub-terahertz range generated by photomixing in a GaAs photoconductor," *Appl. Phys. Lett.*, vol. 99, p. 223508, Nov. 2011.
[20] H. Roehle, R. J. B. Dietz, H. J. Hensel, J. Böttcher, H. Künzel, D. Stanze, M. Schell, B. Sartorius, "Next generation 1.5 μm terahertz antennas: mesa-structuring of InGaAs/InAlAs photoconductive layers," *Opt. Express*, vol. 18, pp. 2296-2301, Feb. 2010.
[21] Z. D. Taylor, E. R. Brown, J. E. Bjarnason, "Resonant-optical-cavity photoconductive switch with 0.5% conversion efficiency and 1.0W peak power," *Opt. Lett*., vol. 31, pp. 1729-1731, Jun. 2006.
[22] M. Jarrahi, "Terahertz radiation-band engineering through spatial beam-shaping," *Photon. Technol. Lett*., vol. 21, pp. 830-832, Jul. 2009.
[23] M. Beck, H. Schäfer, G. Klatt, J. Demsar, S. Winnerl, M. Helm, T. Dekorsy, "Impulsive terahertz radiation with high electric fields from an amplifier-driven large-area photoconductive antenna," *Opt. Express*, vol. 18, pp. 9251-9257, Apr. 2010.
[24] A. Dreyhaupt, S. Winnerl, T. Dekorsy, and M. Helm, "High-intensity terahertz radiation from a microstructured large-area photoconductor," *Appl. Phys. Lett.*, vol.86, p. 121114, 2005.
[25] S. Preu, M. Mittendorff, H. Lu, H. B. Weber, S. Winnerl, A. C. Gossard, "1550 nm ErAs:In(Al)GaAs large area photoconductive emitters," *Appl. Phys. Lett*., vol. 101, p. 101105, Sep. 2012.
[26] S. Winnerl, "Scalable Microstructured Photoconductive Terahertz Emitters," *J. Infrared. Milim.. Teahz Waves*, vol. 33, pp. 431-454, 2012.
[27] F. Peter, S. Winnerl, S. Nitsche, A. Dreyhaupt, H. Schneider, M. Helm, "Coherent terahertz detection with a large-area photoconductive antenna," *Appl. Phys. Lett.*, vol. 91, p. 081109, 2007.
[28] C. W. Berry, M. Jarrahi, "Terahertz generation using plasmonic photoconductive gratings," *New J. Phys*., vol. 14, p. 105029, Oct. 2012.
[29] C. W. Berry, N. Wang, M. R. Hashemi, M. Unlu, M. Jarrahi, "Significant Performance Enhancement in Photoconductive Terahertz Optoelectronics by Incorporating Plasmonic Contact Electrodes," *Nat. Commun*., vol. 4, p. 1622, Mar. 2013.
[30] S. H. Yang, M. R. Hashemi, C. W. Berry, M. Jarrahi, "7.5% optical-to-terahertz conversion efficiency offered by photoconductive emitters with three-dimensional plasmonic contact electrodes," *IEEE Trans. Terahertz Sci. Technol*, vol. 4, pp. 575-581, Sep. 2014.
[31] C. W. Berry, M. R. Hashemi, S. Preu, H. Lu, A. C. Gossard, M. Jarrahi, "High Power Terahertz Generation Using 1550 nm Plasmonic Photomixers", *Appl. Phys. Lett.*, vol. 105, p. 011121, 2014.
[32] C. W. Berry, M. R. Hashemi, M. Jarrahi, "Generation of High Power Pulsed Terahertz Radiation using a Plasmonic Photoconductive Emitter Array with Logarithmic Spiral Antennas", *Appl. Phys. Lett.*, vol. 104, p. 081122, 2014.
[33] N. Wang, M. R. Hashemi, M. Jarrahi, "Plasmonic photoconductive detectors for enhanced terahertz detection sensitivity", *Opt. Express*, vol. 21, pp. 17221-17227, 2013.

[34] B. Heshmat, H. Pahlevaninezhad, Y. Pang, M. Masnadi-Shirazi, R. B. Lewis, T. Tiedje, R. Gordon, T. E. Darcie, "Nanoplasmonic Terahertz Photoconductive Switch on GaAs," *Nano Lett.*, vol. 12, pp. 6255-6259, Nov. 2012.
[35] S.-G. Park, K. H. Jin, M. Yi, J. C. Ye, J. Ahn, and K.-H. Jeong, "Enhancementof terahertz pulse emission by optical nanoantenna," *ACS Nano*, vol. 6, pp. 2026–2031, Feb. 2012.
[36] S. Liu, X. Shou, A. Nahata, "Coherent Detection of Multiband Terahertz Radiation Using a Surface Plasmon-Polariton Based Photoconductive Antenna," *IEEE Trans. Terahertz Sci. Technol*., vol. 1, pp. 412-415, Nov. 2011.
[37] S.-G. Park, Y. Choi, Y.-J. Oh, K.-H. Jeong, "Terahertz photoconductive antenna with metal nanoislands," *Opt. Express*, vol. 20, 25530, Nov. 2012.
[38] B-Y. Hsieh, M. Jarrahi, "Analysis of periodic metallic nano-slits for efficient interaction of terahertz and optical waves at nano-scale dimensions", *J. Appl. Phys.*, vol. 109, 084326, 2011.
[39] C. A. Balanis, *Antenna Theory: Analysis and design*, 3rd ed. (John Wiley & Sons, Hoboken, New Jersey, USA, 2005).
[40] C. W. Berry, N. T. Yardimci, M. Jarrahi, "Responsivity Calibration of Pyroelectric Terahertz Detectors," arXiv:1412.6878v1, 2014.
[41] H. Nemec, A. Pashkin, P. Kuzel, M.Khazan, S. Schnull, I. Wilke, "Carier dynamics in low-temperature grown GaAs studied by terahertz emission spectroscopy," *J. Appl. Phys.*, vol. 90, p. 1303, 2001.
[42] S.-H. Yang, M. Jarrahi, "Enhanced light-matter interaction at nanoscale by utilizing high aspect-ratio metallic gratings", *Opt. Lett.*, vol. 38, pp. 3677-3679, 2013.